You might find this additional information useful...

This article cites 347 articles, 156 of which you can access free at:
http://physrev.physiology.org/cgi/content/full/83/4/1401#BIBL

This article has been cited by 4 other HighWire hosted articles:

A model of thalamocortical relay cells
P. A Rhodes and R. Llinas
J. Physiol., June 15, 2005; 565 (3): 765-781.
[Abstract] [Full Text] [PDF]

Functional Characterization and Neuronal Modeling of the Effects of Childhood Absence Epilepsy Variants of CACNA1H, a T-Type Calcium Channel
I. Vitko, Y. Chen, J. M. Arias, Y. Shen, X.-R. Wu and E. Perez-Reyes
J. Neurosci., May 11, 2005; 25 (19): 4844-4855.
[Abstract] [Full Text] [PDF]

Reverberation, storage, and postsynaptic propagation of memories during sleep
S. Ribeiro and M. A.L. Nicolelis
Learn. Mem., November 1, 2004; 11 (6): 686-696.
[Abstract] [Full Text] [PDF]

Neuronal Oscillations in Cortical Networks
G. Buzsaki and A. Draguhn
Science, June 25, 2004; 304 (5679): 1926-1929.
[Abstract] [Full Text] [PDF]

Medline items on this article's topics can be found at http://highwire.stanford.edu/lists/artbytopic.dtl
on the following topics:
Physiology .. Sleep
Physiology .. Slow-Wave Sleep
Neuroscience .. Central Nervous System
Neuroscience .. Thalamus
Neuroscience .. Seizures

Updated information and services including high-resolution figures, can be found at:
http://physrev.physiology.org/cgi/content/full/83/4/1401

Additional material and information about *Physiological Reviews* can be found at:
http://www.the-aps.org/publications/prv

This information is current as of August 1, 2005 .

Interactions Between Membrane Conductances Underlying Thalamocortical Slow-Wave Oscillations

A. DESTEXHE AND T. J. SEJNOWSKI

Unité de Neurosciences Intégratives et Computationnelles, Centre National de la Recherche Scientifique,
Gif-sur-Yvette, France; Howard Hughes Medical Institute and the Salk Institute; Department of Biology,
University of California at San Diego, La Jolla, California

Destexhe, A., and T. J. Sejnowski. Interactions Between Membrane Conductances Underlying Thalamocortical Slow-Wave Oscillations. *Physiol Rev* 83: 1401–1453, 2003; 10.1152/physrev.00012.2003.—Neurons of the central nervous system display a broad spectrum of intrinsic electrophysiological properties that are absent in the traditional "integrate-and-fire" model. A network of neurons with these properties interacting through synaptic receptors with many time scales can produce complex patterns of activity that cannot be intuitively predicted. Computational methods, tightly linked to experimental data, provide insights into the dynamics of neural networks. We review this approach for the case of bursting neurons of the thalamus, with a focus on thalamic and thalamocortical slow-wave oscillations. At the single-cell level, intrinsic bursting or oscillations can be explained by interactions between calcium- and voltage-dependent channels. At the network level, the genesis of oscillations, their initiation, propagation, termination, and large-scale synchrony can be explained by interactions between neurons with a variety of intrinsic cellular properties through different types of synaptic receptors. These interactions can be altered by neuromodulators, which can dramatically shift the large-scale behavior of the network, and can also be disrupted in many ways, resulting in pathological patterns of activity, such as seizures. We suggest a coherent framework that accounts for a large body of experimental data at the ion-channel, single-cell, and network levels. This framework suggests physiological roles for the highly synchronized oscillations of slow-wave sleep.

Physiological Reviews

I. INTRODUCTION

A. Brain Rhythms

The rhythmic nature of electrical activity in the brain was first discovered in electroencephalographic (EEG) recordings from the scalp by Caton in 1875, and later by Berger in humans (25). They observed that the frequency and amplitude of the oscillations vary widely across different behavioral states. Awake and attentive states are characterized by low-amplitude, high-frequency EEG activity, with significant power in the beta (20–30 Hz) and gamma (30–80 Hz) frequency bands. Large-amplitude alpha rhythms (8–12 Hz) appear mostly in occipital cortex in aroused states with eyes closed and are reduced with eyes open (25). The early stages of sleep are characterized by spindle waves (7–14 Hz), which consist of short bursts of oscillations lasting a few seconds and displaying a typical waxing-and-waning appearance. When sleep deepens, slow-wave complexes, such as delta (1–4 Hz) and slower waves (~1 Hz), progressively dominate the EEG. Slow-wave sleep is interrupted by periods of rapid-eye-movement (REM) sleep, during which the EEG activity has a low amplitude and high frequencies, similar to that during arousal. Finally, the cortex participates in several forms of epileptic seizures, such as the 3-Hz "spike-and-wave" complexes (241).

B. The Building Blocks of EEG Rhythms

The earliest explanation for the EEG rhythmicity was the "circus movement theory" proposed by Rothberger in 1931 (cited in Ref. 38). According to this theory, the rhythms are due to action potentials traveling along chains of interconnected neurons. The period of the rhythmicity corresponded to the time needed for a volley of action potentials to traverse a loop in the chain. Inspired by the circus movement theory, Bishop (28) proposed the concept of "thalamocortical reverberating circuits," in which the rhythmicity was generated by action potentials traveling back and forth between thalamus and cortex. Although the reverberating circuit theory remained prevalent for several years, subsequent experiments demonstrated that the EEG activity is not generated by action potentials (260), invalidating a fundamental premise of the circus movement theory.

An alternative proposal by Bremer (38–40) suggested instead that brain rhythms reflect the autorhythmic properties of cortical neurons and that the EEG is generated by nonpropagated potentials, in analogy with the electrotonic potentials in the spinal cord (33). Bremer (39) also proposed that cortical oscillations should depend on the "excitability cycle" of cortical neurons. He emphasized that cortical neurons are endowed with intrinsic properties that participate in rhythm generation and that brain rhythms should not be described as the passive driving of the cerebral cortex by impulses originating from pacemakers (37, 40). Bremer's proposal for the genesis of EEG rhythmicities rested on four core ideas: *1*) the EEG rhythmicity is generated by the oscillatory activity of cortical neurons; *2*) the genesis of these oscillations depends on properties intrinsic to cortical neurons; *3*) EEG oscillations are generated by the synchronization of oscillatory activity in large assemblies of cortical neurons; and *4*) the mechanisms responsible for synchronization are due to intracortical excitatory connections. Most of these assumptions have been validated, and the modern view of EEG genesis is largely based on these principles (see below).

Experiments on motoneurons in the spinal cord (110) provided convincing evidence that the EEG reflects summated postsynaptic potentials. To explain the slow time course of EEG waves, Eccles (110) postulated that distal dendritic potentials, and their slow electrotonic propagation to soma, participate in the genesis of the EEG. This assumption was confirmed by intracellular recordings from cortical neurons, which demonstrated a close correspondence between the EEG and synaptic potentials (68, 69, 184). This view of the genesis of the EEG is still widely held (243).

C. Interaction Between Intrinsic and Synaptic Conductances

Spinal motoneurons integrate synaptic activity and, when a threshold membrane potential is reached, emit an action potential that is followed by a prolonged hyperpolarization (43, 110). This led to an early model of the neuron based on the concept of "integrate and fire" followed by a reset. Early views about activity in other parts of the central nervous system, particularly the cerebral cortex, were strongly influenced by studies of motoneurons, and brain activity was thought to arise by interactions between similar neurons connected in different ways. In this "connectionist" view, the function of a brain area was determined primarily by its pattern of connectivity (110).

Studies on invertebrates during the 1970s revealed that neurons are endowed with complex intrinsic firing properties that depart from the traditional integrate-and-fire model (2, 55–57, 176). Further evidence against the integrate-and-fire view came from studies of small invertebrate ganglia showing that connectivity was insufficient by itself to specify function (126, 274) and that the modulation of intrinsic properties needed to be taken into account (146). The generality of these results was con-

firmed in intracellular recordings from vertebrate slice preparations (6, 171, 172, 204–207), which revealed that central neurons also have complex intrinsic properties (202).

The nonlinear interactions between ionic conductances are complex. Computational models can make a significant contribution in linking the microscopic properties of ion channels and cellular behavior. This approach was used by Hodgkin and Huxley (157) to understand the genesis of action potentials, and essentially the same approach has been used in modeling studies to understand the complex behavior of central neurons. Perhaps the best characterized neurons in the vertebrate brain are those in the thalamus, which we review here (see sect. II).

In addition to having complex intrinsic properties, neurons also interact in various ways, including chemical synaptic transmission, electrical coupling through gap junctions, and ephaptic interactions through electric fields. Whole cell and patch-clamp recording techniques (264) have been used to investigate the detailed mechanisms underlying the conductances of ionic channels involved in synaptic transmission. An extraordinarily rich variety of dynamic properties of synaptic interactions between central neurons has been uncovered on a wide range of time scales. Many neurotransmitters and receptor types have been identified in the thalamocortical system (222), each of which confers characteristic temporal properties to synaptic interactions. The properties of the main receptor types mediating synaptic interactions are now well understood.

It is now well accepted that rhythmicity arises from both intrinsic and synaptic properties (106b, 310, 312). Some neurons generate oscillations through intrinsic properties and interact with other types of neurons through multiple types of synaptic receptors. These complex interactions generate large-scale coherent oscillations. Understanding how the interactions between ionic conductances can generate rhythms is difficult, and computational models can help in exploring the underlying mechanisms. This review shows how this approach has been used to understand how the interplay between intrinsic and synaptic conductances generate oscillations at the network level (see sect. III).

D. Thalamocortical Loops

We focus here on two types of rhythms: spindle oscillations and absence seizures, both of which are generated in the thalamocortical system schematized in Figure 1. Sensory inputs from visual, auditory, and somatosensory receptors do not reach the cerebral cortex directly, but synapse first on thalamocortical (TC) relay
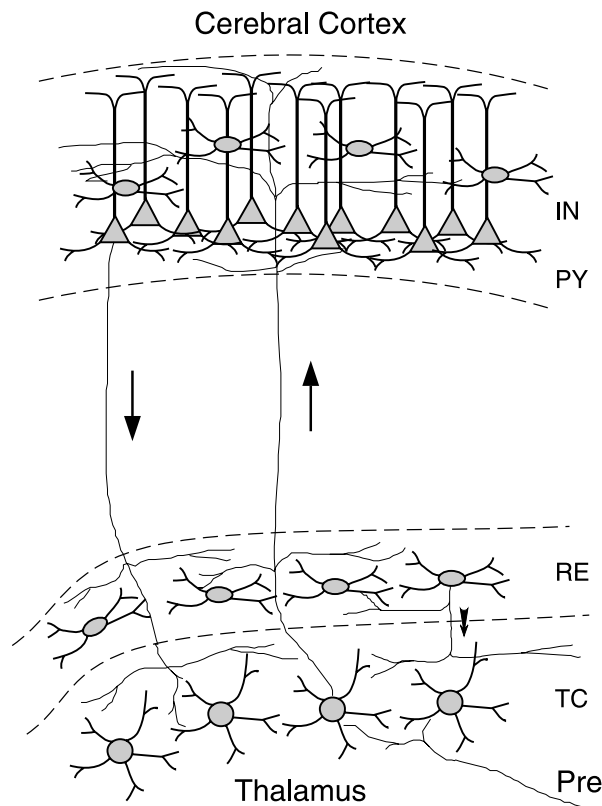

FIG. 1. Arrangement of inputs and output projections in the thalamocortical system. Four cell types and their connectivity are shown: thalamocortical (TC) relay cells, thalamic reticular (RE) neuron, cortical pyramidal cells (PY), and interneurons (IN). TC cells receive prethalamic (Pre) afferent connections, which may be sensory afferents in the case of specific thalamic nuclei involved in vision, audition, and somatosensory modalities. This information is relayed to the corresponding area of cerebral cortex through ascending thalamocortical fibers (upward arrow). These axons have collaterals that contact the RE nucleus on the way to the cerebral cortex, where they arborize in superficial layers I and II, layer IV, and layer VI. Corticothalamic feedback is mediated primarily by a population of layer VI PY neurons that project to the thalamus. The corticothalamic fibers (downward arrow) also leave collaterals within the RE nucleus and dorsal thalamus. RE cells thus form an inhibitory network that surrounds the thalamus, receive a copy of nearly all thalamocortical and corticothalamic activity, and project inhibitory connections solely to neurons in the thalamic relay nuclei. Projections between TC, RE, and PY cells are usually organized topographically such that each cortical column is associated with a given sector of thalamic TC and RE cells. [Modified from Destexhe et al. (100).]

cells in specific regions of the thalamus. These relay cells in turn project to their respective area in primary sensory cortex. These topographically organized forward projections are matched by feedback projections from layer 6 of cortex to the corresponding afferent thalamic nucleus (174, 278).

Within the thalamus, there are reciprocal connections between TC and thalamic reticular (RE) neurons. The RE cells are GABAergic and send their projections exclusively to relay nuclei, but they also receive excitatory collaterals from both ascending (thalamocortical)

and descending (corticothalamic) fibers. Thalamocortical loops therefore include both bidirectional excitatory interactions between the cortex and thalamus and inhibition through the collaterals of ascending and descending fibers to GABAergic neurons. These inhibitory interactions are needed to explain the large-scale synchrony of thalamocortical oscillations (see sect. IV).

Several types of brain rhythms originate in the thalamocortical system. Spindle waves are by far the best understood type of rhythmicity in this system, in part because they can be enhanced by anesthetics such as barbiturates (8, 81). The thalamic origin of spindles was first suggested by Bishop (28), who observed the suppression of rhythmic activity in the cortex after sectioning connections with the thalamus and was confirmed in experiments on decorticated animals (3, 234). The cellular events underlying this rhythmic activity have been identified in vivo (305, 310) and in isolated thalamic slices in vitro (346). The biophysical mechanisms underlying spindle rhythmicity were uncovered in slice preparations, particularly the voltage-dependent conductances and receptor types involved. Theories for the genesis and termination of spindle oscillations need to be rigorously tested.

Absence seizures also originate in the thalamocortical system. Because they are generalized and involve large-scale synchrony, Jasper and Kershman (173) suggested that they may have foci in thalamic nuclei that widely project to cortex. This hypothesis was supported by chronic recordings during absence seizures in humans, showing that signs of a seizure were observed first in the thalamus before appearing in the cortex (360; but see Ref. 240). Experimental models of absence seizures, such as the penicillin model in cats (256), showed that although the thalamus is critical for generating seizures, it was not sufficient to explain all of their properties. Seizures can be obtained from injection of convulsants limited to cerebral cortex, but not when the same drugs are injected into the thalamus (130, 258, 302). It is now clear that both the thalamus and the cortex are necessary partners in these experimental models of absence seizures, but the exact mechanisms are unknown (74, 129). Computational models can help identify the critical parameters involved in the genesis of pathological behavior, as well as suggest ways to resolve apparently inconsistent experimental observations, as explored in section IV.

Despite progress in understanding how the EEG is generated, the possible significance of brain oscillations for the large-scale organization of information processing in the brain remains a mystery. After summarizing current knowledge of the mechanisms that generate spindle oscillations, absence seizures, and other types of thalamocortical oscillations, we explore possible functions for these rhythms (see sect. IVC) suggested by the computational models.

II. SINGLE-CELL PACEMAKERS: OSCILLATIONS AND BURSTS EMERGING FROM THE INTERPLAY OF INTRINSIC CONDUCTANCES IN SINGLE NEURONS

We first review how interactions between conductances within a single cell can generate phenomena like bursting or intrinsic oscillations, and how these properties are tuned by calcium and neuromodulators. We examine these mechanisms through computational models constrained by experimental data.

A. Thalamic Relay Cells

1. Rebound bursts in thalamic relay cells

In addition to relaying sensory input to cortex, TC neurons have intrinsic properties that allow them to generate activity endogenously. Following inhibition, these cells can under some circumstances produce bursts of action potentials, called a "low-threshold spike" (LTS) or "postinhibitory rebound." The importance of the rebound response of TC cells was first established by Andersen and Eccles (9), who called it "postanodal exaltation." It was later characterized in vitro by Llinás and Jahnsen (209) and in vivo by Deschênes et al. (84) and has become generally known as the "rebound burst" or LTS. Andersen and Eccles (9) were the first to show that TC cells display bursts of action potentials tightly correlated with the offset of inhibitory postsynaptic potentials (IPSPs).

In vitro studies (209, 171) demonstrated that TC cells possess two different firing modes. In the "tonic" mode, near the resting membrane potential (approximately -60 mV), the relay neuron fires trains of action potentials at a frequency proportional to the amplitude of the injected current (Fig. 2A, *left panel*). This is similar to the response of many other neurons and is explained by the voltage-dependent Na$^+$ and K$^+$ currents that generate action potentials. In contrast, at hyperpolarized membrane potentials, thalamic neurons can enter a "burst mode" (Fig. 2A, *right panel*), firing high-frequency bursts of action potentials ($\sim$300 Hz) at the offset of hyperpolarizing current injection. A burst can also occur following a strong IPSP, which provides hyperpolarization and return to rest similar to the conditions simulated by current injection. The response of a neuron to a depolarizing current injection depends on its previous state, producing a steady low-frequency firing rate if injected at a depolarized level, but eliciting a burst followed by a long afterhyperpolarization if injected in a sufficiently hyperpolarized state.

The ionic mechanism underlying the "low-threshold" behavior of thalamic neurons is a slow, low-threshold Ca^{2+} current (171, 172), which was characterized in voltage-clamp experiments (67, 71, 148, 319). This current is
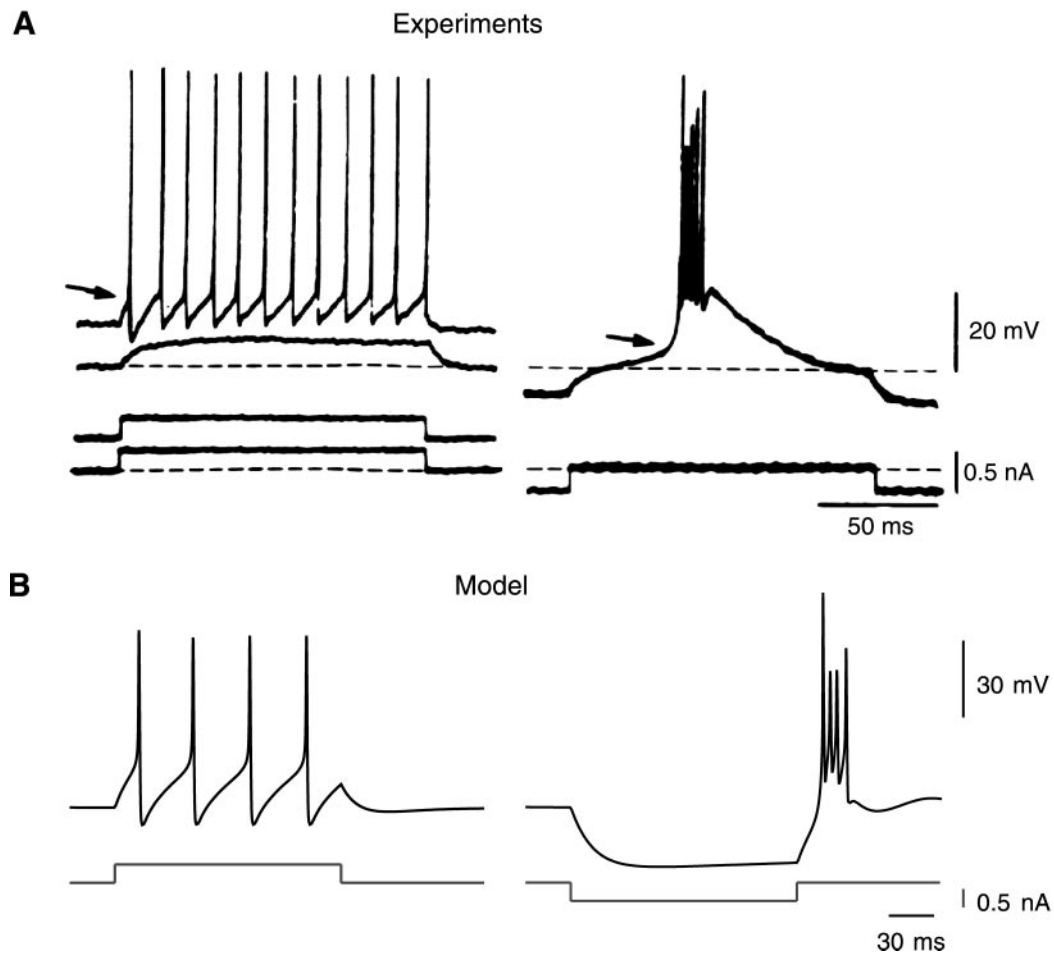
A Experiments

B Model

FIG. 2. Intrinsic electrophysiological properties of thalamic relay neurons. *A*: intracellular recordings of guinea pig thalamic relay neurons in vitro. *Left*: a depolarization that is subthreshold at resting level (*bottom trace*) produced repetitive firing if delivered at a depolarized direct-current (DC) level (*top trace*). *Right*: when the same stimulus was given at a hyperpolarized DC level, the cell produced high-frequency bursts of action potentials. [Modified from Llinas and Jahnen (209).] *B*. computational model. Tonic and burst responses were obtained in a single-compartment model including various voltage-dependent currents, such as I_T and the I_{Na} and I_{Kd} currents for generating action potentials. Tonic and burst responses could be obtained either by various stimuli at the same membrane voltage (*left*) or by the same stimulus applied at different membrane potential levels (*right*). [Modified from McCormick and Huguenard (225).]

carried by low-voltage activated Ca^{2+} channels described previously (49, 50) and later called "T-type" Ca^{2+} channels (242). Cloning of the T-type channels revealed several distinct subunits, which may account for functional difference according to the type of subunit assembling the channel (192). Like the Na^+ current described by Hodgkin and Huxley (157), the T current (I_T) of thalamic neurons is transient and shows activation followed by inactivation. However, the voltage range over which I_T activates is close to the resting potential, in contrast to the Na^+ current, which activates at more depolarized levels. The kinetics of I_T are considerably slower than the Na^+ current. A voltage-clamp characterization of the I_T in thalamic cells performed in dissociated TC cells by Huguenard and Prince (163) provided the quantitative data on

the kinetics of activation and inactivation of this current used in the computational models below.

2. Models of the rebound burst and the role of dendrites

Hodgkin and Huxley (157) introduced computational models to determine whether the ionic mechanisms identified in their voltage-clamp measurements were sufficient to account for the generation of the action potential. The same approach was taken to study the genesis of bursting behavior. Hodgkin-Huxley-type models of TC neurons were first introduced by McMullen and Ly (230) and Rose and Hindmarsh (262) based on the experiments of Jahnsen and Llinás (171). The more recent characterization of the I_T by voltage-clamp methods (see above) pro-

vided precise measurements for the time constants and steady-state values of activation and inactivation processes. Several Hodgkin-Huxley-type models based on voltage-clamp data replicate the rebound-burst properties of TC cells (95, 96, 106, 162, 214, 225, 332, 352, 356). The most salient features of the rebound burst can be reproduced by single-compartment models containing Na^+, K^+, and T-type currents described by Hodgkin-Huxley-type kinetics (Fig. 2B). Simplified "integrate-fire and burst" models have also successfully reproduced the most salient features of TC cells bursts (284). However, to reproduce all the features of the rebound burst in TC cells, the I_T must be concentrated in the dendrites, where a large number of synaptic terminals are located (174, 197).

Imaging experiments clearly show dendritic calcium signals during bursts in TC cells (238, 373), consistent with results from current-clamp and voltage-clamp experiments (106, 371). The dendritic localization of the I_T was shown by direct measurements of channel activity in dendrites (361). To estimate the I_T density in dendrites, a TC neuron was recorded in slices of the ventrobasal thalamus (163), stained with biocytin, and reconstructed using a computerized camera lucida (106). Two sets of data were used to constrain the amount of calcium current in dendrites. First, recordings of the I_T were made from dissociated TC cells (163), which lack most of the dendritic structure and are electrotonically compact, therefore minimizing voltage-clamp errors. These recordings were then compared with voltage-clamp measurements of the I_T in intact TC cells, which were ~5–14 times larger than in dissociated cells (106).

Models based on the reconstructed dendritic morphology of TC cells were used to explore the consequences of varying the density of the current in the different dendritic and somatic regions (106). The low amplitude of I_T in dissociated cells could be reconciled with the high-amplitude currents observed in intact cells if the concentration of T-type calcium channels was 4.5–7.6 times higher in the dendrites than in the soma (106). The same density gradient of calcium channels in the model also reproduced the bursts of spikes evoked in the current-clamp protocols (106). Similar findings were reported in another modeling study (12), which predicted that the dendrites of TC cells must contain the I_T (in addition to delayed-rectifier K^+ current I_{Kd}). This was needed for the model to generate tonic or burst firing with the correct voltage-dependent behavior and oscillations (12).

The predicted high densities of T-type calcium channels in the dendrites of TC cells were confirmed by direct measurements of channel activity using cell-attached recordings (361). The density was, however, not uniform, but was concentrated mostly in stem dendrites up to 40 μm from the soma, while distal dendrites had low T-

channel densities. The results based on this type of distribution were equivalent to those based on the distribution of I_T density discussed above.[1] Thus it is essential that most of the T channels are dendritic, but how they are distributed within the dendrites is not critical. A similar conclusion about dendritic currents was reached in a model of delta oscillations in TC cells (113).

The localization of dendritic calcium currents in dendrites has several functional consequences. First, the presence of the calcium current at the same sites as inhibitory synapses is likely to enhance the rebound responses of TC cells (106c). Second, the shunting effects of tonic excitatory cortical synapses and inhibitory synapses on burst generation would be more effective if the I_T were dendritic (106). As a consequence, the activity of corticothalamic synapses can counteract bursting, and rapidly switch the TC neuron from the burst mode (cortical synapses silent) to the tonic mode (sustained cortical drive). Local dendritic interactions thus allow corticothalamic feedback to potentially control the state of thalamic neurons on a millisecond time scale compared with conventional neuromodulatory mechanisms, which operate over hundreds of milliseconds (222).

3. Bursts in awake animals

The TC cells in the thalamus generate powerful synchronized bursts of action potentials during sleep; in comparison, the activity in alert animals is dominated by single-spike (tonic) firing (201, 309). There is, however, evidence for the presence of bursts in the thalamus of awake animals (142, 143, 278). These thalamic bursts may represent a special type of information in alert states, such as novelty detection (278). However, the occurrence of bursts is rare in the thalamus of aroused animals and may instead signify that the animal is drowsy (296); this possibility is supported by observations that thalamic bursts are negatively correlated with attention (357).

The occurrence of bursts as a rebound to inhibition during oscillatory states similar to sleep oscillations (9, 305, 312) has been intensively studied with computational models (reviewed in Ref. 106b), but bursts following excitatory inputs have not been as well studied (106c). Excitatory stimulation by sensory synapses was modeled by a constant density of glutamatergic (AMPA) synapses on proximal TC dendrites (174, 197), up to 40 μm from the soma. The threshold for action potential generation was

---

[1] All the conclusions of the model with high uniform density of I_T in dendrites (1.7×10^{-5} cm/s in soma and 8.5×10^{-5} cm/s in dendrites; Ref. 106) could be obtained using a nonuniform distribution of T channels (10.3×10^{-5} cm/s in soma, 20.6×10^{-5} cm/s in proximal dendrites <40 μm from soma, and 2.5×10^{-5} cm/s elsewhere), similar to the pattern estimated by Williams and Stuart (361).

estimated by increasing the conductance of this synapse and, as expected, when the cell was hyperpolarized (less than -65 mV), the synaptic stimulus could evoke bursts of action potentials. At more depolarized resting values (more than -65 mV), excitatory stimuli evoked tonic firing. In control conditions, the region of membrane potential corresponding to the burst mode was large, and the minimal excitatory postsynaptic potential (EPSP) amplitude to evoke a burst was about 0.035 μS (106c), which represents $\sim$230–350 simultaneously releasing glutamatergic synapses, based on an estimated quantal amplitude of 100–150 pS (246, 247). Models therefore predict that an excitatory stimulus should efficiently evoke bursts only when the TC cell is in the right range of membrane potentials.

In contrast, when the membrane of model TC cells was more leaky, as occurs during tonic activity of the network in vivo, the burst region narrowed, and there was a large range of stimulus amplitudes for which the only possible spike output was the tonic mode (106c). Under these conditions, the minimal EPSP amplitude needed to evoke bursts was $\sim$0.09 μS, which corresponds to $\sim$600–900 simultaneously releasing synapses. In the visual thalamus, the evoked conductance from a single retinal afferent is 0.6–3.4 nS (1.7 nS on average), which represents from 4 to 27 quantal events (246). This suggests that the simultaneous release of all terminal sites from 8 to 87 retinal axons are required to evoke bursts in relay cells (from 22 to 220 under in vivo conditions). However, one morphological study reported that a single retinal axon can make a large number of synaptic terminals onto the same relay neuron, forming a significant proportion of all of its retinal synapses (145). It is therefore possible that the convergence of a relatively small number of afferent axons could evoke bursts, which would support the notion that bursts are easily triggered by afferent excitatory synapses. More precise measurements of the number of synaptic terminals from single axons are needed to determine the convergence of afferent activity needed to trigger bursts in relay cells.

Models of TC neurons based on reconstructed morphologies and dendritic I_T therefore suggest that sensory-initiated bursts are possible, but they require a large convergence of excitatory stimuli and are more likely to occur under conditions of low activity. This is consistent with the view that in burst mode the thalamus strongly filters afferent information (223). This also supports the view that bursts may be a "wake-up call" signal during drowsiness or inattentive states (278), although it is not clear how the cortex would distinguish these "wake-up" bursts from bursts occurring spontaneously (or in an oscillation) during states of low vigilance.

4. Intrinsic oscillations in thalamic relay cells

In addition to displaying burst and tonic modes, TC cells can also generate sustained oscillations. In experiments performed in cats in vivo, TC cells generated oscillations in the delta frequency range (0.5–4 Hz) after removal of the cortex (73). Oscillations in the same frequency range were also observed in TC cells in vitro (190, 191, 226). These intrinsic slow oscillations consisted of rebound bursts recurring periodically and have been also called "pacemaker oscillations" (190, 191). These slow oscillations were resistant to tetrodotoxin, suggesting that they were generated by mechanisms intrinsic to the TC cell.

The intrinsic delta oscillations depend on the membrane potential (226). Oscillations were only possible if TC cells were maintained at relatively hyperpolarized potentials, within the range of the burst mode, suggesting that the I_T actively participated in its generation. Another property, illustrated in Figure 3A, is that these oscillations disappeared following blockade of another current, called I_h (226) with Cs^+. I_h is a mixed Na^+/K^+ cation current responsible for anomalous rectification in TC cells (253). In voltage-clamp, I_h is activated by hyperpolarization in the subthreshold range of potentials (226, 290). These data indicate that intrinsic oscillations in TC cells are generated by an interplay between I_T and I_h.

5. Models of the conductance interplay to generate intrinsic oscillations

Several computational models have shown that the interaction between I_h and I_T can account for the genesis of low-frequency oscillations in TC cells (91, 95, 96, 214, 217, 225, 332, 352). In addition to I_T (see above), these models included Hodgkin-Huxley-type models of I_h based on voltage-clamp data obtained in TC cells. Several types of models have been used for this current, beginning with simple one-variable models based on a single activation gate (96, 214, 217, 225, 332, 352). This class of models only has one gate and cannot account for the observation that the I_h activates slowly, with a time constant greater than 1 s at 36°C (226, 290), but deactivates faster (114, 125, 175, 335, 340). A model with a dual gating process, combining fast and slow activation gates, can reproduce the voltage-clamp behavior of I_h in detail (91, 95).

Although both types of models of I_h gave rise to slow oscillations when I_h is combined with I_T, the double-activation model generated more complex oscillatory patterns, such as waxing-and-waning oscillations (see below). Figure 3B illustrates the oscillations generated by a single-compartment model of a TC cell comprising I_T and I_h, as well as I_{Na}/I_K responsible for action potentials. Examination of I_T and I_h conductances during the oscillation revealed that the activation of I_h depolarizes the
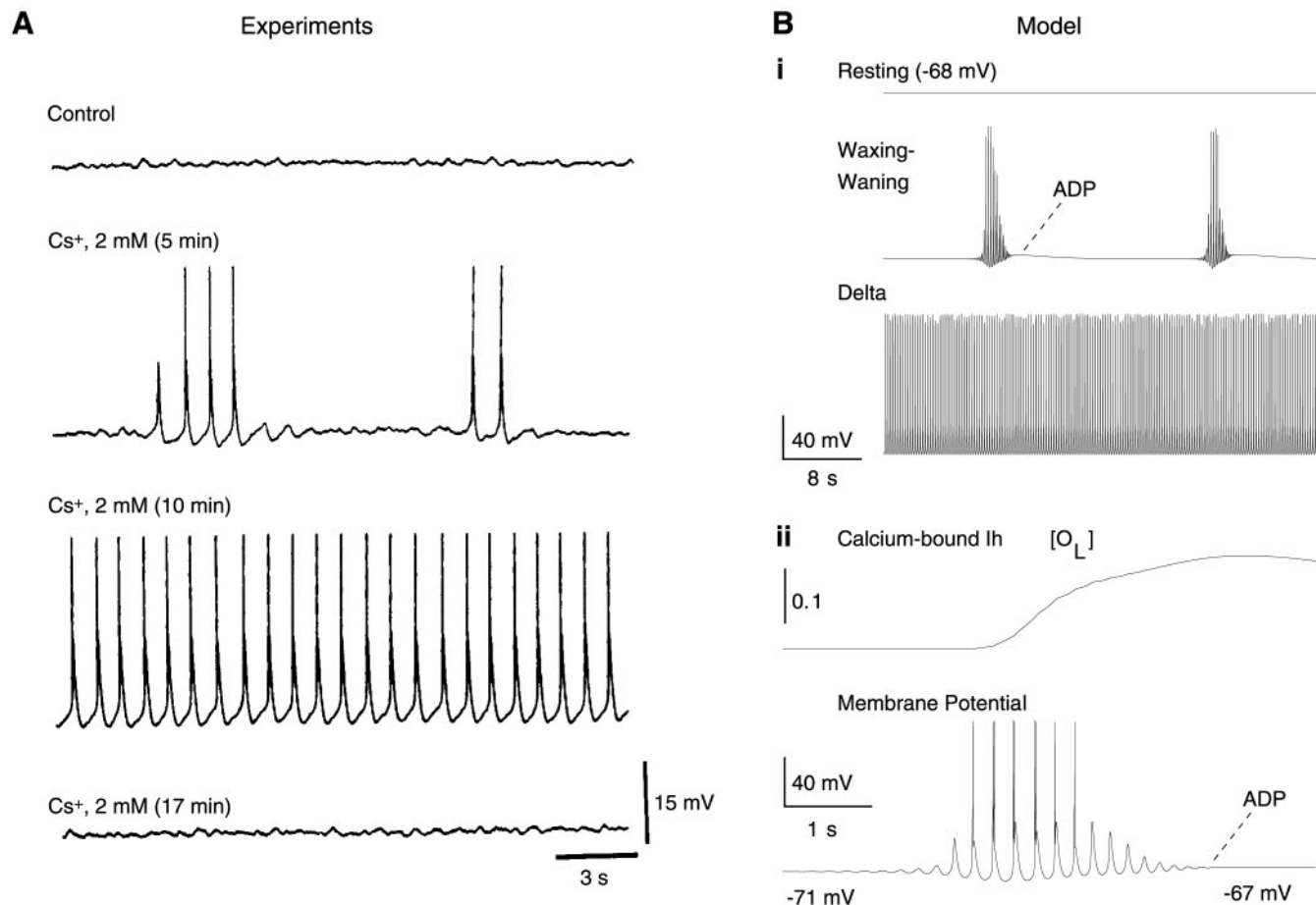
FIG. 3. Intrinsic oscillatory properties of thalamic relay neurons. *A*: intracellular recordings of a cat thalamic relay neuron in vitro showing different oscillatory modes following application of cesium (Cs^+). Cs^+ was applied extracellularly to a cell that had no spontaneous oscillations (control). Four minutes after the application of Cs^+, spontaneous waxing-and-waning oscillations began (silent periods of 4–9 s and oscillatory sequences lasting for 2–6 s). After an additional 4 min, the oscillations became sustained (frequency of 1–2 Hz) and persisted for ~6 min before all activity ceased. [Modified from Soltesz et al. (290).] *B*: computational model of intrinsic oscillations in thalamic relay cells. The model had a calcium-mediated regulation of I_h. *i*: Three different modes with different conductance values of I_h. From *top* to *bottom*: relay state ($g_h = 0.025$ mS/cm^2), slow waxing-and-waning ("spindle-like") oscillations ($g_h = 0.02$ mS/cm^2), and delta oscillations ($g_h = 0.005$ mS/cm^2). *ii*: Intrinsic waxing-and-waning oscillation at higher time resolution. *Top trace* shows the fraction of channels in the calcium-bound open state (O_L), and the membrane potential is shown at *bottom*. [Modified from Destexhe et al. (96).]

membrane slowly until a LTS is generated by activation of I_T. During the depolarization provided by the LTS, I_h deactivates, and together with the termination of the LTS the membrane becomes hyperpolarized. This hyperpolarization allows I_T to deinactivate to prepare for the next LTS, and as I_h slowly activates, the cycle restarts. The same mechanism has been explored, with minor variations, in several modeling studies that used different models of I_T and I_h (91, 95, 96, 152, 214, 217, 225, 332, 352), suggesting that the interplay between I_T and I_h is a highly robust way to generate slow oscillations. This conclusion is also supported by a dynamic-clamp study showing that delta oscillations are lost in TC cells if I_h is blocked, but can be restored by injection of a computer-generated I_h conductance (161).

6. Waxing-and-waning oscillations

The slow intrinsic oscillations generated by TC cells can be modulated by different factors. Cat TC cells studied in a low-Mg^{2+} medium in vitro displayed either a resting state, sustained slow oscillations, or intermittent "waxing-and-waning" oscillations (190, 191) (second trace in Fig. 3*A*). The latter consisted of an alternation between periods of oscillation (0.5–3.2 Hz), lasting 1–28 s, with periods of silence, lasting 5–25 s, during which the membrane progressively hyperpolarized. The waxing-and-waning envelope was resistant to tetrodotoxin (191), suggesting mechanisms intrinsic to the TC neuron. In analogy with the waxing and waning of spindles observed in vivo, they have also been called "spindlelike oscillations" (190,

191). However, in vivo spindles oscillate at a higher frequency (7–14 Hz) and depend on interactions with neurons of the thalamic reticular nucleus (see sect. IIIC), which distinguishes them from the waxing-and-waning oscillations intrinsic to TC cells.

The pharmacology of intrinsic waxing-and-waning oscillations was investigated by Soltesz et al. (290), who found that they were dependent on I_h. Slow delta-like oscillations and waxing-and-waning oscillations can be observed in the same TC cell by altering I_h (290) (Fig. 3A). Increasing the amplitude of I_h by norepinephrine can transform delta-like oscillations into waxing-and-waning oscillations; application of Cs^+, an I_h blocker, transforms the depolarized state into waxing-and-waning oscillations, the delta-like oscillations, and finally a hyperpolarized resting state (290) (Fig. 3A). In addition, the intrinsic waxing-and-waning oscillations can be transformed into sustained slow delta-like oscillations by applying a depolarizing current (190, 191).

7. Models of waxing-and-waning oscillations

Several ionic mechanisms for generating waxing-and-waning oscillations have been suggested. The first model (95) was inspired by experiments on the I_h current in heart cells demonstrating regulation of I_h by intracellular Ca^{2+} (144). The steady-state activation of I_h is dependent on the intracellular Ca^{2+} concentration ($[Ca^{2+}]_i$), shifting toward more positive membrane potentials with increasing $[Ca^{2+}]_i$ (144). Because calmodulin and protein kinase C were not involved in the Ca^{2+} modulation of I_h, Ca^{2+} may affect the I_h channels directly (144), with the binding of Ca^{2+} increasing the conductance of I_h, or indirectly through the production of cAMP (213). Different variants of calcium-dependent regulation of I_h have been proposed (72, 85, 222).

The modulation of I_h by Ca^{2+} was studied in several bursting models of the TC cells. The simplest model was based on the assumption that Ca^{2+} bind directly to the open state of the channel, thereby "locking" I_h into the open configuration and shifting its voltage dependence as observed experimentally (95). Calcium upregulation was also proposed to occur according to a model in which the calcium indirectly affects the I_h channel through an intermediate messenger, which itself binds to the open state of I_h channels (96). Another ionic mechanism for waning has been proposed (350) based on activity-dependent adenosine production, which affects the voltage dependence of I_h but in the opposite direction (244). Waxing-and-waning oscillations were also modeled by the interaction between I_T, I_h, and a slow potassium current (91, 152).

All models generated waxing-and-waning oscillations, but only those based on the upregulation of I_h by Ca^{2+} reproduced the slow periodicity, the slow oscillation frequency, and the progressive hyperpolarization of the membrane during the silent period. Moreover, the Ca^{2+}-dependent models also displayed the correct coexistence of oscillatory and resting states in TC cells, as shown in Figure 3Bi. For fixed I_T conductance, increasing I_h conductance led successively to slow oscillations in the delta range (1–4 Hz), then to waxing-and-waning slow oscillations and, finally, to the relay resting state, consistent with in vitro studies (290) (compare with Fig. 3A). According to this mechanism for waxing-and-waning oscillation (Fig. 3Bii), calcium enters through I_T channels on each burst, resulting in an increase of Ca^{2+} (or Ca^{2+}-bound messenger) and a gradual increase of I_h channels in the open state (O_L). This produces a progressive afterdepolarization (ADP) following each burst until the cell ceases to oscillate (Fig. 3Bii). The membrane then progressively hyperpolarizes during the silent period, as I_h channels unbind the messenger.

The presence of this ADP was observed during waxing-and-waning oscillations in cat TC cells maintained in low magnesium in vitro (191), as well as in ferret thalamic slices (19). It is possible to artificially induce this ADP by evoking repetitive burst discharges in TC cells (19). The ADP is responsible for a marked diminution of input resistance in successive responses (19). These features were observed in a model based on the upregulation of I_h by Ca^{2+} (96).

Recent experiments provide direct evidence for the Ca^{2+}-dependent regulation of I_h channels predicted in modeling studies. Although Ca^{2+} does not directly modulate I_h channels in thalamic neurons (44), experiments with caged Ca^{2+} in thalamic neurons have demonstrated an indirect calcium-dependent modulation of I_h (212), with cAMP acting as the intermediate messenger (213).

B. Thalamic Reticular Neurons

1. Rebound bursts in thalamic reticular cells

RE neurons recorded in awake animals fire tonically, but during slow-wave sleep the activity of these cells changes to rhythmic firing of bursts (307). A typical burst of action potentials in an RE cell during natural sleep shows an accelerando-decelerando pattern of action potentials (Fig. 4A). In intracellular recordings, both modes of firing in RE cells could be elicited, depending on the membrane potential. Depolarizing current pulses from −68 mV produced tonic firing, whereas the same pulse delivered at more hyperpolarized levels elicited a burst. The burst in a model RE cell shows a slowly rising phase and is broader than in TC cells, and there is always an accelerando-decelerando pattern of sodium spikes, typical of RE cells recorded from anesthetized, naturally sleeping animals as well as in animals under different anesthetics (59, 107, 237, 307) (Fig. 4A).

The rebound burst of RE cells studied in vitro (14, 17), like that of TC cells, is mediated by a low-threshold
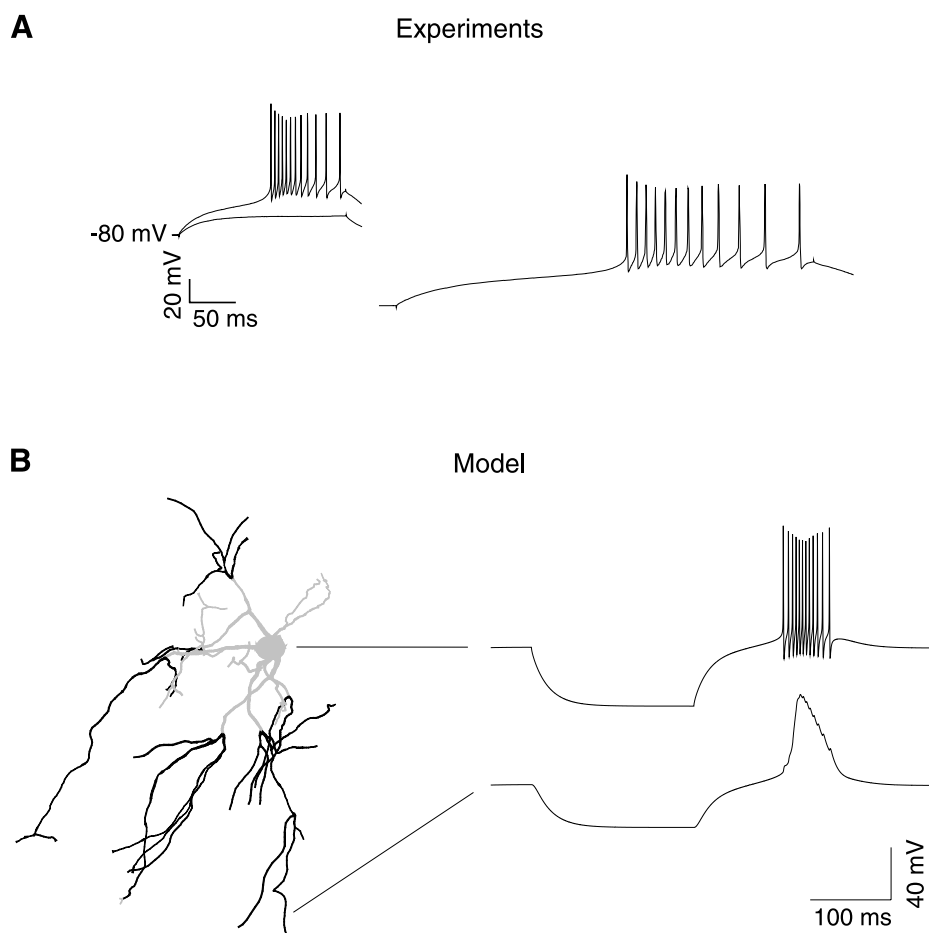
A   Experiments

B   Model

FIG. 4. Bursting properties of thalamic reticular neurons. *A*: bursts evoked in a rat thalamic reticular neuron in vitro. Bursts were obtained after intracellular injection of depolarizing current pulses. A slight change in injected current amplitude resulted in an apparently all-or-none burst response. *Bottom trace* indicates a burst on a 5 times faster time scale. *B*: computational model of burst generation in thalamic reticular neurons with dendritic I_T. *Left*: morphology of a thalamic reticular neuron from rat ventrobasal thalamus, which was reconstructed and incorporated in simulations. The dark areas indicate the dendrites with high density of T-type current (0.045 mS/cm² in soma, 0.6 mS/cm² in distal dendrites). *Right*: burst generated in this model following current injection in the soma (*top trace*; 0.3 nA during 200 ms). The voltage in distal dendrites (*bottom trace*) shows a slow rising and decaying calcium spike mediated by I_{Ts}. In both cases, the bursts had a slow rising phase, and sodium spikes within a burst showed a typical accelerando-decelerando pattern. [Modified from Destexhe et al. (99).]

Ca^{2+} current. However, the characterization of the T-type Ca^{2+} current in RE cells by voltage-clamp methods revealed marked differences with the I_T of TC cells. In RE cells, the kinetics were slower and the activation was less steep and more depolarized than that found in TC cells (163). This current was named "slow I_T", or I_{Ts}. In some preparations, however, the I_T of RE cells appears to be similar to that of TC cells (333). Nevertheless, the observation of two distinct types of T channels is consistent with the differences observed after reconstitution of cloned T channels, which displayed different voltage dependence and kinetics and regional distribution (321). In particular, thalamic relay and reticular neurons express different T-channel subtypes (321), consistent with the electrophysiological differences found between TC and RE neurons (163).

2. Models of the rebound burst in RE cells and the role of dendrites

The properties of burst generation in RE cells were examined in Hodgkin and Huxley (157) types of models derived from voltage-clamp measurements. Early models (90, 355) used a I_T similar to that found in TC cells, based

on the data available at that time (14, 208, 228). More recent characterization of the kinetics of the I_T in RE cells (163) has led to more accurate models of I_{Ts} in these cells (97, 348).

Although single-compartment Hodgkin-Huxley type models were able to account for the genesis of bursts in RE cells, not all features of these bursts were found. For example, the slowly rising phase of the burst, its broad structure, and the accelerando-decelerando pattern of sodium spikes within RE bursts were not apparent (14, 17, 99, 165). Another feature not found in the models was that RE bursts show qualitative differences between preparations: RE cells generate bursts in an all-or-none fashion in vitro (99, 165), but bursts can be activated gradually in vivo (59, 99).

The failure of a Hodgkin-Huxley model to simulate these properties could reflect an incomplete knowledge of the biophysical parameters of the I_T because of errors in voltage-clamp measurements. This is unlikely, however, because these measurements were done in dissociated RE neurons, which are electrotonically compact, and the recordings had high resolution and low error. Another possibility, proposed previously (237), is that because the

I_T of intact cells is located in the dendrites, the electrophysiological behavior recorded in the soma is significantly distorted. This possibility was tested using compartmental models of the dendritic morphology of RE cells (99).

Following a similar approach to that taken with TC cells in section II*A2*, an RE neuron was recorded in the reticular sector of the ventrobasal thalamus in rat thalamic slices (163), stained with biocytin, and reconstructed using a computerized camera lucida (Fig. 4*B*, *left*). Voltage-clamp recordings were also obtained from dissociated RE cells (163), which are mostly devoid of dendrites, and intact RE cells (99). Computational models were then used to estimate how much current density must be located in dendrites to reproduce all the experimental results. The conclusion was that high densities of I_T must be located in dendrites to account for these measurements.

Bursts generated with dendritic I_T are shown in Figure 4*B*. The calcium spike generated in the dendrites slowly injects current into the soma/axon, where action potentials are generated. The slowly rising phase of the burst as well as the accelerando-decelerando pattern result from an interaction between the soma and dendrites and the slow kinetics of the I_T (99). Dendritic I_T also accounts for the broader currents seen in intact RE cells under voltage clamp. Moreover, bursts were all or none under control conditions but were graded in simulations of in vivo conditions when synaptic background activity was included. These features were a direct consequence of dendritic Ca^{2+} currents and were confirmed by presumed intradendritic recordings (see details in Ref. 99).

3. Physiological consequences of dendritic calcium currents

In contrast to TC cells, RE cells are highly noncompact electrotonically. Comparing neurons reconstructed from the same animal, the maximal electrotonic length of TC cells was 0.34 (106), compared with 2.7 in RE neurons (99). Consequently, the dendrites are relatively decoupled from the soma in RE cells, and the dendritic localization of voltage-dependent currents is likely to have significant consequences in these cells.

The first consequence is that the colocalization of dendritic I_T with dendritic GABAergic synapses may enhance the rebound properties of these neurons. RE neurons contact their neighbors through GABAergic axon collaterals (21, 174, 197) or dendro-dendritic GABAergic synapses (83, 252, 368). Intracellular recordings revealed GABAergic IPSPs in RE cells (21, 97, 265, 266, 280, 336, 372), but they are of relatively low amplitude and might not be sufficient to elicit a rebound burst at short latency (338). However, if the I_T is dendritic, IPSPs arising from neighboring RE cells might initiate rebound bursts in localized dendritic regions, without a trace of IPSP in somatic recordings (106c). The possibility that mutual inhibitory interactions between RE cells may generate rebound bursts and oscillatory behavior is considered in section III*B*.

Alternatively, if the dendrites of RE cells at rest are close to the reversal potential of the IPSPs, GABAergic inputs could counteract the initiation of burst discharges by shunting inhibition. In this case, mutual inhibition between RE cells would prevent them from generating large bursts, which may protect the cells from epileptic discharges (see sect. IV*B*). Thus interactions between RE cells will critically depend on the dendritic membrane potential and the reversal potential of IPSPs. The range of possible interactions, and their impact at the network level, is considered in section III*B*.

Dendritic I_T make RE cells exquisitely sensitive to cortical EPSPs. Models have shown that glutamatergic (AMPA) EPSPs, which are subthreshold in the tonic mode, can evoke full-blown bursts of action potentials if the cell is more hyperpolarized (88, 106c). The threshold for burst generation by excitatory synapses was ~0.03 μS and increased to 0.065 μS under in vivo conditions, somewhat less than for relay cells. Given that the quantal conductance of glutamatergic synapses on reticular neurons is ~266 ± 48 pS (137), these threshold values predict a convergence of ~113 excitatory releasing sites in control conditions, and ~244 releasing sites under in vivo conditions. However, for focal or "hot-spot" distributions, the threshold was much lower, 0.007 μS, corresponding to ~26 releasing sites, but it was not possible to evoke bursts under in vivo conditions in this case (106c).

This remarkable sensitivity occurs only if the dendrites contain a high density of I_{Ts}, and if they are hyperpolarized enough to deinactivate the I_T. Consistent with this sensitivity, in vivo recordings show that corticothalamic excitatory volleys are extremely efficient in triggering bursts in RE cells and eliciting oscillations (59, 66). The sensitivity of RE cells to cortical EPSPs is the basis for the "inhibitory dominance" hypothesis (100), according to which cortical influence on the thalamus occurs primarily through the feed-forward inhibitory pathway through RE cells rather than the direct excitatory one onto TC cells and is critical for understanding the large-scale synchrony of oscillations (see sect. IV*A*).

With dendritic localization of I_{Ts}, high levels of synaptic background activity may prevent bursts (88, 99, 106c). This suppression of bursting does not occur in a single compartment model, suggesting that the interaction between the soma with sodium spikes and the dendrites with calcium spikes depends on the level of synaptic background activity. The dendrites of RE cells would "sample" the overall synaptic activity between the thalamus and the cortex and tune the responsiveness of the RE cells according to these inputs. For high levels of back-

ground activity, which occur during tonic activity in the thalamus and cortex, the RE cell does not have a tendency to fire bursts. For lower levels of background activity, or more phasic inputs such as during synchronized sleep, the dendrites would no longer be bombarded in a sustained manner, and bursting behavior would be enhanced. It is possible that this type of interplay of currents in the dendrites acts in concert with neuromodulation to efficiently switch the thalamus between tonic and bursting modes, which may be an efficient way to implement attentional mechanisms controlled by cortical activity (88).

4. Intrinsic oscillations in thalamic reticular cells

In addition to generating bursts, RE cells also participate in oscillations. In intracellular recordings from cat RE cells in vivo (59, 237), rhythmic bursting activity at a frequency of 8–12 Hz occurred either spontaneously or after stimulation of the internal capsule or thalamus. Typically, a depolarizing envelope accompanied this oscillatory behavior and a slow afterhyperpolarization (AHP) following each burst; the termination of the oscillatory sequence was followed by a tonic tail of spike activity (107). The same features were observed in intracellular recordings of RE cells in vitro (14, 17). A rebound sequence of rhythmic bursts could be elicited in RE cells after current injection. In an in vitro study of rodent RE cells (17), this rhythmic behavior was resistant to tetrodotoxin and was, therefore, intrinsic to the cell. The same study also showed that blocking the AHP with apamin, which blocks a class of calcium-activated potassium current [$I_{K(Ca)}$], abolished the rhythmic activity. Rhythmic oscillations in RE cells therefore reflect interactions between the T-type Ca^{2+} current and $I_{K(Ca)}$.

In an in vitro study of spindles in thalamic slices (17), rhythmic oscillations at 7–12 Hz were often followed by a short tonic tail of spikes. Application of TTX revealed an ADP mediated by a nonspecific cation current, activated by intracellular calcium, called I_{CAN}. This current, encountered in many other cell types in the nervous system (245), could underlie the tonic tail of spikes in RE cells (17).

5. Models of the interacting conductances underlying intrinsic oscillations

Several models have been introduced to investigate the repetitive bursting properties of RE cells. All models with I_{Ts}, Ca^{2+}, and $I_{K(Ca)}$ robustly generated oscillations at low frequency (2–4 Hz) (97, 105, 355). These oscillations could be elicited as a rebound rhythmic bursting activity in response to a hyperpolarizing pulse. The 2- to 4-Hz frequency was mainly dependent on the level of the resting potential and on the kinetics of I_{Ts} and $I_{K(Ca)}$. This mechanism was similar to that suggested by current-

clamp experiments (14): following an LTS, Ca^{2+} enters and activates $I_{K(Ca)}$, which then hyperpolarizes the membrane and deinactivates I_{Ts}. When the membrane depolarizes due to the deactivation of $I_{K(Ca)}$, a new LTS is produced and the cycle repeats. The robustness of this mechanism was confirmed in several modeling studies (97, 105, 151, 348, 355).

Despite the ease with which these low-frequency oscillations could be generated, none of the kinetic parameters tested for $I_{K(Ca)}$ was able to produce frequencies in the range 7–14 Hz. The correct oscillations frequencies occurred, however, when the outward current I_{CAN} was included. This current produces a marked ADP after application of tetrodotoxin and apamin (17). In the model (97), such an ADP occurred in the presence of I_{Ts} and I_{CAN} as a rebound following a hyperpolarizing pulse. Simulations of a single compartment containing the combination of currents I_{Ts}, $I_{K(Ca)}$, and I_{CAN} produced a rebound bursting oscillations at 9- to 11-Hz frequencies. The activation of I_{CAN} accelerated the rising phase of the burst and increased the frequency of the rebound burst sequence. The presence of I_{CAN} also terminated the oscillatory behavior by producing a tonic tail of spikes before the membrane returned to its resting level. Varying the conductance of $I_{K(Ca)}$ and I_{CAN} modulated both the frequency and the relative importance of rhythmic bursting relative to tonic tail activity. These results were confirmed in another modeling study (348), in which the same set of conductances was found to produce oscillations and tonic tail activity. In particular, this study reported a similar dependence of the repetitive firing frequency on the membrane potential, with in addition a dependence on the leak K^+ conductance (348).

III. NETWORK PACEMAKERS: OSCILLATIONS THAT DEPEND ON BOTH INTRINSIC AND SYNAPTIC CONDUCTANCES

How the intrinsic neuronal properties reviewed above combine at the network level to generate collective behaviors in a population of neurons is a complex problem. We show here how a combination of experimental data and models was used successfully to investigate this problem. We illustrate how interacting intrinsic and synaptic conductances generate oscillations in circuits of thalamic neurons.

A. Experimental Characterization of Thalamic Oscillations

1. Early experiments

In humans, spindle oscillations are grouped in short 1- to 3-s periods of 7- to 14-Hz oscillations, organized

within a waxing-and-waning envelope, recurring periodically every 10–20 s. These oscillations typically appear during the initial stages of slow-wave sleep (stage II) and later during transitions between REM and slow-wave sleep. In cats and rodents, spindle waves with similar characteristics appear during slow-wave sleep and are typically more prominent at sleep onset. They are enhanced by some anesthetics, such as barbiturates, which, when administered at an appropriate dose, generate an EEG dominated by spindles (8).

Bishop (28) showed that rhythmical activity was suppressed in cerebral cortex following destruction of its connections with the thalamus and suggested that spindles are generated in the thalamus. Bremer (37) showed that rhythmical activity is still present in the white matter after destruction of the cortical mantle. Later, Adrian (3) and Morison and Bassett (234) observed that spindle oscillations persist in the thalamus upon removal of the cortex, providing strong evidence for the genesis of these oscillations in the thalamus. These experiments led to the development of the "thalamic pacemaker" hypothesis (8, 305), according to which rhythmic activity is generated in the thalamus and communicated to the cortex, where it entrains cortical neurons and is responsible for the rhythmical activity observed in the EEG.

Spindles have also been observed in thalamic slices from different preparations. In the ferret visual thalamus, slices that contain the dorsal (lateral geniculate nucleus or LGN) and reticular nuclei (perigeniculate nucleus or PGN) as well as the interconnections between them (346) can display spindles (Fig. 6A). Spindles have also been observed in mouse (351) and rat (170) thalamic slices, as well as in rat thalamocortical slices (322), where they survived in the thalamus following inactivation of the cortex. These in vitro observations are definitive proof that thalamic circuits are capable of endogenously generating spindle oscillations. Moreover, in vitro preparations have made it possible to precisely characterize the ionic mechanisms involved in spindle oscillations, as shown below.

2. Different hypotheses for generating spindles

Based on their intracellular recordings of thalamic neurons during spindles, Andersen and Eccles (9) reported that TC cells fired bursts of action potentials interleaved with IPSPs. They suggested that TC cells fire in response to IPSPs (postinhibitory rebound), which was later demonstrated to be a characteristic electrophysiological feature of thalamic cells (see sect. IIA). In particular, they suggested that the oscillations arose from the reciprocal interactions between TC cells and inhibitory local-circuit interneurons. This mechanism was then in-

corporated into a computational model that provided a phenomenological description of the inhibitory rebound (10) (see also Ref. 210).

Although remarkably forward looking, the mechanism of Andersen and Eccles (9) was not entirely correct. Reciprocal connections between TC cells and thalamic interneurons have not been observed in anatomical studies, but intrathalamic loops of varying complexity have been found between TC cells and the inhibitory neurons of the thalamic RE nucleus, which receive collaterals from corticothalamic and thalamocortical fibers and project to specific and nonspecific thalamic nuclei (269). That "TC-RE" loops could underlie recruitment phenomena and spindle oscillations was suggested by Scheibel and Scheibel (269–271), replacing the interneuron in the "TC-interneuron" loops of Andersen and Eccles with the reticular thalamic neurons. They specifically predicted that the output of the RE nucleus should be inhibitory (271) and that the inhibitory feedback from RE cells onto TC cells should be critical for the genesis of thalamic rhythmicity. This hypothesis was supported by the observation that the pattern of firing of RE neurons was tightly correlated with IPSPs in TC neurons (272, 305, 369).

Subsequent experiments have firmly established the involvement of the RE nucleus in the generation of spindles in cats in vivo (306, 308). First, cortically projecting thalamic nuclei lose their ability to generate spindle oscillations if deprived of input from the RE nucleus (306). Second, the isolated RE nucleus can itself generate rhythmicity in the spindle frequency range (308) (Fig. 5A). In these experiments, the thickest region of the RE nucleus, the rostral pole, was surgically isolated from dorsal thalamic and cortical afferents. This procedure created an isolated "island" of RE cells whose blood supply was preserved and in which the only remaining afferents were fibers from the brain stem and basal forebrain. Extracellular field potentials from the isolated RE nucleus showed rhythmicity in the same frequency range as in the intact thalamus (308) (Fig. 5A). This observation suggested that the RE nucleus is the pacemaker of spindle activity and that oscillations in TC cells were entrained by rhythmic IPSPs from RE cells.

The occurrence of spindle waves in slices (170, 322, 346, 351) (Fig. 6A) confirmed earlier experimental evidence (3, 234) for the genesis of spindles in the thalamus. The spindle waves disappeared after the connections between TC and RE cells were physically cut (346), after application of excitatory amino acid blockers (170, 346, 351), or if TC cells were selectively inactivated (322), consistent with the mechanism based on intrathalamic TC-RE loops proposed by Scheibel and Scheibel (269–271). These in vitro experiments also confirmed the in vivo observation that the input from RE neurons is necessary to generate spindles (306). However, the RE nu-
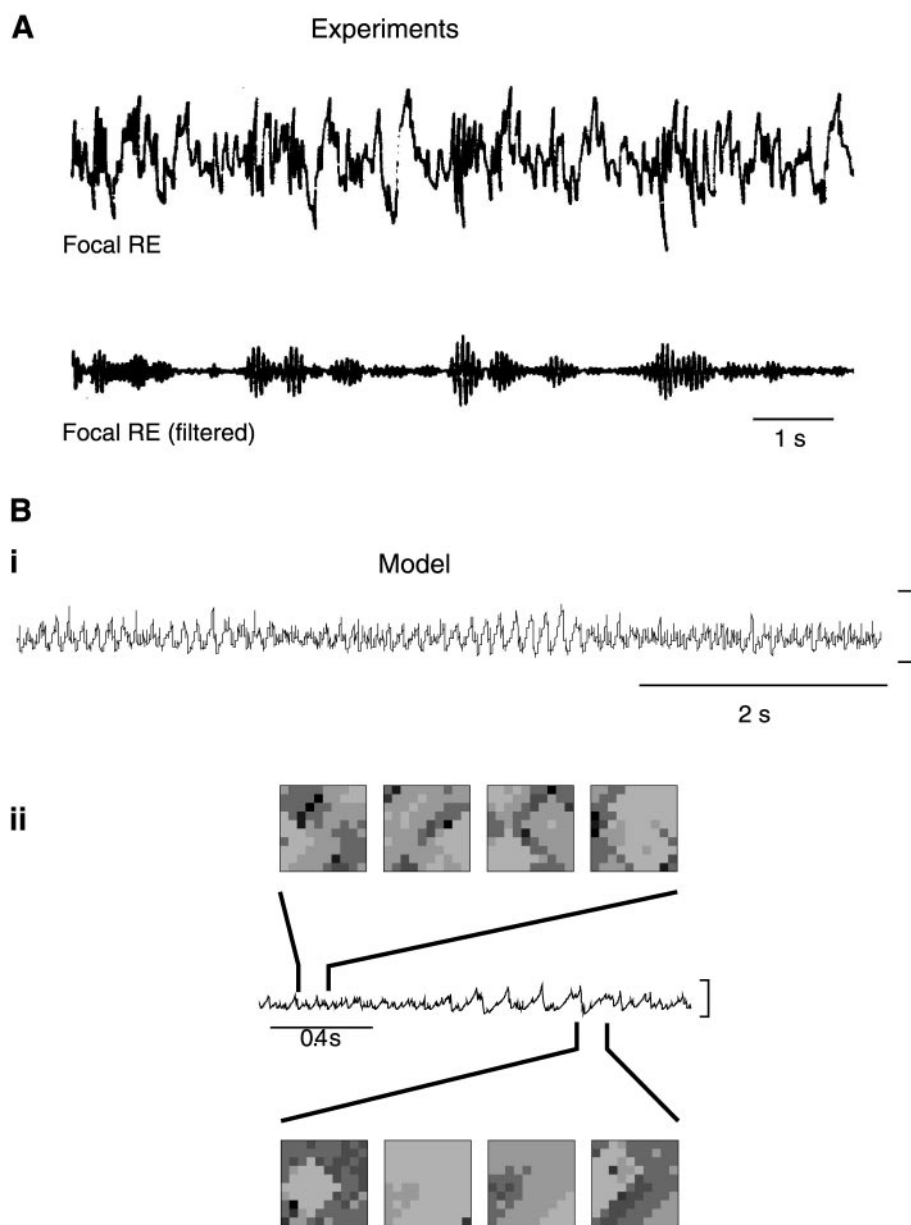
FIG. 5. Oscillations in the isolated reticular nucleus. *A*: spontaneous oscillations in the spindle frequency range obtained in the deafferented thalamic reticular nucleus in vivo. The field potentials recorded in the isolated RE nucleus show rhythmicity in the spindle frequency range (*bottom trace* was filtered between 7 and 14 Hz). [Modified from Steriade et al. (308).] *B*: model of oscillations mediated by GABA$_A$ synapses in the RE nucleus. *i*: Oscillations in a network of 400 RE neurons in which each cell was connected to its 24 nearest neighbors. The average value of the membrane potentials shows oscillations with a similar frequency as in the experiments. *ii*: Snapshots of activity in a 100 RE neuron network during waxing-and-waning oscillations corresponding to the regions of the averaged membrane potential as indicated. The top series of snapshots was taken during the "desynchronized" phase and shows highly irregular spatiotemporal behavior. The bottom series of snapshots was taken during the "oscillatory" phase, when the network is more synchronized and coherent oscillations were found in the averaged activity. The time interval between frames was 40 ms. [Modified from Destexhe et al. (97).]

cleus maintained in vitro did not generate oscillations without connections from TC cells (322, 346), in contrast to the observation of spindle rhythmicity in the isolated RE nucleus in vivo (308).

In summary, three different mechanisms have been proposed to explain the genesis of thalamic rhythmicity: the TC-interneuron loops of Andersen and Eccles (9), the TC-RE loops of Scheibel and Scheibel (269–271), and the RE pacemaker hypothesis of Steriade et al. (308). In vitro experiments appear to support the "TC-RE" loop mechanism, in contrast to in vivo experiments that support the RE pacemaker hypothesis. We show below how computational models suggest a way to reconcile these apparently contradictory experimental observations.

B. Models of the Thalamic Reticular Pacemaker

1. Early models

The thalamic RE nucleus is a network of interconnected inhibitory neurons that might not be expected to generate oscillations. The discovery that thalamic RE neurons were capable of a rebound burst (14, 208) suggested that these cells could sustain oscillations through repetitive reciprocal inhibitory rebound. The genesis of oscillations in such inhibitory networks was investigated in central pattern generators of invertebrates (249). However, in this structure, the neurons typically oscillate antiphase, inconsistent with the synchronized oscillations observed in the RE nucleus.
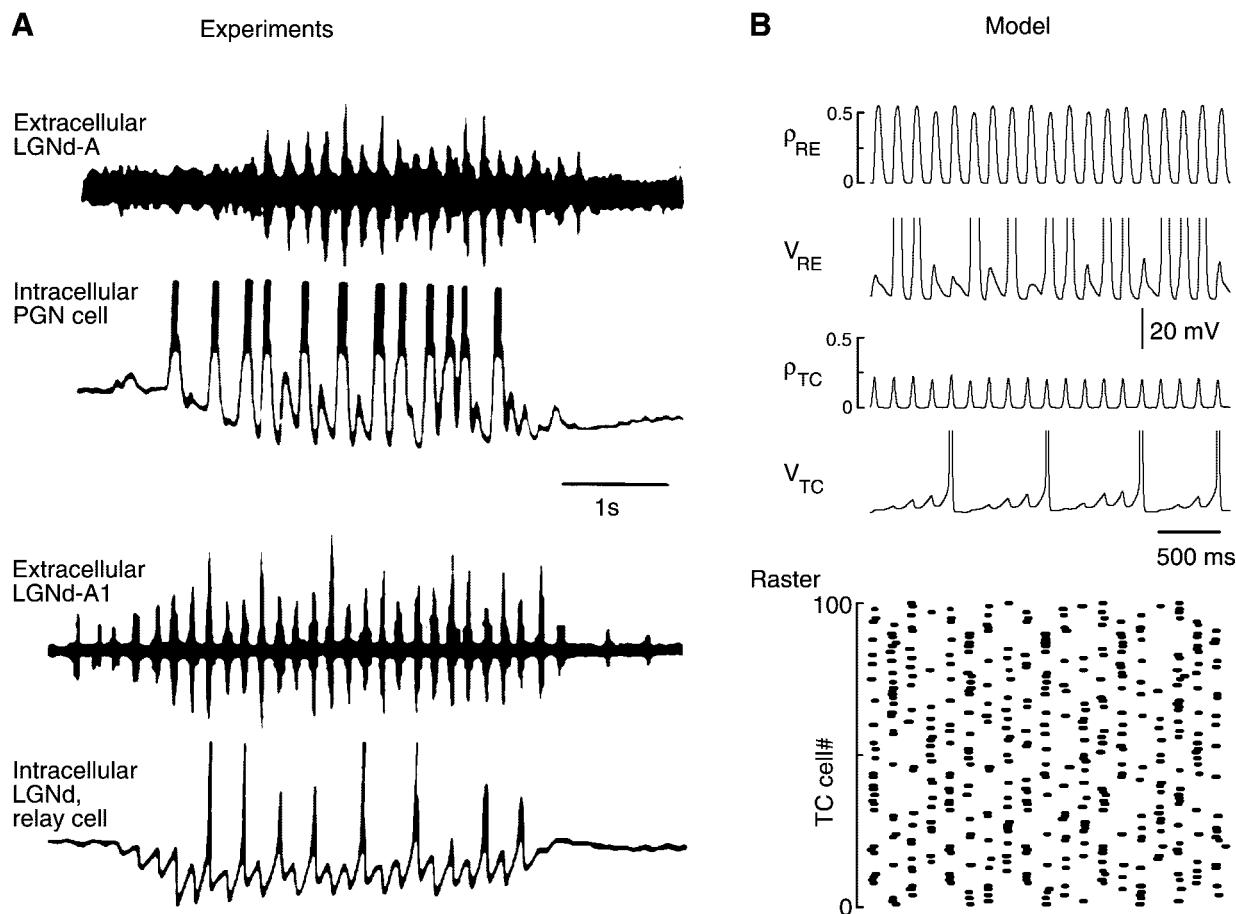
A Experiments **B** Model

FIG. 6. Spindle waves resulting from interactions between thalamic relay and reticular neurons. *A*: spindle sequence recorded both intracellularly and extracellularly in ferret visual thalamus in vitro. An intracellular recording was performed in a thalamic reticular neuron (*second trace*), located in the perigeniculate (PGN) sector of the thalamic slice, together with an extracellular recording (*top trace*) of relay cells in the dorsal lateral geniculate (LGNd) sector of the slice. Another spindle sequence is shown recorded intracellularly in a relay neuron (LGNd, *bottom trace*), together with an extracellular recording of relay cells (LGNd, *third trace*). RE cells tended to burst at every cycle of the oscillation, while TC cells burst every 2 or 3 cycles. [Modified from von Krosigk et al. (346).] *B*: spindle oscillations in a 100-neuron network of thalamic relay and reticular cells. Synaptic interactions were mediated by AMPA receptors (from TC to RE), a mixture of GABA$_A$ and GABA$_B$ receptors (from RE to TC), and GABA$_A$-mediated lateral inhibition between RE cells (see Ref. 353 for details of the model). The fraction of TC and RE cells that are simultaneously active (ρ_{TC} and ρ_{RE}) are indicated together with one representative example of the membrane potential for each cell type (V_{TC} and V_{RE}) during spindle oscillations. Individual TC cell produced bursts at a subharmonic frequency of the network oscillation, but the population of TC cells oscillated at the spindle frequency (see raster plot in bottom graph). [Modified from Wang et al. (353).]

Several computational models have been used to explain the genesis of synchronized oscillations within the RE nucleus (23, 90, 97, 98, 133, 134, 354). Two different hypotheses were proposed at about the same time. Wang and Rinzel (354, 355) investigated the "slow-inhibition hypothesis," postulating that networks of inhibitory neurons can generate synchronized oscillations if they interact through slow (presumably GABA$_B$-mediated) inhibition. In contrast, other investigators proposed a "fast-inhibition hypothesis" for generating synchronized oscillations based on fast (presumably GABA$_A$-mediated) type of inhibition (23, 90, 97). In the Wang and and Rinzel model,

the oscillatory behavior of two coupled RE neurons depended on the decay rate of inhibition: antiphase oscillations typically arose for fast inhibition, whereas slow inhibition led to in-phase oscillations (355). These two different mechanisms for producing oscillations can be explained most clearly with phase plane diagrams (354). One problem with the slow-inhibition hypothesis was that it generated synchronized oscillations slower than the ~10- to 15-Hz frequency observed in the thalamic RE nucleus in vivo (308).

In a model of the fast-inhibition hypothesis, faster oscillation frequencies (~10 Hz) arose from fast inhibi-

tory interactions, and the synchrony of the oscillations was due to dense interconnections between RE cells (90). The rebound burst properties of RE cells were based on the data available at that time (14, 208, 228). Two-dimensional networks of RE cells were investigated, in which each RE neuron was densely connected with its neighbors within some diameter. Anatomical studies show that RE cells are connected through GABAergic dendro-dendritic synapses over a significant distance (83, 252, 368). In addition, the axons emanating from RE cells give rise to collaterals in the RE nucleus before projecting to relay nuclei (174, 252, 368). As these collaterals generally extend over distances greater than the size of the dendritic tree, a given RE cell probably receives inputs from cells outside its immediate neighborhood. Under these conditions, the network generated synchronized oscillations at a frequency of ~ 7 Hz (90). Unlike models with slow inhibition, this fast-inhibition model did not generate fully synchronized oscillations. Instead, the neurons in the network had phases distributed around zero, and the average membrane potential displayed oscillations reflecting the synchrony of the population.

Experiments have demonstrated that RE cells interact through GABA$_A$-mediated interactions. This was first suggested by the strong effects of GABA$_A$ agonists in slices of the RE nucleus (17, 164, 227, 291). Intracellular recordings of RE cells later revealed the presence of fast hyperpolarizing IPSPs in vivo (97), which were shown to be GABA$_A$ mediated in vitro (21, 265, 266, 280, 336, 372). In some preparations, the GABA$_A$-mediated currents between RE cells have slower kinetics compared with TC cells (337), although still far from the slow time course of GABA$_B$ currents. These data revealed the ingredients necessary for the fast inhibition hypothesis. However, a low-amplitude postsynaptic GABA$_B$ component was detected in some cases (336), and gap junctions were recently identified between RE neurons in mouse thalamic slices (189), suggesting that the spectrum of interaction between RE cells is more complex than pure GABA$_A$-mediated inhibition.

2. Models of oscillatory behavior in networks of reticular neurons

Models of the RE nucleus have yielded insights into the mechanisms underlying oscillations based on GABA$_A$-mediated synaptic interactions (23, 97). These models incorporated biophysical measurements of the I_T current (163), as well as other currents (17), in RE cells.

The first step was to identify the different oscillatory modes generated by circuits composed of Hodgkin-Huxley-type models of RE cells, connected by either GABA$_A$ or GABA$_B$ synapses (97, 355). Different types of oscillatory modes were observed, such as antiphase bursting (as in Ref. 249) and synchronized oscillations (97). The latter

type was the most frequent and depended on the connectivity. Two-dimensional networks of RE cells with dense proximal connectivity (the same connectivity as in Ref. 90), with GABA$_A$ synapses, robustly generated synchronized oscillations at a frequency of 6.5–9 Hz (Fig. 5*Bi*). The synchrony was not perfect, but the phases of the individual bursts were distributed around zero, and the overall synchrony of the network was visible in the average membrane potential, in cross-correlations (data not shown), and in computer-generated animations of network activity (Fig. 5*Bi*).[2] Interestingly, these animations revealed that, at any given moment, all neurons that were firing in phase form a coherent, moving patch of activity, or "traveling wave," that swept across the network. This suggests that the spindle rhythmicity observed in the average firing activity of neurons in the network is a reflection of coherent waves of activity that recur on every cycle of the oscillation (Fig. 5*Bii*). Both rotating and spiral waves were observed (97) (see also Ref. 23; see below).

Spatiotemporal analysis also revealed that the coherence of the oscillations fluctuated with time. The network alternated between periods of high and low synchronization between the activity of the RE cells, which translated into waxing-and-waning patterns of oscillations in the average activity of the network (Fig. 5*Bii*). This pattern of activity was consistent with the waxing-and-waning field potentials recorded extracellularly in the RE nucleus after deafferentation (308) (Fig. 5*A*). The model therefore predicts that the type of waxing and waning observed in the RE nucleus is not due solely to intrinsic cellular properties but is associated with spatiotemporal patterns of coherent waves that continuously form and dissolve (97).

Different patterns of connectivity between RE cells affected the patterns of oscillations in RE network models. When RE cells were connected globally (all-to-all coupling), the networks displayed synchronized oscillations in only two cases (135): when interactions were GABA$_B$ mediated and when GABA$_A$ synapses had a reversal potential around rest ("shunting" synapses). However, the oscillations had frequencies <6 Hz in both cases. Partial synchrony was observed at higher frequencies (~ 10 Hz) when the properties of the neurons were randomized (135). GABA$_A$-mediated waxing-and-waning oscillations at 10 Hz with partial with synchrony at 10 Hz, as observed in experiments, were obtained in another model (97). These GABA$_A$-mediated oscillations were generated by mutual inhibition-rebound sequences in RE cells, which arose from the interactions between the I_{Ts} and GABA$_A$ currents. They were robust to changes in connectivity, connection strength, and network size, provided

---

[2] Computer-generated animations of the membrane voltage are available at http://cns.iaf.cnrs-gif.fr or http://www.salk.edu/~alain.

that the IPSPs were strong enough to deinactivate the I_T and evoke rebound bursts. Oscillations were not dependent on currents such as I_{CAN}, $I_{K(Ca)}$, or the details of the kinetics of fast IPSPs. However, they critically depended on the membrane potential (see below). Thus, although these two different models (97, 135) differed in details such as connectivity and the kinetics of the currents, both found that RE cells connected with $GABA_A$ synapses can show synchronized (or partially synchronized) oscillations at 10 Hz.

Another type of model of the reticular nucleus is based on depolarizing interactions between RE cells (23). The (chloride) reversal potential for $GABA_A$ IPSPs is generally more depolarized in RE cells compared with TC cells (265, 337) and in some preparations it was reported to be as high as -70 mV, which is depolarized compared with the resting potential of RE neurons (337). In contrast, other preparations showed that fast IPSPs in RE cells are hyperpolarizing (21, 97, 265, 266, 280, 336, 372). The effect of depolarizing $GABA_A$ IPSPs on RE cells was tested using computational models of two-dimensional networks of RE cells (23). When the RE cells were resting at around -80 mV, the network displayed slow synchronized oscillations at a frequency of ~2.5 Hz, consisting of synchronous bursts of action potentials triggered by the depolarizing IPSPs between RE cells. When RE cells had a more depolarized resting level (just below the $GABA_A$ reversal potential), the network showed oscillations at a higher frequency of ~9 Hz. In this case, individual cells oscillated at ~4.5 Hz, and the population activity showed oscillations at ~9 Hz. As in the other RE models, sustained oscillatory behavior was accompanied by spatiotemporal traveling waves of activity. The periodicity of the spiral-like waves was related to the frequency of oscillation of the network.

In another model (326), spindle oscillations in thalamic and thalamocortical circuits arose from the pacemaker role of the RE nucleus. In this model, as in others, oscillations occurred among RE cells through their rebound burst properties and fast GABAergic interactions. However, this model could not generate oscillations with frequencies higher than 5 Hz. The possibility that higher frequency complex spatiotemporal patterns may emerge was not tested.

In summary, the known intrinsic voltage- and calcium-dependent currents in RE neurons, combined with their patterns of interconnectivity and synaptic interactions through GABAergic receptors, could account for the generation of oscillations in the spindle frequency range, and some models could also account for the waxing-and-waning envelope. These models were different in detail (23, 97, 135), but all consistently showed that the reticular nucleus can generate ~10-Hz oscillations, consistent with in vivo observations in the deafferented RE nucleus (308). A recent study demonstrated the presence of gap junc-

tions between some RE neurons (189). The possibility that electrical interactions also participate in generating synchronized oscillations should be investigated in future models.

C. Models of the TC-RE Pacemaker

1. Elementary TC-RE oscillator

The observation of spindle waves in different thalamic slice preparations (20, 21, 170, 346, 351) (Fig. 6*A*) as well as in rat thalamocortical slices (322) suggests that oscillations are generated by an interaction between TC and RE cells. The synaptic interactions are AMPA (from TC$\rightarrow$RE) and a mixture of $GABA_A$ and $GABA_B$ (from RE$\rightarrow$TC) (346). The kinetics of the synaptic currents mediating these interactions, combined in a model with the intrinsic properties of TC and RE cells, are sufficient to account for spindle oscillations at the correct frequency. The simplest TC-RE oscillator circuit consists of one TC interconnected with one RE cell. This model generated 8- to 10-Hz spindle oscillations separated by silent periods of 8–40 s (105). The bursts of activity in the TC and RE cells were mirror images, as observed experimentally in anesthetized cats (310), in the whole brain in vitro (236), as well as in ferret thalamic slices (346). The spindle oscillations began in the TC cell in a manner similar to the waxing-and-waning slow oscillations of isolated TC cells. The first burst of spikes in the TC cell elicited a series of EPSPs, which activated I_{Ts} in the RE cell. The RE cell started bursting and entrained the TC cell to 8–10 Hz, but the excitatory feedback from the TC cell was necessary to maintain this rhythmicity. At each cycle of the oscillation, the Ca^{2+}-mediated upregulation of I_h shifted its voltage activation curve. The oscillations in the circuit terminated by the same mechanism that caused the slow oscillations in isolated TC cells to wane (see sect. II*A7*).

2. Oscillations generated by TC-RE networks

The model above shows that spindle oscillations can be generated in a simple network model, but two features of the oscillation were not consistent with experiments. The first is that the TC cell spontaneously began to oscillate, but both TC and RE cells stop oscillating if their interconnections are cut (346). Second, the TC cell in the model rebounded on every cycle of the spindle oscillation, but skipping and "subharmonic bursting" is observed in intracellular recordings of TC cells during spindle oscillations (8, 20, 236, 310, 346) (see LGNd cell in Fig. 6*A*). Because RE cells receive barrages of EPSPs at ~10 Hz from several TC cells (21), the population of TC cells may still generate a 10-Hz output although individual cells do

not fire on every cycle. These features were explored in network models (96, 136, 353) (see below).

The subharmonic bursting of TC cells during spindle oscillations depends on the type of receptor, the IPSP conductance, and the frequency of stimulation. Repetitive stimulation of $GABA_A$ receptors at 10 Hz in a TC cell showed that subharmonic bursting is observed only when the strength of the $GABA_A$ conductances is weak or moderate (96). Computational models of thalamic networks investigated the genesis of spindle oscillations with subharmonic bursting in TC cells (96, 136, 353). The models showed that spindle oscillations arise in these networks with different bursting frequency at the single-cell level, but the population oscillated at ~10 Hz. The minimal system for this type of oscillation consisted of a circuit of two TC and two RE cells (96) which generated oscillations at 10 Hz, but TC cells produced bursts in alternation once every two cycles, such that their combined output was 10 Hz. This type of dynamics is illustrated in Figure 6B for larger networks. RE cells generated repetitive bursts at around the spindle frequency (~6–7 Hz in this case), but TC cells produced subharmonic bursting and fired bursts at a lower frequency (~1.5–2 Hz). Similar findings were obtained in several computational models of thalamic networks (96, 136, 353).

The mechanisms underlying subharmonic bursting, investigated earlier (185), are due to an interaction between IPSPs with I_T and I_h in TC cells (352, 353). For strong $GABA_A$ conductances, models of TC cells do not produce subharmonic bursting and can follow 10-Hz IPSPs, similar to the two-cell TC-RE model of spindles (105). This situation is not atypical, because some TC cells do not display subharmonic bursting. For example, intralaminar TC cells typically burst on every cycle of spindle oscillations (304). Strong $GABA_A$ conductances could explain the patterns of spindling in these cells.

In larger network models of interconnected TC and RE cells, the properties of the spindle oscillations were consistent with all the experiments (96). Spontaneous waxing-and-waning oscillations were only present if upregulation of I_h was included, and if TC cells had heterogeneous intrinsic properties,[3] consistent with experiments (191). A simpler model of the TC-RE network, in which cells did not include action potentials, also generated 8- to 12-Hz oscillations with mirror image and correct phase relations between cells, subharmonic bursting, and propagating patterns of activity (136) (see below and also Ref. 353).

---

[3] Heterogeneity was created by randomizing the values of the I_h conductance, such that the majority of TC cells was resting around −60 mV, while only a small minority were spontaneous oscillators, similar to the proportion found in vitro (191). This minority served as "initiators" of the oscillation in the entire network.

3. Traveling patterns of spindle waves in vitro

Spindle waves in ferret thalamic slices show systematically propagating traveling waves in the dorsal-ventral axis (182) (Fig. 7A). A spindle started by the spontaneous discharge of either TC or RE cells and propagated through the recruitment of adjacent cells through localized axonal projections. Andersen and Andersson (8) proposed a similar progressive recruiting mechanism based on local interactions between TC cells and inhibitory interneurons rather than RE cells. Models in which TC and RE cells formed topographically connected local networks (119, 138, 174, 232, 268) could reproduce the traveling spindle waves (96, 136) (Fig. 7B). The oscillation started at one site and propagated by recruiting more TC and RE cells on each cycle of the oscillation. The velocity of the propagation was directly proportional to the extent of the axonal projections (136). Similar results were found with different sets of parameters as long as the connectivity was topographically organized. The average propagation delay between two neighboring neurons was ~19.4 ms. If the fan-out of the projections between the TC and RE cells in the model (11 neurons) is assumed to be equivalent to 200 μm in the slice, then the velocity in the model is ~1.03 mm/s for spindles, within the 0.28–1.21 mm/s range observed experimentally.

Models that incorporated the waxing-and-waning properties of individual TC cells (96) produced propagating patterns similar to the propagating patterns of spindles found in vitro (182) (Fig. 7A). The "waxing" propagated as more and more cells were recruited. Similarly, the "waning" also propagated, as TC cells progressively lost their ability to participate in rebound bursting activity. The resulting pattern had the appearance of "waves" of oscillatory activity propagating through the network, and separated by periods of quiescence for 15–25 s.

4. Dynamic clamp reconstruction of the TC-RE oscillator

A powerful technique to test predictions from modeling studies is to build a system that includes computer simulations coupled with real recordings. In the dynamic clamp technique (261, 276, 277), ionic conductances in the simulation are injected in a real neuron through the intracellular electrode. It is also possible to simulate an entire neuron, simulating synaptic inputs when the recorded cell fires, and, when the simulated neuron fires, inject the appropriate synaptic currents into the recorded cell (193, 194, 259, 367). Another variant is to provide artificial synaptic connections between simultaneously recorded cells, by identifying spikes in each cell and injecting an artificially generated current into the companion cell (275). With these hybrid techniques it is possible to study phenomena arising from the interaction between different types of cells, such as of spindle rhythmicity, and test the
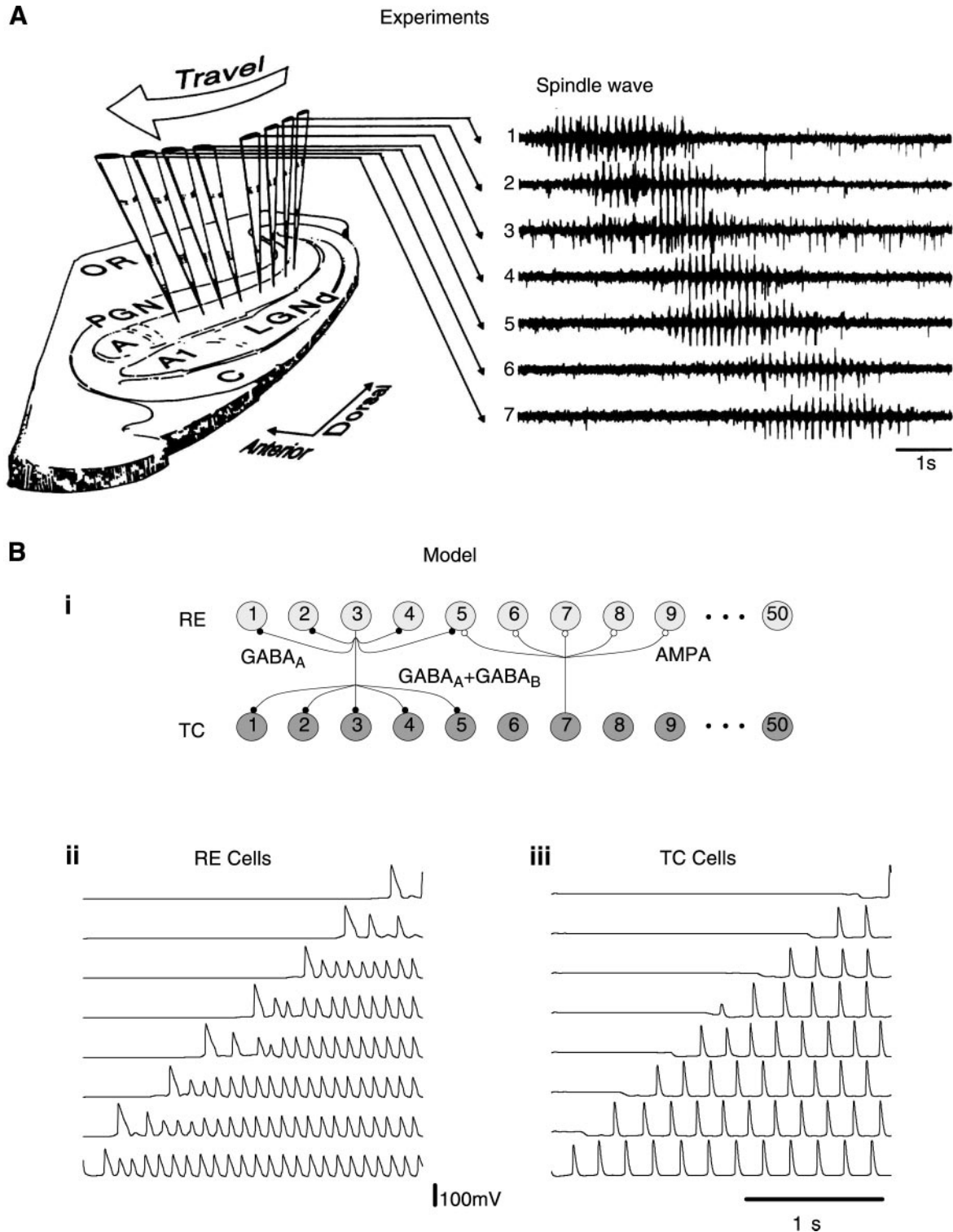
FIG. 7. Propagation of spindle waves in isolated thalamic networks. *A*: propagating spindle waves in ferret thalamic slices. *Left:* drawing of a sagittal ferret dorsal lateral geniculate nucleus (dLGN) slice with an array of 8 multiunit electrodes arranged in lamina A. Electrodes were separated by 250–400 μm, extending over 2–3 mm in the dorsoventral axis. *Right*: example of a propagating spindle wave. The spindle wave started in the dorsal end of the slice and propagated ventrally. Each spindle wave consisted of waxing-and-waning rhythmic action potential bursts with interburst frequency of 6–10 Hz. [Modified from Kim et al. (182).] *B*: propagating spindle oscillations in a network of thalamocortical and thalamic reticular cells. *i*: Schematic diagram of connectivity of a one-dimensional network of TC and RE cells with localized axonal projections. *ii*: Membrane potential of 8 RE cells equally spaced in the network during spindle oscillations. *iii*: Membrane potential of 8 TC cells equally space in the network (same simulation as in *ii*). [*ii* and *iii* modified from Golomb et al. (136).]

role of individual conductances, of synaptic or voltage-dependent type. The key is to use models that can be simulated in real time, while maintaining a sufficient degree of realism, which has only become possible with the availability of powerful digital computers in the laboratory.

The TC-RE oscillator has been investigated using hybrid recordings (193). The single-compartment models described above were used with minor modifications. In the first setup, a real RE cell was recorded and connected to an artificial TC cell (Fig. 8*A*). In a second setup, a real TC cell was recorded and connected to an artificial RE cell (Fig. 8*B*). In both cases, ~10-Hz spindle oscillations were obtained from the interacting real-artificial pair, even though none of the cells was spontaneous oscillators. The oscillation observed resembled that found in model two-neuron circuits (105). This hybrid approach provides a clear demonstration that spindle oscillations can be generated by interacting TC and RE cells, confirming earlier modeling studies.

D. Reconciling Different Pacemaker Mechanisms

The models demonstrate that the voltage-dependent currents generating the intrinsic properties of thalamic cells and the type of synaptic receptors mediating their synaptic interactions are consistent with properties of spin-

dle generation, both by TC-RE circuits and by the isolated RE nucleus. However, an explanation is still needed for why the isolated RE nucleus does not show spontaneous oscillations in vitro (14, 21, 165, 351, 346). Possible reasons for this discrepancy (312) include the possibility that the RE nucleus was not completely deafferented in the in vivo experiments or that there are too few interconnected RE cells in the slice to sustain oscillations.

Another possible explanation for this discrepancy is a different state of neuromodulation of RE cells (98). One major difference in the thalamus between the slice preparation and the living brain is that there is a tonic level of activity in neuromodulatory pathways in vivo, including acetylcholine (ACh), norepinephrine (NE), and serotonin (5-HT). These pathways densely innervate thalamic nuclei, and the release of neuromodulators alters channel conductances and the resting level of thalamic neurons (222). In particular, ACh was shown to affect the firing pattern of RE cells by activating a leak K^+ current (227), whereas NE and 5-HT depolarize thalamic cells by blocking a leak K^+ current (228).

The effects of neuromodulators on networks of RE cells were examined with computational models to help understand why spontaneously oscillations are observed in vivo but not in vitro (98). The histology in vivo showed that the rostral pole of the RE nucleus was perfectly
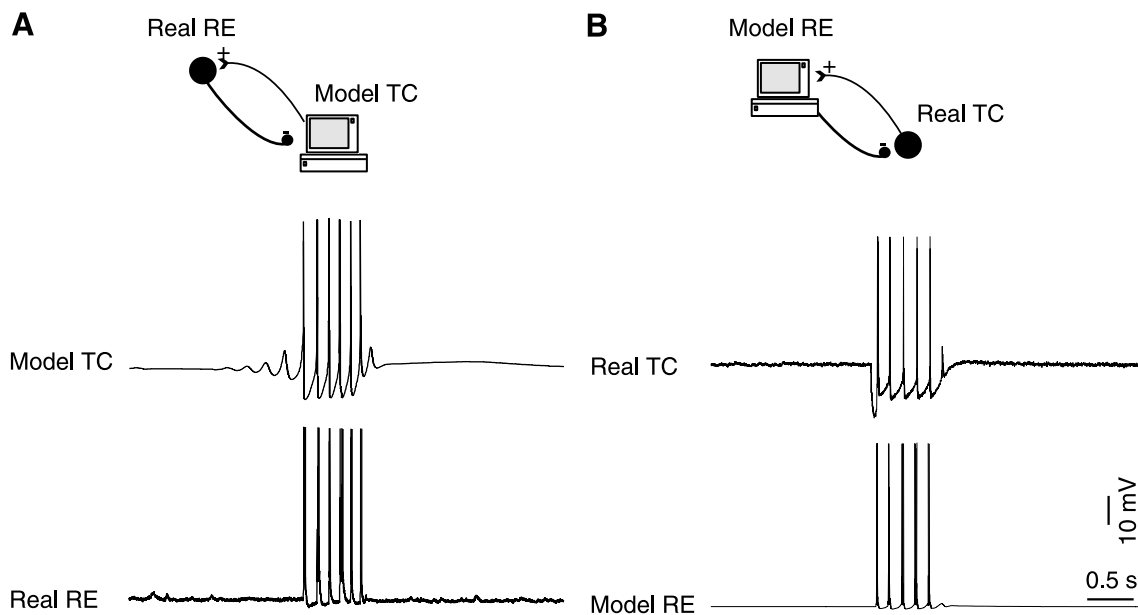
FIG. 8. Reconstruction of spindle waves from hybrid thalamic circuits. Thalamic neurons were recorded intracellularly in ferret thalamic slices and were coupled to computational models in real time. *A*: intracellularly recorded thalamic reticular neuron (nRt/PGN) coupled to a model thalamic relay cell (TC). Synaptic interactions were mediated by AMPA receptors (from TC to nRt/PGN) and GABA$_A$ receptors (from nRt/PGN to TC) and were simulated using the dynamic-clamp technique. *B*: intracellularly recorded thalamic relay neuron (TC) coupled to a model thalamic reticular cell (nRt/PGN) using a similar coupling procedure. In both cases, oscillations in the spindle frequency range emerged from these circuits, although none of the cells was a spontaneous oscillator. The oscillations waxed and waned due to calcium-mediated upregulation of I_h in the TC cell. Models were single-compartment modifications from Ref. 105. [Modified from LeMasson et al. (193).]

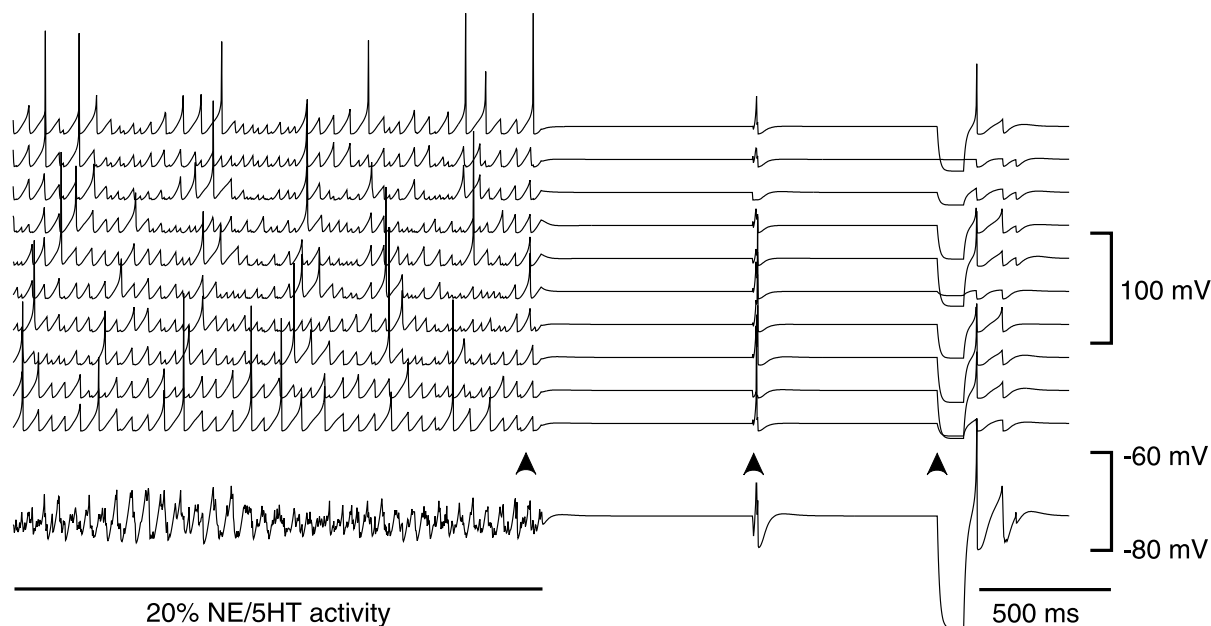FIG. 9. Neuromodulation can explain why networks of RE cells spontaneously oscillate in vivo but not in vitro. Simulation of a network with 100 RE cells locally interconnected through GABA$_A$ synapses. Oscillations were possible only if RE cells had a sufficiently depolarized resting membrane potential (about -65 mV in this case), close to in vivo measurements. This depolarization was provided here using kinetic models of the block of K$^+$ conductances by noradrenergic/serotonergic (NE/5-HT) neuromodulatory synapses. In the absence of this neuromodulatory drive, leak K$^+$ conductances were fully activated, and the resting level of RE cells was more hyperpolarized (-75 mV in this case), close to in vitro measurements. In this case, the network of RE cells was unable to sustain oscillations. The figure shows the transition between these two states: NE/5-HT synapses were initially active, as in vivo, allowing the network to display waxing-and-waning oscillations at a frequency of 10–16 Hz. After 2 s (first arrow), all NE/5-HT synaptic activity was suppressed; the resulting hyperpolarization prevented the network from sustaining oscillations. Depolarizing (second arrow) or hyperpolarizing (third arrow) current pulses injected simultaneously in all neurons (with random amplitude) could not restore spontaneous oscillations. This latter situation may correspond to the conditions of RE cells in vitro. [Modified from Destexhe et al. (98).]

isolated from the dorsal thalamus and the cerebral cortex, but projections of the most ventral fibers arising from the brain stem could reach the RE nucleus as well as the basal forebrain, which was still present in the isolated island (308). These fibers may constitute the noradrenergic projections from the raphe nucleus and locus coeruleus, as well as glutamatergic projections from various forebrain areas. It is therefore plausible that a reduced, but not entirely suppressed, neuromodulatory drive was still present in these experiments, bringing the RE neurons to more depolarized levels consistent with oscillations.

If the resting membrane potential of RE neurons in the model were adjusted to that typically observed in vitro (-65 to -80 mV), then networks of interconnected RE neurons could not sustain oscillations because the resting level was too close to the reversal potential of GABA$_A$ currents. On the other hand, simulating the depolarizing action of neuromodulators such as NE or 5-HT, by blocking ~20% of the leak K$^+$ currents, depolarized RE cells between -60 and -70 mV. This value was closer to the resting level observed in vivo (59). Under these conditions, the RE network showed waxing-and-waning oscillations as described in section IIIB, even though the intrin-

sic bursting properties of RE neurons were not affected (98). Incorporating NE/5-HT synapses and their effect on leak K$^+$ channels showed that a network of RE cells can be switched from oscillatory mode to silent mode by controlling these synapses (Fig. 9). This behavior was robust to changes in parameters; the critical parameter was the reversal potential of GABAergic currents (98).

The need for a depolarized level to sustain oscillations in the RE is compatible with reports of the presence of gap junctions between RE neurons (189). Symmetric electrical interactions between RE cells could be particularly effective in generating synchronized oscillations, but only if the resting level of RE cells is sufficiently depolarized. With depolarized rest close to threshold, spikes from one RE cell could in principle induce spikes directly in other electrically coupled RE cells.[4] Several

---

[4] It is also conceivable that RE cells coupled through gap junctions could induce bursts in each other if their resting level is hyperpolarized enough to deinactivate the I_T. In this case, oscillations should be observed in slices of the RE nucleus, where the level of RE cells is typically very hyperpolarized (see, for example, Ref. 337). Such oscillations have, however, never been reported.

different factors, such as mutual GABA$_A$ synapses and symmetric electrical coupling, may cooperate in generating oscillations in networks of depolarized RE cells.

The presence of a weak neuromodulatory drive may explain why the isolated RE nucleus oscillates in vivo but not in vitro. The model predicts that spontaneous sustained oscillations should be observed in slices of the RE nucleus if the resting level of RE cells could be brought to more depolarized values and the connections between RE cells in the slice were sufficiently strong. This could be achieved by bath application of NE/5-HT agonists at low concentrations to depolarize all RE neurons to the −60 to −70 mV range. Another prediction is that NE/5-HT antagonists should suppress oscillatory behavior in the isolated RE nucleus in vivo. The same results should also be found in other models of networks of inhibitory neurons displaying rebound bursts (135, 355) or in models incorporating gap junctions.

IV. THALAMOCORTICAL PACEMAKERS: CONTROL AND SYNCHRONIZATION OF OSCILLATIONS FROM INTERACTING NETWORKS

The pacemaker behavior of thalamic networks gives this region of the brain autonomy, but these thalamic models need to be scaled up in size and integrated into models for other brain systems. This leads to the problem of understanding the often highly complex behaviors that occur in vivo, and how to reconcile this behavior with the data obtained in reduced preparations or isolated networks maintained in vitro (297). We review here large-scale network behavior, such as coherent activity in the cortex, synchronized oscillations in unconnected thalamic and cortical areas, and pathological states such as epileptic seizures. We show that key to reconciling results from different preparations is the prominent role of corticothalamic projections, from which a unified framework emerges that explains the genesis of normal and pathological behavior.

A. The Large-Scale Synchrony of Slow-Wave Oscillations

1. Experimental characterization of large-scale synchrony

A consistent feature of oscillations recorded in vivo during slow-wave sleep or anesthesia is their high level of synchrony (8, 61, 102). This high coherence is also present in the human EEG during sleep (see Ref. 61 and references therein). Spindle oscillations are coherent across broad regions of the central, parietal, and occipital corti-

ces. A similar high level of coherence is found in EEG recordings from the suprasylvian cortex of naturally sleeping cats.

Andersen and Andersson (8) extended their model of a thalamic pacemaker and proposed that the large-scale synchrony observed in cortical systems could be generated by "distributor" TC cells, which would connect different thalamic nuclei by intrathalamic excitatory axon collaterals (8). According to this view, spindling could start in any thalamic neuron and be transmitted to inhibitory interneurons through intranuclear recurrent collaterals; these in turn would project IPSPs back to the TC neurons, which would fire rebound spike bursts at the offset of the IPSPs. This mechanism explicitly predicted propagating patterns of spindle oscillations through the thalamus and consequently through the cortex (8, 11) by progressive recruitment through intrathalamic axonal projections, consistent with earlier experimental observations (345) and more recent observations in thalamic slices (182).

According to this thalamocentric view, not only does the thalamus generate oscillations, but it also serves to synchronize large-scale cortical activity. Recent experiments suggest that although the thalamus is important for initiating spindle activity, the cortex is itself actively engaged in generating large-scale synchrony. Multisite recordings from the thalamus of intact and decorticate cats have confirmed that spindle waves are highly synchronous in the thalamus within the intact brain, but revealed that this large-scale synchrony was lost after removing the cortex (60) (Fig. 10A). Without the cortex, the thalamus still generated spindle oscillations, in agreement with the well-known thalamic origin of these oscillations (234, 305, 346), but the different thalamic sites oscillated quasi-independently (Fig. 10A). Subsequent experiments confirmed that the loss of the cortical influence on the thalamus was responsible for this loss of thalamic coherence (60). First, intracellularly recorded thalamic cells in the decorticate preparation all showed typical features of spindle oscillations. Second, dual intracellular recordings in the decorticate thalamus demonstrated that closely spaced electrodes (~1 mm) displayed highly synchronized oscillations, consistent with the intactness of the local thalamic synchronizing mechanisms, but synchrony was lost for larger intrathalamic distances. Third, the large-scale synchrony was still present after deep coronal cuts in cortex, suggesting that horizontal cortico-cortical connections were not necessary.

Thus the cortex is not passively driven by the thalamus and plays an active role in generating large-scale synchrony, which depends on a functional connectivity between cortex and thalamus.

A   Experiments

Intact

Decorticated

200 mV

1 s

B   Model

Thalamus with cortex   Isolated thalamic network
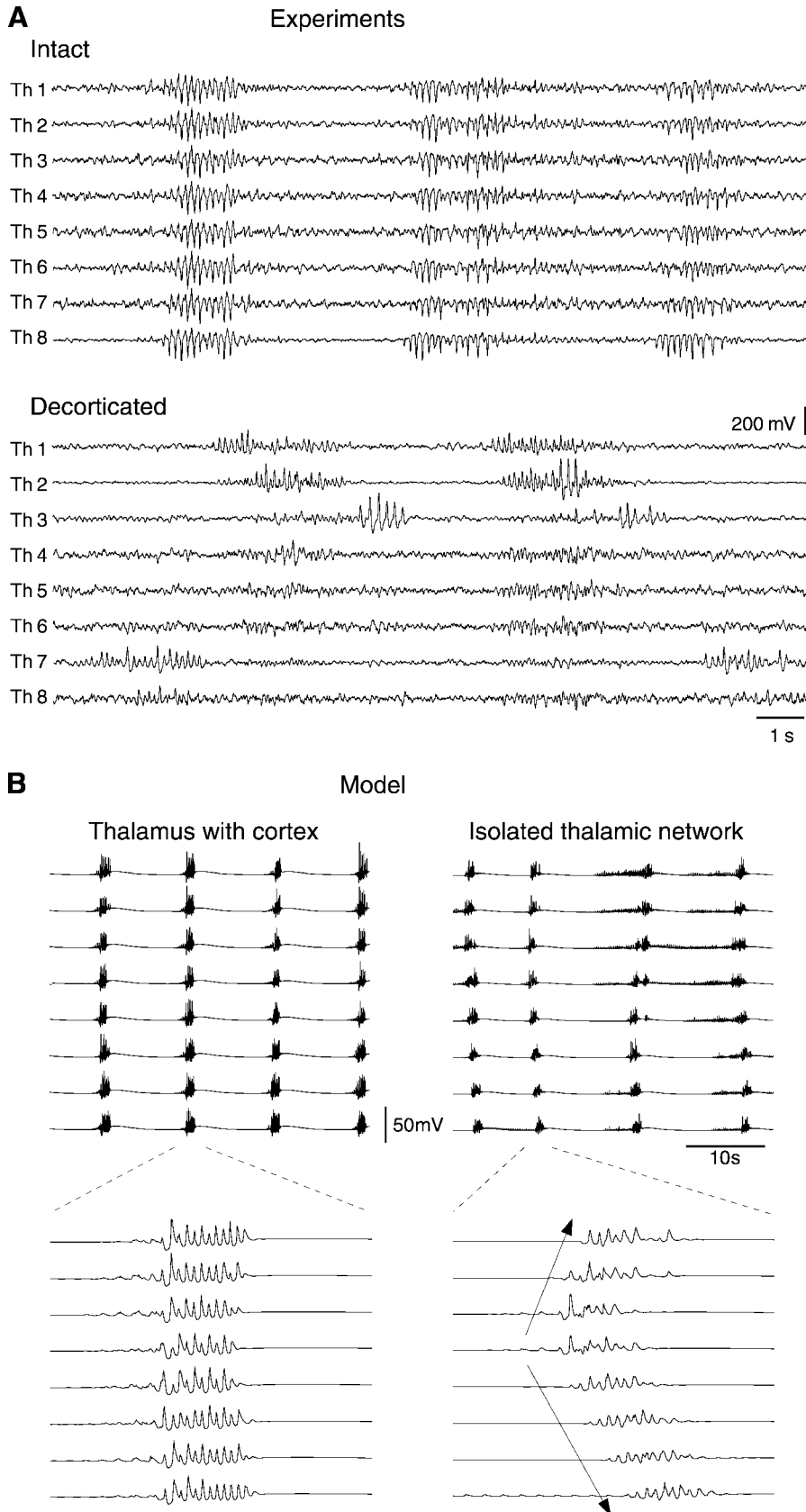

50mV

10s

FIG. 10. The large-scale synchrony of spindle oscillations depends on corticothalamic feedback. *A*: removal of the cerebral cortex affects the pattern of spindle oscillations in the thalamus. Field potentials were recorded using 8 tungsten electrodes equidistant of 1 mm (Th1-Th6) inserted in the cat thalamus under barbiturate anesthesia in the intact brain (Intact) and after removal of the cortex (Decorticated). After decortication, recordings from approximately the same thalamic location showed that spindling continued at each electrode site, but their coincidence in time was lost. The 8-electrode configuration was positioned at different depths within the thalamus (from -2 to -6) and different lateral planes (from 2 to 5); all positions gave the same result. [Modified from Contreras et al. (60).] *B*: computational model of large-scale coherence in the thalamocortical system. Spontaneous spindles are shown in the presence of the cortex (*left panels*) and in an isolated thalamic network (*right panels*) under the same conditions. The traces indicate local averages computed from 21 adjacent TC cells sampled from 8 equally spaced sites on the network. *Bottom graphs* represent averages of a representative spindle at 10 times higher temporal resolution. The near-simultaneity of oscillations in the presence of the cortex is qualitatively different from the propagating patterns of activity in the isolated thalamic network (arrows). [Modified from Destexhe et al. (100).]

2. Mechanisms underlying large-scale synchrony in the thalamocortical system

A thalamocortical network model was developed to explain these observations. The model consisted of the thalamic network as described in section IV*A* and a one-dimensional representation of cortical layer 6, whose neurons are the major source of corticothalamic projections, and which receives collaterals from ascending thalamocortical fibers, thus forming monosynaptic loops (149, 358). With the use of this model (see details of connectivity and receptor types in Ref. 100), the cortical oscillations were highly synchronized in the presence of the corticothalamic loops (Fig. 10*B*, thalamus with cortex), but this large-scale synchrony was lost if cortical cells were removed (Fig. 10*B*, isolated thalamic network).

To reproduce the large-scale synchronized oscillations observed in vivo, it was necessary for the corticothalamic projections in the model to recruit thalamic relay cells predominantly through inhibition (100). This inhibitory dominance might seem surprising since corticothalamic fibers have excitatory synaptic terminals on TC cells (174). However, corticothalamic fibers also excite RE cells, which mediate feedforward IPSP onto TC cells. Intracellular recordings of TC cells in response to stimulating the anatomically related cortical area typically show an EPSP-IPSP sequence dominated by the IPSP component (Fig. 11*A*). In the model, cortical simulation reproduced the EPSP/IPSP sequences observed experimentally in the thalamus only if cortical EPSPs on RE cells were stronger than the EPSPs on TC cells (see Fig. 11*B*). If the conductance of AMPA-mediated cortical drive on TC and RE cells as well as the GABA$_A$-mediated IPSP from RE cells were of the same order of magnitude, cortical EPSPs were shunted by reticular IPSPs, and cortical stimulation did not evoke oscillations in the thalamic circuit (Fig. 11*B*). The EPSP-IPSP sequence in the model resembled intracellular recordings, and cortical stimulation was effective in evoking oscillations when the cortical conductances of the EPSPs on TC cells were at least 5–20 times smaller than those on RE cells (88, 100) (Fig. 11*C*).

The dominance of inhibition in corticothalamic interactions is supported by a large body of experimental data.

The fact that the strong IPSP component is mediated by RE cells is consistent with the high sensitivity of these cells to cortical EPSPs; even low stimulus intensities evoke bursts in RE cells in vivo (59, 237) and in vitro (328). Inhibitory dominance has also been reported in recordings of thalamic relay neurons after stimulation of the corresponding cortical areas (4, 45, 66, 82, 196, 263, 315, 330, 359). In vitro experiments are also consistent with a dominance of inhibition; stimulation of the internal capsule in thalamic slices (328) or cortical stimulation in thalamocortical slices (177) produced EPSP-IPSP sequences dominated by inhibition in a significant proportion of the recorded TC cells. In agreement with these observations, the majority of excitatory synapses on RE cells are from cerebral cortex (198), and the number of glutamate receptors and the conductances of these synapses were approximately three to four times larger in RE cells compared with that of cortical synapses on TC cells (137). Perhaps the strongest evidence for inhibitory dominance was provided by Deschênes and Hu (82), who compared the effect of corticothalamic feedback before and after lesion or inactivation of the thalamic reticular nucleus. The "IPSP-dominant" cortical feedback was transformed into "EPSP-dominant" feedback after functional disconnection of the RE nucleus (82).

Why does inhibitory dominance promote large-scale synchrony in the thalamocortical system? A possible mechanism is shown in Figure 12 (100). In the isolated thalamus, the topographic structure of intrathalamic connections favors local propagation phenomena (Fig. 12*A*). Oscillations initiated at a given site (asterisk in Fig. 12*A*) recruit progressively larger areas of the thalamus at each cycle, through divergent TC-RE projections (see sect. III*C3*). In the presence of the cortex, initiation sites in the thalamus (asterisk in Fig. 12*B*) recruit first cortical neurons, and if the cortical feedback is inhibitory dominant, cortical discharges then recruit first RE neurons and consequently TC cells through IPSPs. During thalamo-cortico-reticulo-thalamic recruitment, a cascade of divergent axonal projection systems are activated (TC-to-CX, CX-to-RE, RE-to-TC). These thalamocortical loops are highly efficient at generating large-scale synchrony during oscil-

---

FIG. 11. "Inhibitory dominance" of corticothalamic feedback on thalamic relay cells. *A*: intracellular recording of a TC cell in the lateral posterior (LP) thalamic nucleus while stimulating the anatomically related part of the suprasylvian cortex in cats during barbiturate anesthesia. Cortical stimulation (arrow) evoked a small excitatory postsynaptic potential (EPSP) followed by a powerful biphasic inhibitory postsynaptic potential (IPSP). The IPSP gave rise to a rebound burst in the TC cell. This example was representative of the majority of recorded TC cells. *B*: simulation of cortical EPSPs (AMPA-mediated) in a circuit of 4 interconnected thalamic cells. Cortical EPSPs were stimulated by delivering a presynaptic burst of 4 spikes at 200 Hz to AMPA receptors. The maximal conductance was similar in TC and RE cells (100 nS in this case), and no rebound occurred after the stimulation (arrow). *C*: simulation of dominant IPSP in TC cell. In this example, the AMPA conductance of stimulated EPSPs in the TC cell was reduced to 5 nS. The stimulation of AMPA receptors evoked a weak EPSP followed by strong IPSP, then by a rebound burst in the TC cells, as observed experimentally. [Modified from Destexhe et al. (100).]

lations because each cycle through the loop recruits a large area of cortical or thalamic tissue.

Other factors may also enhance large-scale synchrony between thalamic areas that have no direct connection. Computational models suggest that the refracto-

riness of thalamic circuits, as observed in vitro (182), may serve to phase set thalamocortical activity (100). If unconnected thalamic nuclei end their period of refractoriness at roughly the same time, the initiation of activity in these areas may occur simultaneous and further promote

A Isolated thalamus
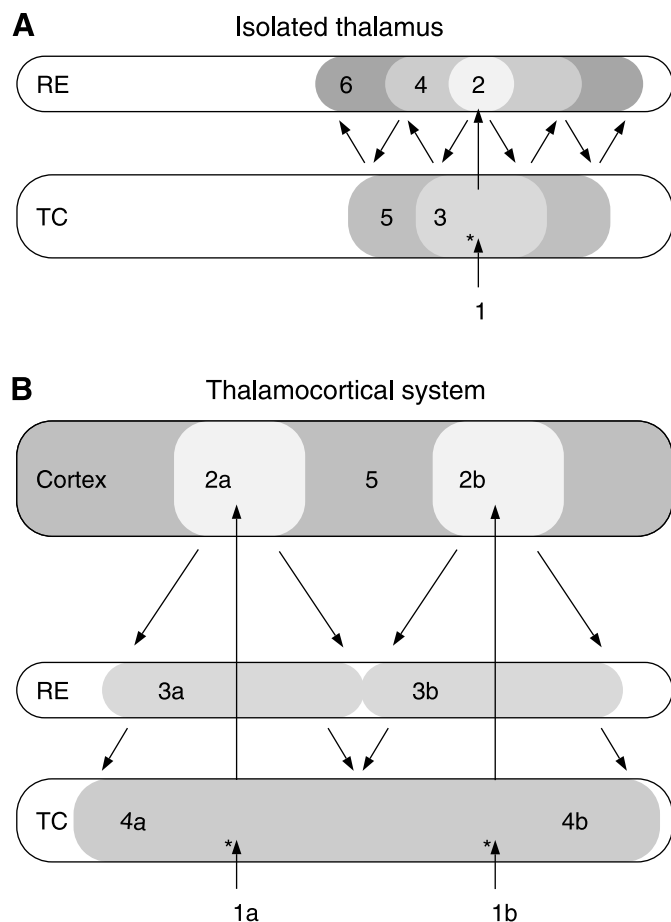

B Thalamocortical system
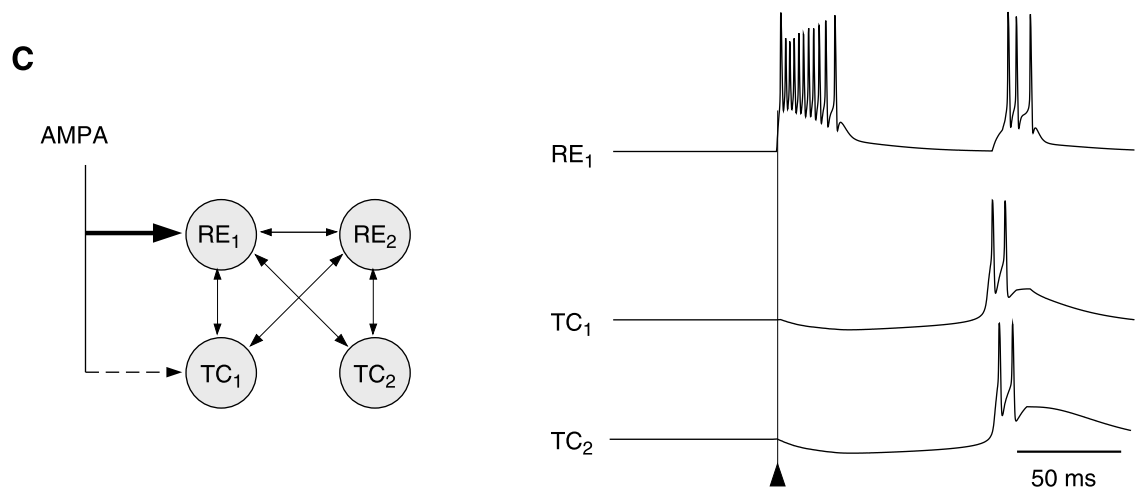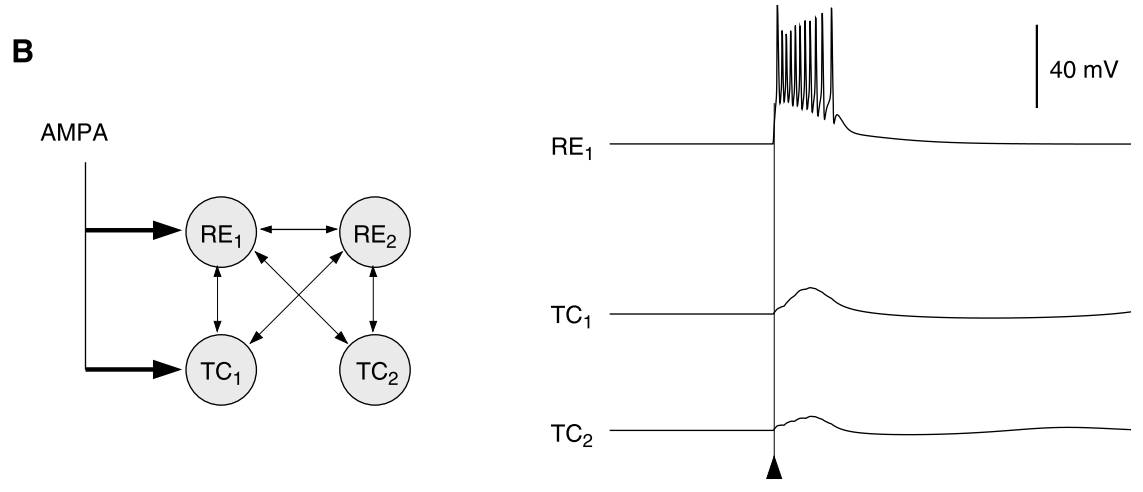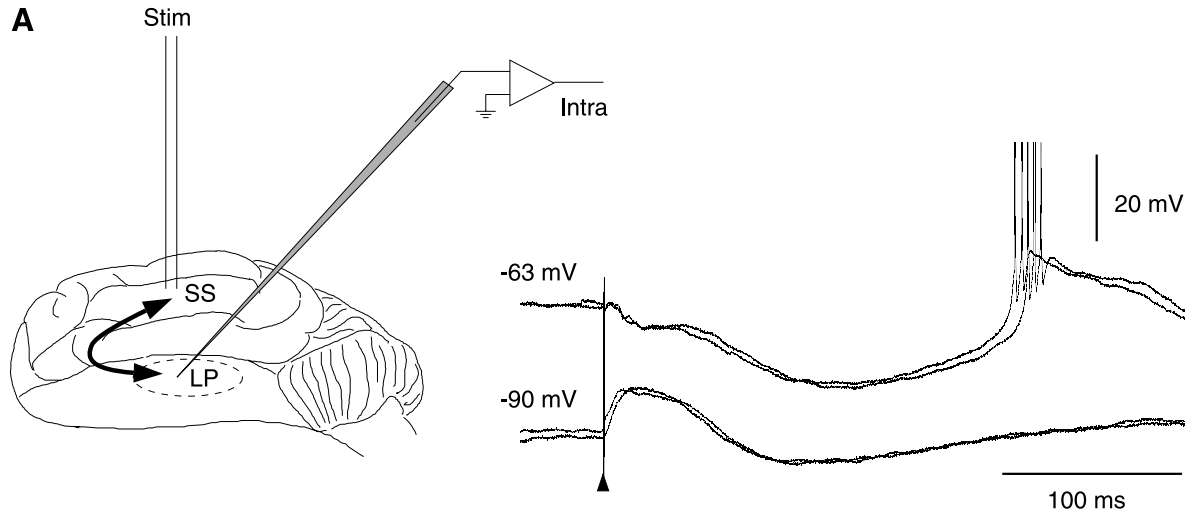
FIG. 12. Proposed mechanisms for large-scale synchrony. *A*: reciprocal recruitment of thalamocortical (TC) relay cells and thalamic reticular (RE) cells synchronize cells in the isolated thalamus. From an initial discharge of a TC cell (*1*; asterisk), a localized area of RE cells was recruited (*2*), which in turn recruited a larger neighboring TC cells (*3*), and so forth. Progressively larger areas of the thalamus were recruited on each successive cycle (*4*, *5*, *6*,...) through the topographic structure of the connectivity. An array or electrodes would record propagating oscillations, as found in thalamic slices (181). *B*: thalamic recruitment mechanism involving the cortex. Two approximately simultaneous initiation sites in the thalamus (*1a*, *1b*) recruited localized cortical areas (*2b*, *2c*), which in turn recruited the connected areas of the RE nucleus (*3a*, *3b*), which in turn recruited larger areas of TC cells (*4a*, *4b*), etc. At the next cycle, the entire cortical area was recruited (*5*). The corticothalamic connections overshadowed the local thalamic recruitment mechanisms shown in *A*, and oscillations achieved large-scale synchrony within a few cycles, consistent with in vivo data (63). [Modified from Destexhe et al. (100).]

large-scale synchrony. This mechanism was modeled by Ca^{2+}-dependent modulation of I_h in TC cells (100), similar to the way that it was modeled in isolated thalamic cells (see sect. II*A7*). In networks with randomly distributed I_h conductance in TC cells, different initiation sites "synchronized" because all TC cells had the same refractory period (see details in Ref. 100). The length of the refractory period depends on biochemical rate constants that may be similar in all TC cells that possess this mechanism. In vivo experiments have demonstrated that tha-

lamic refractoriness is visible from oscillations evoked by cortical stimulation (61). Oscillations could be evoked by cortical stimulation only after a 2- to 8-s period of silence, depending on stimulation intensity (61), and similar results were found in the thalamocortical model (100). These experiments and models suggest that thalamic refractoriness allows the network to "learn" large-scale synchrony by setting these mechanisms in phase in different thalamic nuclei.

Other synchronizing factors were proposed and tested by computational models. These include the synchronizing role of the long-range connections from RE to TC (288), which were not taken into account by other thalamic models, or a synchronized activity intrinsic to the RE network (24), which may also help synchronizing thalamocortical oscillations.

Another factor that promotes large-scale synchrony is the contribution of cortico-cortical fibers. Because *trans*-callosal fibers are myelinated and are fast-conducting, *trans*-callosal interhemispheric interactions may promote large-scale synchrony. Indeed, interhemispheric synchrony was diminished following callosal sections in cats (41). Recent experiments have shown that interhemispheric synchrony is larger than intrahemispheric synchrony in absencelike seizures in rats (231). The contribution of cortico-cortical interactions is examined in section IV*A4*.

Although the large-scale synchrony of thalamocortical spindle oscillations has not been the focus of investigation in other computational models, such models have also been used to investigate other related issues. In a model circuit comprising cortical and thalamic cells, transitions between spindle and delta sleep rhythms were obtained by modulating leak K^+ conductances in RE cells (323). Interestingly, this model predicted a synchronizing role for the RE neurons during the delta rhythm, through slow $GABA_B$-mediated IPSPs, which synchronized TC cells in their intrinsic delta oscillation. In another model (326), spindling was generated inside the RE nucleus, but a thalamocortical network comprising such a pacemaker could only generate oscillations at low frequencies ($\sim$5 Hz). Spindle rhythms were also modeled using continuum-based approaches (188, 364), or by simple cortical neuronal networks driven by a thalamic pacemaker (89).

3. Traveling patterns of spindle waves in vivo

In contrast to the large-scale synchrony observed in intact brains (Fig. 10*A*, intact), the isolated thalamus displays traveling waves (Fig. 7*A*). Traveling patterns were also observed by Verzeano and Negishi (344, 345) in early studies in the thalamus in vivo using multiple extracellular recordings. In the intact brain, the interelectrode distance was 1 mm, and the recorded area of the thalamus was $\sim$7 mm, which nearly covers the entire anterior-

posterior axis of the cat thalamus. In Verzeano's experiments, the electrodes covered a much smaller thalamic area (30–100 μm interelectrode distance). It is possible for local traveling patterns to occur within a globally synchronized network. Indeed, there is evidence for local propagation between Th1-Th6 in Figure 10*A*, although the spindle oscillations occurred approximately within the same time window at all sites. Moreover, with the use of the same electrode setup, propagating patterns of oscillations were found in the thalamus of decorticate cats in vivo (61). The isolated thalamus has a tendency to generate traveling waves, but these oscillations quickly evolve toward large-scale coherent patterns in the intact thalamocortical system. Fine-scale recording from local areas of the thalamus and measurements of the fine-time structure of the initiation of the oscillation (see below) might reveal wave propagation.

Evoked traveling waves have been observed in the intact thalamocortical system using low-intensity electrical stimulation of the cortex (61). This stimulus typically evoked oscillations that propagated away from the stimulation site. Distant recording sites began oscillating after a delay proportional to the distance from the stimulation site, but within the oscillation, all sites were synchronized. This type of propagating wave was seen both in local field potentials and in multiunit activity (61). It was not dependent on intracortical horizontal connections, because a deep coronal cut did not affect the traveling patterns (61), suggesting that they depend mainly on thalamocortical loops. These observations were all reproduced in computational models (100), in which the stimulation activated a local cortical area, which progressively recruited the entire network through successive cortico-thalamo-cortical loops.

4. The contribution of cortico-cortical connectivity to large-scale coherence

The evidence presented above suggests that the large-scale synchrony of spindle oscillations arises from the mutual interactions between cortex and thalamus. These experiments were performed during barbiturate anesthesia, which could be different in nonanesthetized preparations. In early experiments, interhemispheric synchrony was reduced in cats following section of the corpus callosum (41), suggesting that at least some intracortical connections are important. This aspect was quantified in a series of studies that compared the patterns of cortical spindles in natural sleep before and after artificial depression of cortical activity (62, 102). During natural sleep, spindle oscillations are characterized by a high coherence and initiate almost simultaneously in cortical sites up to 7 mm apart. Under barbiturate anesthesia, the initiation is less precise, and signs of propagating activity are visible in the first 500 ms of the oscillatory sequences.

Interestingly, similar patterns of imprecise initiation could be reproduced during natural sleep after cortical depression (102). These differences were also apparent in spatiotemporal maps of activity as well as in patterns of cross-correlations (102). Finally, it was observed that a synchronous negative EEG deflection always precedes spindles during natural sleep in cats, but is absent in barbiturate anesthesia or when the cortex has been depressed (62). Taken together, these experiments suggest that during natural sleep, the large-scale synchrony is further enhanced by intracortical interactions.

A thalamocortical network model was proposed to account for these observations (102). The hypothesis was that spindles are more coherent during natural sleep because of higher cortical excitability due to neuromodulatory drive. In the early phases of natural sleep, during which most spindles occur, the level of discharge of activating systems from brain stem, basal forebrain, and posterior hypothalamus is still relatively high (311). The model incorporated in vitro data (222) on the effect of neuromodulators such as ACh, 5-HT, and NE on reducing leak and voltage-dependent K^+ currents. In control conditions, the model displayed coherence similar to that observed during barbiturate spindles (see above), which correspond to unaffected leak and K^+ conductances, as expected from states of low levels of neuromodulation such as barbiturate anesthesia. When a downregulation of these ion channels was simulated, representing the moderate neuromodulatory drive during early stages of sleep, cortical excitatory neurons were depolarized and their excitability was augmented. The spindle oscillations during this state of moderate downregulation showed highly coherent patterns similar to those that occur during natural sleep. The augmented coherence was due to several factors (102): *1*) facilitation of the intracortical spread of excitatory discharges, *2*) augmented responsiveness of cortical neurons to thalamic EPSPs, and *3*) more powerful and more coherent feedback of the cortex to the thalamus.

Models thus predict that highly coherent patterns of oscillation in the cortex can be generated by cortex-thalamus-cortex loops in which the excitability of cortical neurons are enhanced due to partial downregulation of their K^+ channels by neuromodulators. Experiments and models provide converging evidence that the cortex is intimately involved in triggering and synchronizing oscillations generated in the thalamus through corticothalamic feedback projections. If cortical excitability is further augmented, the system may generate pathological activity, such as absence seizures, as analyzed below.

B. Pathological Behavior: Absence Seizures

The model of thalamocortical interactions that has been developed for understanding spindle oscillations,

without any additional mechanisms, also accounts for the activity that occurs during pathological states, such as some forms of spike-and-wave seizures. We discuss here the experimental evidence that the thalamus is involved in generating paroxysmal rhythms, and how models provide insights into plausible network mechanisms for generating seizures, as well as possible ways to suppress them.

1. Thalamic and cortical contributions to generalized seizures

Absence or "petit-mal" seizures, which are particularly common in children, are spontaneous, generalized, and accompanied by a brief loss of consciousness that typically lasts a few seconds. High-amplitude spikes in the EEG alternate with slow positive waves at a frequency of ~3 Hz (241). These generalized "spike-and-wave" seizures appear suddenly and invade the entire cerebral cortex nearly simultaneously. Similar spike-and-wave EEG patterns are observed in other neurological disorders as well as in experimental models of absence seizures in cats, rats, mice, and monkeys.

The large-scale synchrony observed during absence seizures and their sudden appearance suggest that they are generated in a central structure projecting widely to the cerebral cortex. The involvement of the thalamus in spike-and-wave seizures was initially proposed by Jasper and Kershman (173) and is now supported by several findings. First, in simultaneous thalamic and cortical recordings in humans during absence attacks, thalamic participation was directly demonstrated (360). Second, thalamic activation in human absence seizures was observed with positron emission tomography (255). Third, electrophysiological recordings in experimental models of spike-and-wave seizures support a strong thalamic involvement. Cortical and thalamic cells fire prolonged discharges in phase with the "spike" component, while the "wave" is characterized by silence in all cell types (16, 48, 168, 229, 254, 273, 293, 294). Electrophysiological recordings also indicate that spindle oscillations, which are generated by thalamic circuits (see sect. IIIC), can be gradually transformed into spike-and-wave activity and that any intervention that promotes or antagonizes spindles has the same effect on spike-and-wave oscillations (186, 187, 229). Finally, spike-and-wave patterns disappear following thalamic lesions or inactivation (15, 248, 341).

These observations suggest a direct involvement of the thalamus in seizure activity. Other experiments, however, indicate that the cortex is also involved. Thalamic injection of high doses of $GABA_A$ antagonists, such as penicillin (130, 258) or bicuculline (302, 52), lead to highly synchronized 3- to 4-Hz oscillations, but not to spike-and-wave discharge. On the other hand, injection of the same drugs into the cortex, without altering the thalamus, re-

sulted in full-blown spike-and-wave seizures (130, 302). The threshold for epileptogenesis was extremely low in the cortex compared with the thalamus (302). Finally, a diffuse application of a dilute solution of penicillin to the cortex produced spike-and-wave seizures although the thalamus was intact (130) (Fig. 13A).

A form of spike-and-wave activity that is intracortically generated has been observed in cats. In seizures occurring during ketamine-xylazine anesthesia, or in seizures induced by focal application of bicuculline to the cortex, a large proportion (60%) of TC cells is steadily hyperpolarized, suggesting few thalamic participation to these seizures. Indeed, a slow type of spike and wave (1.8–2.5 Hz), with a less prominent "spike" component, was recorded in the isolated cortex or athalamic preparations after administration of convulsants in cats (219, 248, 302). However, this type of intracortical spike and wave appears not to occur in rats (341) and has never been reported in neocortical slices. It has been argued that these seizures may represent an experimental analog of the "Lennox-Gastaud" syndrome (297), which also presents spike-and-wave or poly-spike-wave patterns similar to these preparations. Further experiments are certainly needed to characterize the differences between intracortical and thalamocortical spike-and-wave activity and explain why it appears in cats but not in rats.

In summary, some experimental models of absence seizures suggest that spike-and-wave patterns typically require both cortex and thalamus, whereas other experimental models show a type of slow spike-and-wave activity that is generated intracortically. It is difficult to know where to begin to sort out the different mechanisms that underlie these observations. Computational models have proven to be quite helpful in exploring possible mechanisms underlying these different oscillations, as shown below.

2. The receptor types involved in seizure activity

The fact that $GABA_A$ antagonists are powerful convulsants shows that the inhibition mediated by $GABA_A$ receptors is central in seizure generation. However, the removal of $GABA_A$ inhibition cannot by itself explain the oscillatory mechanism during seizure activity, and a series of experiments point to a critical role for $GABA_B$ receptors as well in the genesis of spike-and-wave oscillations. First, $GABA_B$ agonists exacerbate seizures, while $GABA_B$ antagonists diminish or suppress them in rats (159, 257, 285, 286). Furthermore, blocking $GABA_B$ receptors in thalamic nuclei leads to the suppression of spike-and-wave seizures (200). Second, in rat thalamic slices, the anti-absence drug clonazepam diminished $GABA_B$-mediated inhibition in TC cells, reducing their tendency to burst in synchrony (164). Clonazepam potentiates $GABA_A$ receptors in the RE nucleus (128, 160, 164). Indeed, there
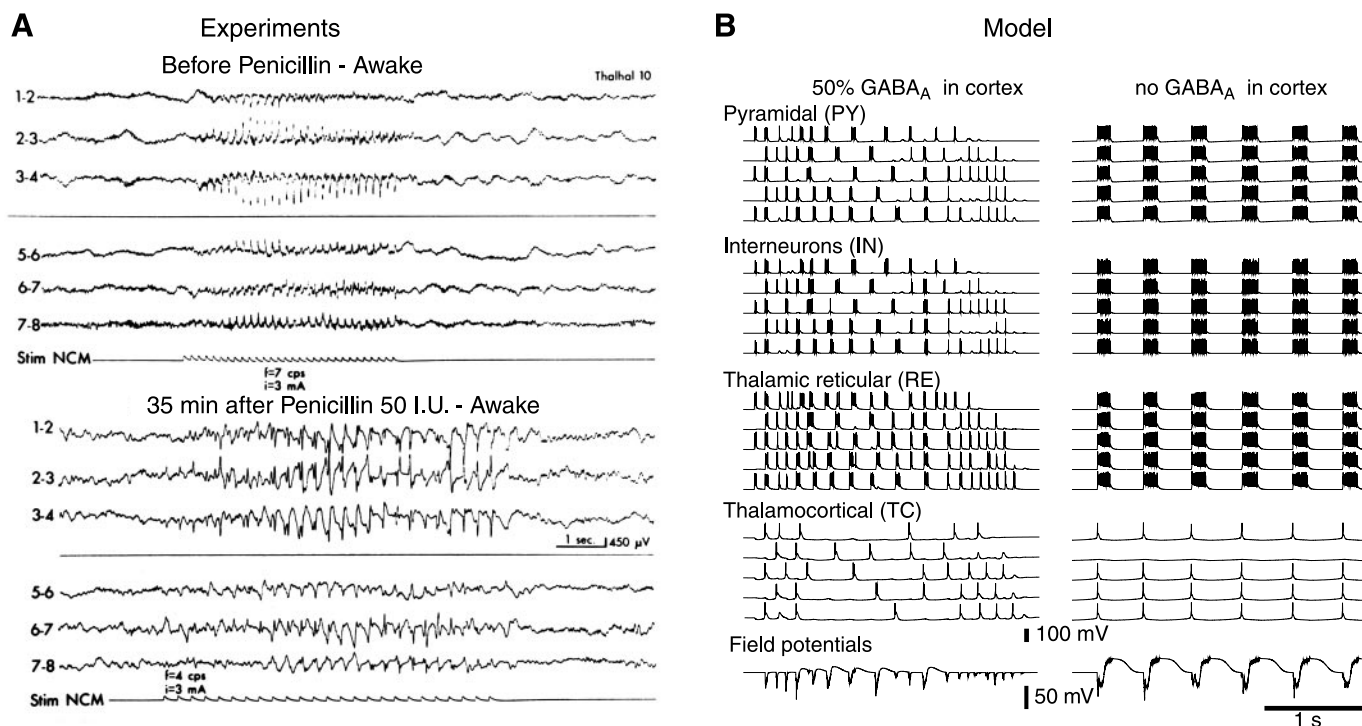
FIG. 13. The 3-Hz spike-and-wave discharges obtained by altering cortical inhibition. *A*: spike-and-wave discharges following diffuse application of penicillin to the cortex of cats. *Top:* stimulation of nucleus centralis medialis (NCM; 7 Hz) induced a recruiting response in the cortex. *Bottom:* after diffuse application of a diluted solution of penicillin to the cortex (50 IU/hemisphere) in the same animal, 4-Hz stimulation of NCM elicited bilaterally synchronous spike-and-wave activity. Similar spike-and-wave discharges also occurred spontaneously. [Modified from Gloor et al. (130).] *B*: computational model of the transformation of spindle oscillations into ~3 Hz spike-and-wave by reducing cortical inhibition. A thalamocortical network of 400 neurons was simulated, and 5 cells of each type are shown from *top* to *bottom*. The last traces show the field potentials generated by the array of pyramidal neurons. *Left*: 50% decrease of GABA$_A$-mediated inhibition in cortical cells. The oscillation begins like a spindle, but strong burst discharges appear after a few cycles, leading to large-amplitude negative spikes followed by slow positive waves in the field potentials. *Right*: fully developed spike-and-wave oscillations following suppression of GABA$_A$-mediated inhibition in cortical cells. All cells had prolonged, in-phase discharges, separated by long periods of silence, at a frequency of ~2 Hz. GABA$_B$ currents were maximally activated in TC and PY cells during the periods of silence. Field potentials displayed spike-and-wave complexes. Thalamic inhibition was intact in *A* and *B*. [Modified from Destexhe (86).]

is a diminished frequency of seizures following infusion of GABA$_A$ receptor agonists in the RE nucleus in rats (199). Third, in ferret thalamic slices, spindle oscillations can be transformed into slower and more synchronized oscillations at ~3 Hz following block of GABA$_A$ receptors (346) (Fig. 14*A*). This behavior is reminiscent of the gradual transformation of spindles into the spike-and-wave discharges in cats found by Kostopoulos and co-workers (186, 187). Similar to the spike-and-wave oscillations in rats, the ~3-Hz paroxysmal oscillations in ferret thalamic slices are suppressed by GABA$_B$ receptor antagonists (346) (Fig. 14*A*).

Although GABA$_B$ receptors seem to play a crucial role in seizures, there seems to be critical differences between experimental models. In the cat penicillin model of absence epilepsy, the spike-and-wave oscillation frequency is ~3 Hz, as in humans; however, GABA$_B$ receptor involvement was never investigated. Ferrets also show ~3-Hz paroxysmal oscillations that are also dependent on GABA$_B$ receptors, but so far it has been described only in thalamic slices. In rats, however, the spike-and-wave oscillations occur at a faster frequency (5–10 Hz) that is inconsistent with the slow kinetics of GABA$_B$-mediated IPSPs (~300 ms). Indeed, intracellular recordings in the generalized absence epilepsy rat from Strasbourg (GAERS) show that thalamic neurons are paced by GABA$_A$ IPSPs (251), consistent with the exacerbation of seizures by GABA$_A$ agonists in rats (160, 342). However, GABA$_B$ receptors must somehow participate in the maintenance of the paroxysmal oscillation, as suggested by the protective effects of GABA$_B$ antagonists (200).

These experiments show that a complex interplay of GABA$_A$ and GABA$_B$ conductances is probably involved in generating spike-and-wave discharges, but the exact mechanisms are unclear. In the next sections, we review models for thalamic ~3-Hz paroxysmal oscillations and for thalamocortical oscillations with spike-and-wave field potentials at either 3 or 5–10 Hz.
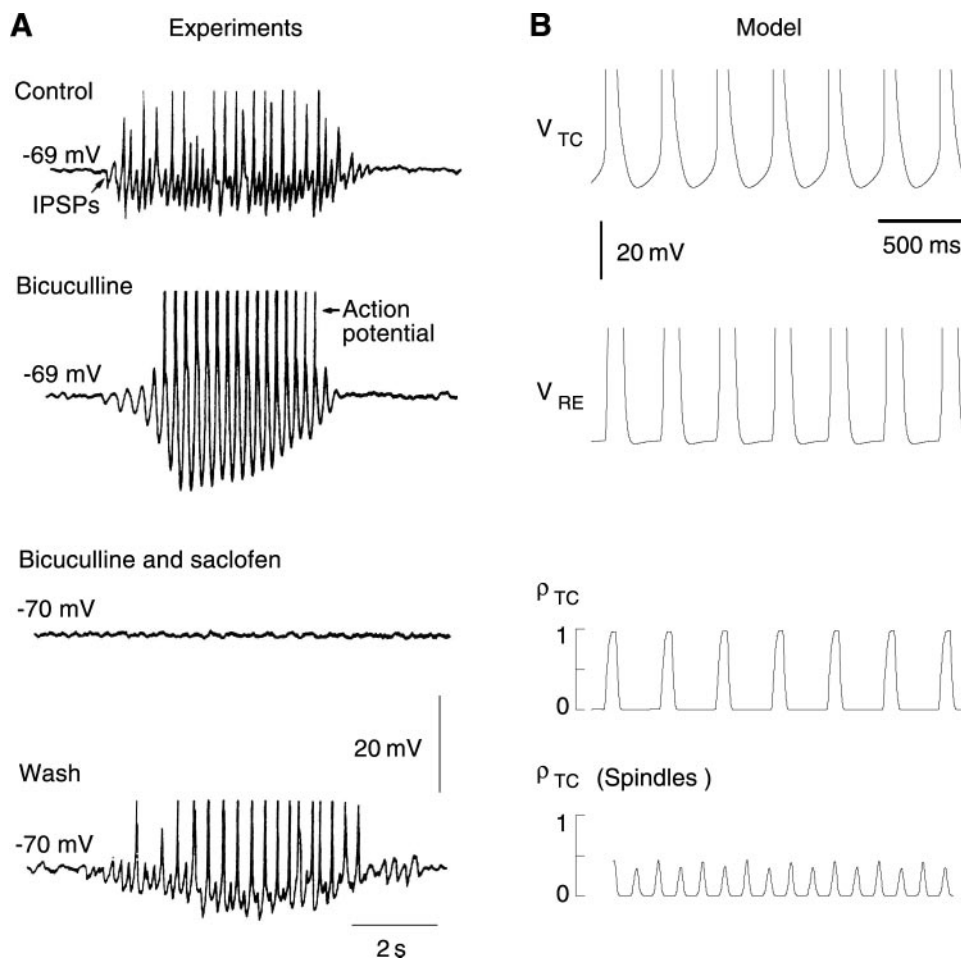
FIG. 14. Slow thalamic oscillation after suppression of GABA$_A$-mediated inhibition. *A*: intracellular recording of a relay neuron in the dorsal lateral geniculate nucleus in ferret thalamic slices during spindle waves. Blocking GABA$_A$ receptors by bath application of bicuculline (second trace) slowed the oscillation to 2–4 Hz and markedly increased rebound burst activity. Further application of the GABA$_B$ receptor antagonist saclofen abolished this slow oscillation (third trace). Recovery after washout of antagonists shows that these effects are reversible (last trace). [Modified from von Krosigk et al. (346).] *B*: computational model of the 3-Hz thalamic oscillation in thalamic networks. The graphs show (from *top* to *bottom*) a representative example of the membrane potential of TC and RE cells (V_{TC}, V_{RE}), the fraction of TC cells (ρ_{TC}) active as a function of time during slow oscillations, as well as during spindle oscillations for comparison (bottom graph). In control conditions, the network generated 6- to 7-Hz spindle oscillations (shown in Fig. 6*B*). After suppressing GABA$_A$ receptors, the circuit showed a slow 2- to 3-Hz oscillation, which was more synchronized than spindle oscillations (see ρ_{TC} in bottom graphs). [Modified from Wang et al. (353).]

3. Models of paroxysmal discharges in the thalamus

Models of spike-and-wave oscillations first addressed the progressive transformation of spindle oscillations into synchronized 3-Hz oscillations following blockade of GABA$_A$ receptors in the thalamus (96, 105, 136, 349, 353). An early model (105) replicated the transformation of spindles into slow 3-Hz oscillations by slowing the decay of GABAergic currents, but this model did not investigate the presence of two types of GABAergic receptors. In another model, disinhibition of interneurons projecting to TC cells with GABA$_B$-specific connections resulted in stronger discharges when GABA$_A$ receptors are antagonized, as proposed by Soltesz and Crunelli (289). This model included TC, RE, and interneurons (349) and reproduced the stronger discharges in TC cells following application of bicuculline. Although it is possible that this mechanism plays a role in thalamically generated epileptic discharges, it does not account for experiments showing the decisive influence of the RE nucleus in preparations devoid of interneurons (164, 165). Increased synchrony and stronger discharges occurred in another model (353), but the synchronous state coexisted with a desynchronized state of the network, which has never

been observed experimentally. Full agreement with experimental data was obtained only when the cooperative activation proposed for GABA$_B$ receptors (106a) was included. Network models including this cooperative activation (96, 136) produced robust synchronized oscillations and traveling waves at the network level, similar to those observed in thalamic slices (182). This property also led to the transformation of spindles to $\sim$3-Hz paroxysmal oscillations following block of GABA$_A$ receptors.

These two modeling studies concluded that the transition from spindle to paroxysmal 3-Hz oscillations can be achieved provided there was cooperativity in GABA$_B$ responses (96, 136). GABA$_B$ responses must depend nonlinearly on the presynaptic pattern of activity; they are elicited only under intense stimulation conditions, for example, after long presynaptic bursts of spikes. The nonlinear activation properties of this response were modeled by an intracellular second messenger system involving multiple G protein bindings to activate the K$^+$ channels associated with GABA$_B$ receptors (106a). This mechanism can account for the different patterns of GABA$_B$ responses observed in the hippocampus (75, 109) and in the thalamus (165, 183). The prediction that the GABA$_B$ nonlinearity is

a property intrinsic to the kinetics of these receptors is consistent with the nonlinearity found in single-axon $GABA_B$ responses in thalamic (183) and neocortical slices (327).

The action of the antiabsence drug clonazepam in rat thalamic slices (164) can also be explained using the nonlinear activation of $GABA_B$ responses (106a). Clonazepam, by reinforcing $GABA_A$-mediated interactions in the RE nucleus, diminishes the number of spikes produced by RE cells and therefore will diminish the tendency of RE cells to activate $GABA_B$ responses in TC cells. A similar mechanism was explored in another modeling study (325), which reported that agents augmenting the $GABA_A$-mediated inhibition in the RE nucleus act as desynchronizers by reducing the IPSP on TC cells, and thereby reduce TC cell's firing probability. This model also indicated that substances such as benzodiazepines may exert their effects through an increase of inhibition in the RE nucleus. Another model (215) suggested that antidromic activation must be taken into account for reproducing in detail the effect of clonazepam in thalamic slices.

The genesis of the slow thalamic oscillation is based on a mechanism opposite to that of clonazepam. The $GABA_A$ antagonist bicuculline suppresses inhibitory interactions between RE cells,[5] allowing them to produce large burst discharges. These bursts constitute the optimal signal to activate $GABA_B$ receptors in TC cells, which are maintained hyperpolarized for ~300 ms, then produce a rebound LTS at the offset of the $GABA_B$ IPSP that reexcites RE cells, and restarts the cycle. A similar oscillatory mechanism was found by several modeling studies (96, 105, 136, 353) that successfully reproduced the oscillation found in thalamic slices following suppression of $GABA_A$ receptors. This slow thalamic oscillation is depicted in Figure 14B, which illustrates the augmented synchrony of thalamic neurons compared with that during spindle oscillations (see bottom graphs; also compare with Fig. 6B). In the next sections, we review biophysical mechanisms that were proposed to link this slow paroxysmal oscillation in the thalamus with spike-and-wave seizures.

4. Model of absence seizures in the thalamocortical system

Evidence from a number of experimental studies indicates that the paroxysmal thalamic 3-Hz oscillation discussed above is a phenomenon distinct from spike-

and-wave seizures. Injections of $GABA_A$ antagonists into the thalamus with the cortex intact failed to generate spike-and-wave seizures (130, 258, 302). In these in vivo experiments, suppressing thalamic $GABA_A$ receptors led to "slow spindles" around 4 Hz, quite different from spike-and-wave oscillations (Fig. 15A). On the other hand, spike-and-wave discharges were obtained experimentally by diffuse application of $GABA_A$ antagonists to the cortex (130) (Fig. 13A). In these in vivo experiments, spindles were transformed into spike-and-wave discharges by altering cortical inhibition without changes in the thalamus. We review below models that explored possible mechanisms to explain these observations and to relate them to the 3-Hz thalamic oscillation (86).

To investigate this problem, it is necessary to compare the field potentials generated by a thalamocortical model in different conditions (86). Altering thalamic $GABA_A$-mediated inhibition in the model slowed the spindle oscillations from ~10 to ~4 Hz (Fig. 15B). Calculation of the extracellular field potentials generated by the array of cortical neurons (see methods in Ref. 86) showed that both of these oscillation types displayed negative deflections (Fig. 15B, *bottom traces*), in agreement with experiments. Thus selectively altering thalamic inhibition generated field potential patterns similar to spindles at the level of the cortex, but no spike-and-wave patterns. This occurs because in both conditions, pyramidal neurons are under strict control of cortical inhibition and fire moderate discharge patterns, generating negative deflections in field potentials.

In contrast, when $GABA_A$-mediated cortical inhibition was selectively altered in the model, prolonged discharges occurred that were strongly reflected in the field potentials. Reduction of intracortical $GABA_A$ conductances to 50% of their normal values increased the occurrences of prolonged high-frequency discharges during spindle oscillations (Fig. 13B, *left panel*). Further decrease in intracortical fast inhibition led to highly synchronized and prolonged discharges, which generated spike-and-wave patterns in the simulated field potentials (Fig. 13B, *right panel*). This agrees with experiments in cats showing that spike-and-wave oscillations can be obtained from a diffuse application of the $GABA_A$ antagonist penicillin to the cortex, with no change in the thalamus (130). In the model, the spike-and-wave field potentials consisted of one or several negative/positive sharp deflections, followed by a slowly developing positive wave (Fig. 13B, *bottom traces*). During the "spike," all cells fired prolonged high-frequency discharges in synchrony, while the "wave" was coincident with neuronal silence in all cell types. This portrait is typical of experimental recordings of cortical and thalamic cells during spike-and-wave patterns (16, 48, 168, 229, 254, 273, 293, 294). Some TC cells remained hyperpolarized during the entire oscillation (second TC cell in Fig. 13B, *right panel*), as also observed

---

[5] Bicuculline was later shown to also block the apamin-sensitive calcium-dependent current in RE cells (76). Because this current is important for controlling burst generation in RE cells (17), bicuculline therefore does not exert specific effects on $GABA_A$ receptors. Other antagonists are used, such as picrotoxin, that also induce slow thalamic oscillations, showing that this oscillation is generated through antagonist actions on $GABA_A$ receptors in the RE nucleus (266).
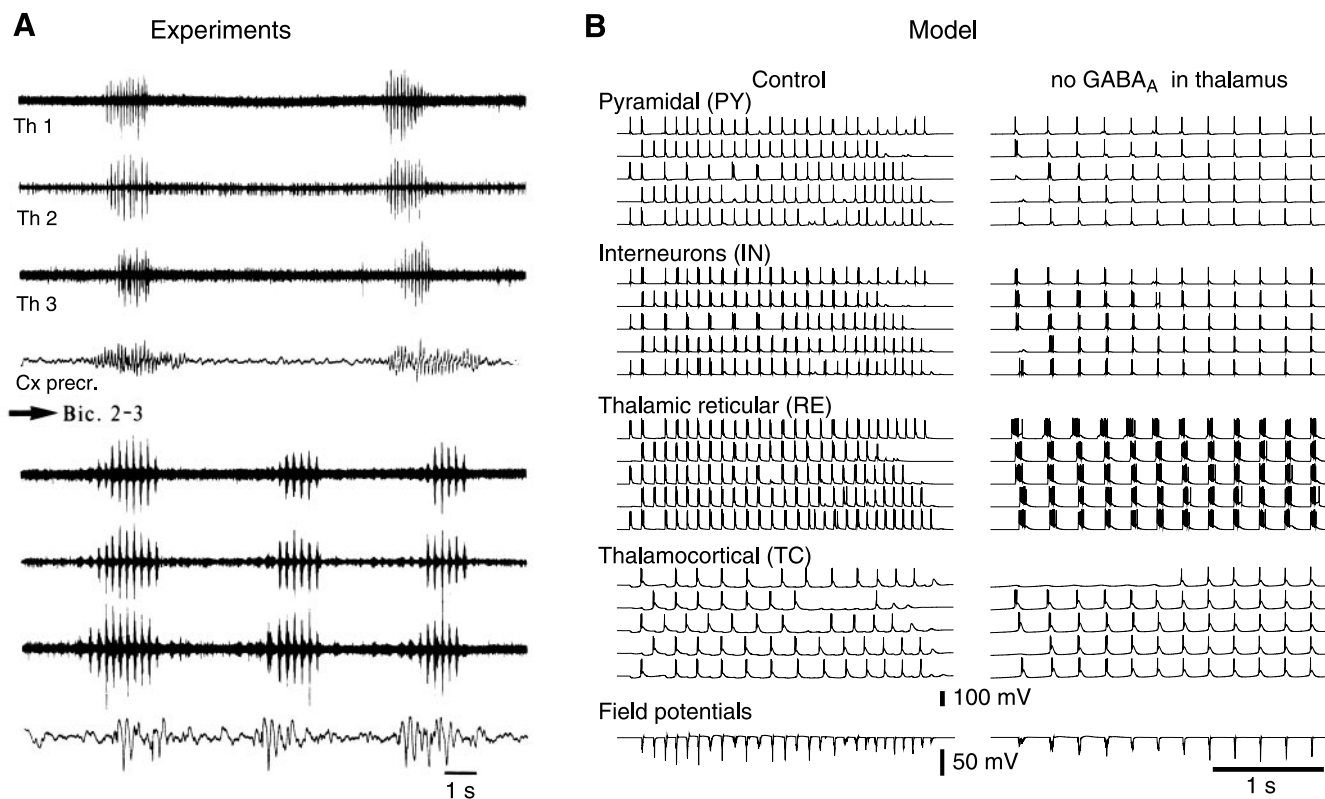
FIG. 15. Block of thalamic GABA$_A$ inhibition does not generate spike-and-wave. *A*: local injection of bicuculline in the thalamus of a cat under barbiturate anesthesia. *Top:* before injection, three thalamic multiunit recordings (Th1-Th3) from foci separated by 2 mm revealed bursts of action potentials corresponding to spindle oscillations. These oscillations are also reflected in the EEG from the ipsilateral pericruciate cortex (Cx prec.). *Bottom*: injection of bicuculline between electrodes 2 and 3 increased the number of action potentials per burst and reduced the oscillation frequency from 10 to ~4 Hz. This reduced frequency was reflected in the EEG, but no spike-and-wave discharges were observed. [Modified from Steriade and Contreras (302).] *B*: suppression of thalamic GABA$_A$ inhibition in a computational model of the thalamocortical system. *Left:* spindle oscillations in the thalamocortical network in control conditions. The field potentials, consisting of successive negative deflections at ~10 Hz, are shown at the *bottom*. *Right*: oscillations following the suppression of GABA$_A$-mediated inhibition in thalamic cells with cortical inhibition intact. The network generated synchronized oscillations at ~4 Hz, with thalamic cells displaying prolonged discharges. The discharge pattern of PY cells resembled spindles but at a lower frequency, as reflected in the field potentials (*bottom*). [Modified from Destexhe (86).]

experimentally (301; see Ref. 216 for a detailed computational model of this condition). The transformation between spindle oscillations and spike-and-wave patterns was continuous (86), as observed in experiments (186, 187). Similar patterns arose when GABA$_A$ receptors were suppressed in the entire network (data not shown).

A slow 2- to 4-Hz frequency oscillation in this model could be elicited by a cortically induced activation of GABA$_B$ receptors in the thalamus. Because of the increase of cortical excitability, the feedback from the cortex onto the thalamus was exceedingly strong, forcing RE cells to fire large burst discharges, which activate full-blown GABA$_B$-mediated responses in TC cells (86). As shown above (see Fig. 11 in sect. IV*A*), moderate activation of corticothalamic synapses can trigger oscillations in thalamic circuits (if correctly timed with respect to their refractory period). However, when corticothalamic synapses were strongly activated, they triggered pro-

longed high-frequency bursts of action potentials in RE cells, which in turn activated GABA$_B$ currents in TC cells. Large burst discharges were indeed observed in RE cells during seizures in GAERS (283). Models therefore predict that strong cortical inputs are able to switch the intact thalamic circuits to a slow oscillatory mode at ~3 Hz. This cortically induced switch of thalamic oscillatory mode was also found experimentally in thalamic slices (see sect. IV*B5*).

In another modeling study of cortical circuits during the transformation of spindle to seizure activity (13), frequency switch from 10 Hz (spindle) to 3 Hz (seizure) occurred because of mechanisms intrinsic to the cortex (13), rather than a switch in the cortical drive to the thalamus as studied in the model described above (86). This assumed that there are no interconnections between interneurons (13). Under these conditions, rhythmic inputs from the thalamus can lead to prolonged discharges

in cortical cells and longer lasting inhibition when the cortex was hyperexcitable, presumably leading to spike-and-wave EEG patterns (although the authors did not confirm this with simulated field potentials). This study also did not include the different GABAergic and glutamatergic receptor types, nor any explicit representation of the intrinsic properties of thalamic neurons. Although the thalamocortical loop was involved in the model, no precise mechanisms were given on how the 3-Hz cortical activity entrained the thalamus at this frequency.

In a thalamocortical model of 3-Hz spike-and-wave seizures (86), the mechanisms for seizure generation depend on a thalamocortical loop where both cortex and thalamus are necessary, but none of them generates the 3-Hz rhythmicity alone. The cycle starts with the genesis of a rebound burst in TC cells, which triggers strong discharges in cortical PY cells and interneurons; the cortical discharge also triggers large bursts in RE neurons so that all cell types fire nearly at the same time, corresponding to "spike" component of the EEG. There is a slight phase advance for TC cells, as observed experimentally in rats (168, 273). Following these concerted discharges, all cell types become silent for ~300 ms. Cortical cells are silenced by the progressive activation of GABA$_B$-mediated and intrinsic voltage-dependent K$^+$ currents. In the thalamus, the large bursts of RE cells elicit a mixture of GABA$_A$ and GABA$_B$ conductances in TC cells, which keep them hyperpolarized for ~300 ms before they rebound and start the next cycle.

Besides reproducing the 3-Hz spike-and-wave oscillations, this mechanism has a number of interesting properties. First, the model was sensitive to intra-RE GABA$_A$ inhibition (86). Reinforcing those connections augmented the threshold for seizure, consistent with the presumed role of the antiabsence drug clonazepam, which may reduce the tendency of the network to produce spike and wave by specifically acting on GABA$_A$ receptors in the thalamic RE nucleus (128, 160, 164). Second, diminishing the AMPA conductance of cortical EPSPs on RE cells significantly shifted the balance from spike-and-wave oscillations in favor of spindles (86). There is as yet no way to selectively targets these synapses. Third, reducing the I_T conductance in RE cells significantly reduced spike-and-wave activity and increased spindle activity (86). This is consistent with the experimental finding that the I_T is selectively increased in RE cells in a rat model of absence epilepsy (333). This conductance affects the oscillation synchrony (324). Fourth, the frequency of spike-and-wave discharges could be effectively controlled by GABA$_B$-mediated IPSPs on TC cells (86). This occurred because, in this model, the duration of the "wave" was mainly determined by GABA$_B$ IPSPs in TC cells, longer IPSPs leading to slower spike-and-waves by further delaying the rebound of TC cells. The frequency varied from 1 to 5 Hz for decay values varying from 50 to 250% of the control value.

These simulations suggest that the different frequencies of the spike-and-wave oscillations in different experimental models may be a consequence of different balances between GABAergic conductances in TC cells. This hypothesis was tested in models by varying these conductances (87). The same model showed a continuum of oscillations, ranging from ~2 to 11 Hz, all of which display spike-and-wave field potentials. In particular, a "fast" (5–10 Hz) type of spike-and-wave oscillation could be observed with intact thalamus but decreased cortical inhibition (87). The mechanism of this oscillation was similar to that depicted above, except that TC cells were paced by GABA$_A$ conductances, as observed experimentally during the fast spike-and-wave oscillations in the GAERS rat (251). The only difference was that this model had stronger GABA$_A$ conductances and weaker GABA$_B$ conductances in TC cells (see details in Refs. 87, 106b).

Finally, models have also been used to investigate mechanisms for intracortical spike-and-wave oscillations. There is a form of spike-and-wave discharge in isolated cortex or athalamic preparations in cats (219, 248, 302). This type of paroxysmal oscillation has a lower 1- to 2.5-Hz frequency and a morphology that is different from that of the typical "thalamocortical" spike-and-wave oscillation (103, 248). Intracortical spike-and-wave discharges have not been observed in athalamic rats (341) and have never been reported in neocortical slices. In the model, if a subset of pyramidal cells had LTS activity, as observed in some cortical areas (103, 79), then isolated cortical networks could sustain a form of purely cortical spike-and-wave discharges, displaying a sequence of GABA$_B$ IPSP and rebound bursts, similar to the mechanism analyzed above. A small number of LTS pyramidal cells were sufficient to generate paroxysmal oscillations with spike-and-wave field potentials in the disinhibited isolated cortex (103). The spike-and-wave oscillations in this model, as in experiments, had a lower frequency (1.8–2.5 Hz) and a different shape from those in the thalamocortical model. Similar findings were also reported recently in a model of cortex consisting of interconnected pyramidal neurons and interneurons (329). This model included an I_h current in pyramidal neurons and the elevated extracellular K$^+$ concentration in the epileptic focus, leading to particularly strong rebound properties of I_h-containing pyramidal neurons, entraining the network in slow hypersynchronized oscillations.

5. Control of thalamic oscillations by corticothalamic feedback

The central mechanism proposed for the genesis of thalamocortical spike and wave predicts that cortical inputs can force physiologically intact thalamic circuits to oscillate at ~3 Hz (see above). To test this prediction in

thalamic slices, one must reconstitute the thalamus-cortex-thalamus loop. This can be accomplished with a dynamic clamp that forms an artificial feedback loop between the TC neurons and the stimulation of corticothalamic fibers (Fig. 16A) (18, 31, 86). This technique was first simulated using a model network of 100 PGN and 100
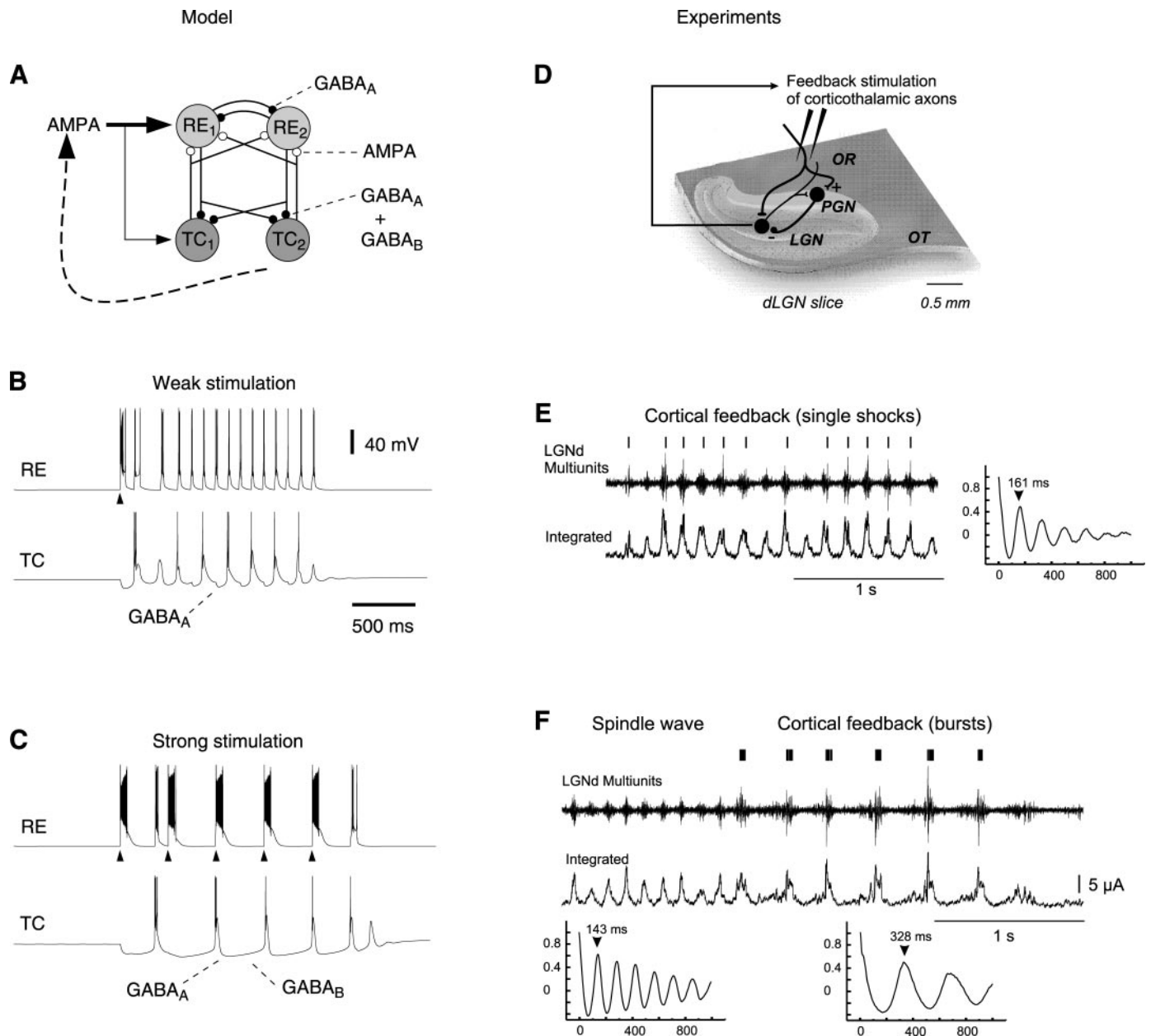
FIG. 16. Cortical feedback can control the frequency and synchrony of thalamic oscillations. A: computational model prediction that cortical feedback can force intact thalamic circuits to oscillate at 3 Hz. A scheme of connectivity and receptor types in a circuit of thalamocortical (TC) and thalamic reticular (RE) neurons is shown. Corticothalamic feedback was simulated through AMPA-mediated synaptic inputs (shown on the *left* of the connectivity diagram) and could be directly triggered by the discharge of TC cells. [Modified from Destexhe (86).] B: a single stimulation of corticothalamic feedback (arrow) entrained the circuit into a 10-Hz mode similar to spindle oscillations. C: after 3-Hz stimulation with high intensity (arrows; 14 spikes/stimulus), RE cells were recruited into large bursts, which evoked IPSPs onto TC cells dominated by GABA_B-mediated inhibition. In this case, the circuit could be entrained into a different oscillatory mode, with all cells firing in synchrony. D: implementation of this paradigm in thalamic slices. Stimulating electrodes were placed in the optic radiation (OR), which contains corticothalamic axons connecting thalamocortical cell in the LGN layers and GABAergic interneurons in the perigeniculate nucleus (PGN). E: weak (single shock) stimulation at a latency of 20 ms after the detection of multiunit bursts activity (*top trace*). *Bottom trace*: smooth integration of the multiunit signal. F: a 7-Hz control spindle is robustly slowed to 3-Hz oscillation by the feedback stimulation (5 shocks, 100 Hz, 20-ms delay). [Modified from Bal et al. (18).]

LGN cells interconnected via AMPA, $GABA_A$, and $GABA_B$ receptors. The spike activity of one TC cell was used to trigger the stimulation of corticothalamic EPSPs across the entire network. A burst of action potential in the trigger TC cell started a high-frequency (100 Hz) burst of AMPA-mediated corticothalamic EPSPs in RE and TC neurons. The strength of the feedback stimulation was adjusted by controlling the number of corticothalamic EPSPs (number of shocks).

For mild feedback (1–4 shocks), the pattern of TC and RE discharge was typical of spindle oscillations (Fig. 16B). Individual TC cells showed subharmonic bursting activity and were not tightly synchronized. The presence of the feedback did not disrupt the spindle oscillations and only slightly increased the synchrony of TC cells. When the number of stimuli was increased to more than five shocks, the pattern of bursting changed qualitatively and the network switched to slow (2–4 Hz) oscillations (Fig. 16C). In this case the degree of synchrony was higher than spindles because all cells fired within the same phase of the oscillation. This activity is consistent with the previous model, in which the entire system switched to synchronized 3-Hz oscillations in the presence of an abnormally strong corticothalamic feedback (86).

Recent experiments performed in ferret thalamic slices (18, 31) have further verified the predictions of this model (Fig. 16, D–F). In these experiments, the activity of thalamic relay cells was used to trigger the electrical stimulation of corticothalamic fibers (Fig. 16D). With this feedback, the activity in the slice depended on the stimulus strength. For mild feedback, the slice generated normal spindle oscillations (Fig. 16E). However, for strong stimulation of corticothalamic fibers, the activity switched to slow synchronized oscillations at ~3 Hz (Fig. 16F). This behavior was dependent on $GABA_B$ receptors, as shown by its sensitivity to $GABA_B$ antagonists (18). These results suggest that strong corticothalamic feedback can force physiologically intact thalamic circuits to oscillate synchronously at 3 Hz. The same results were also obtained in another study (31).

Thus it seems that one of the key hypotheses for generating 3-Hz spike-and-wave oscillations is valid at least in the visual thalamus of ferrets. Excessively strong corticothalamic activation can force the intact thalamus to oscillate at 3 Hz. The model further indicates that this 3-Hz rhythm will lead to spike-and-wave field potentials, but only if the cortex is hyperexcitable. The large-scale synchrony of these oscillations is achieved using the same mechanism as described in section IVA2. Thus seizures and their highly synchronized EEG patterns can be explained by thalamocortical loops with a hyperexcitable cortex.

C. Computational Roles of Synchronized Oscillations

In this final section, we turn to experiments and models suggesting possible physiological roles for the slow oscillations.

1. Evidence for memory reprocessing during slow-wave sleep

Many studies have shown that REM sleep deprivation affects long-term memory (80, 118, 156). However, the effects of stress and REM deprivation were confounded in these studies (158, 282, 343). More recently, sleep deprivation studies have reported that slow-wave sleep may be involved in some forms of memory consolidation. The performance on visual discrimination tasks is significantly enhanced if the training period is followed by sleep, but the enhancement correlates most closely with slow-wave sleep (120, 124, 316, 317). Similar results were reported for ocular dominance plasticity during the critical period in kittens (121). Animals allowed to sleep for 6 h after a period of monocular stimulation developed twice the amount of brain change as those cats with the same stimulation kept awake in the dark for 6 h, consistent with earlier observations (167). Moreover, the amount of change was strongly correlated with the amount of slow-wave sleep and not with the amount of REM sleep. This is direct evidence that one function of slow-wave sleep is to help consolidate the effects of waking experience on cortical plasticity, converting memory into more permanent forms, as suggested previously (120, 235, 303). The different phases of sleep may have different impacts on memory consolidation, with the early part of slow-wave sleep and late part of REM sleep periods having more effect than other phases (reviewed in Ref. 316).

Another line of evidence implicates interactions between the hippocampus and the neocortex in consolidating declarative memories during sleep. Recordings from freely moving rats during wake and sleep states corroborate the idea that the hippocampus and the neocortex interact during sleep (46, 47, 239, 281, 318, 362). In these experiments, neurons that had neighboring place fields and fired together during exploration of a new environment became more highly correlated during subsequent sleep episodes compared with activity during previous sleep episodes. The correlated firing of neurons in the hippocampus during sleep may be a "played back" version of newly acquired experiences to the neocortex through feedback projections (46, 54, 220, 221, 281). Thus the neocortex during the wake state provides the hippocampal formation with a detailed description of the days events; during sleep, the hippocampus may recapitulate some version of these events to the neocortex, where permanent memory representations are gradually formed

over repeated episodes of synchronized slow-wave activity. This scenario is consistent with the finding that lesions limited to the hippocampus and surrounding regions produce memory impairment in monkeys and humans, but only recent memories are impaired while remote memories are intact (7, 374). Together, these experiments suggest that the hippocampal formation is required for memory storage for only a limited time period after learning. As time passes, its role in memory diminishes, and a more permanent memory gradually develops, probably in neocortex, that is independent of the hippocampal formation (34, 131, 178, 221, 292, 374). This gradual consolidation of information in the neocortex may occur during slow-wave sleep.

2. The spatiotemporal structure of slow-wave sleep

Although many experiments show that slow-wave sleep may be important for "off-line" memory reprocessing, there are few that reveal the underlying mechanisms. One of the difficulties is that slow-wave sleep is composed of several types of EEG oscillations, such as spindle (7–14 Hz), delta (1–4 Hz), and slower (0.3–1 Hz) oscillations. There is also evidence that slow-wave sleep contains brief periods during which faster (20–60 Hz) oscillations (beta and gamma range) occur, which are characteristic of wakefulness or REM sleep (see below).

During wakefulness, the EEG is dominated by low-amplitude fast oscillations (Fig. 17A, left panel). Several studies (101, 111, 139, 298) have shown that these fast oscillations are characterized by relatively low spatiotemporal coherence, as shown in the correlations which fluctuated in both space and time, only reaching high values occasionally and only for neighboring sites (Fig. 17B, left panel). Analyzing the correlations between extracellularly recorded units and local EEG revealed that units fired tonically, and wave-triggered averages showed that unit firing was correlated with the depth-EEG negativity (Fig. 17C, left panel). Similar characteristics were found for the fast oscillations during REM sleep (101).

In contrast to the fast oscillations of activated states, the EEG oscillations of slow-wave sleep are remarkably coherent across several millimeters in cortex (101) (Fig. 17A, middle panel). Consistent with this, correlations during slow waves stay high across wide regions of the cortex (Fig. 17B, middle panel). Remarkably, slow-wave complexes are correlated with a concerted decreased/increased firing in single units (Fig. 17C, middle panel). This shows that these high-amplitude EEG waves reflect a remarkably synchronized network dynamics consisting of a generalized silence followed by a concerted firing of the cells. Similar conclusions were drawn for delta waves in various preparations (22, 48, 123), for spontaneous slow oscillations under anesthesia (65, 331), as well as in cortical slices (267).

Perhaps the most interesting observation was that slow-wave sleep also contains a myriad of brief episodes of low-amplitude fast oscillations that are nested within slow-wave complexes (Fig. 17A, right panel). These "wakelike" episodes were observed during natural sleep in cats (101, 300) as well as in anesthetized animals (147, 363). Focusing specifically on these brief episodes showed that their spatial and temporal coherence are similar to the fast oscillations during wakefulness (Fig. 17B, right panel). This similarity applied to the relationship between the fast oscillations and unit discharges, which showed that the depth-negative EEG components are correlated with an increased probability of unit firing (Fig. 17C, right panels). Therefore, these brief wakelike episodes are electrophysiologically indistinguishable from the "sustained" fast oscillations of wake and REM sleep.

The observation that highly coherent slow-wave patterns alternate with brief episodes of low-coherence fast oscillations can be interpreted in several ways. Slow waves and fast oscillations might represent different states of responsiveness of cortical neurons and different receptive field properties (70, 112, 147, 363). We favor another interpretation (101, 106b), in which slow-wave sleep is viewed as a cyclic, iterating process leading to memory reprocessing (see below).

3. The impact of slow waves on cortical neurons

Much is known about the cellular mechanisms that generate spindle and the network mechanisms that control their synchrony. However, little has been done to investigate the impact that these oscillations might have on the cortical network. During spindles, TC neurons generate synchronized high-frequency bursts of action potentials, which are expected to have a strong impact on the cortical recipient neurons. However, intracellular recordings of cortical neurons during spindles do not reveal such a strong impact. Despite the potentially powerful nature of synchronized thalamic burst inputs, pyramidal neurons have a relatively low rate of discharge during spindle oscillations (63, 117, 295), as shown in Figure 18A. Intracellularly recorded pyramidal neurons in the suprasylvian gyrus of cats under barbiturate anesthesia showed that spindle oscillations in the EEG are paralleled with EPSP/IPSP sequences in cortical neurons (Fig. 18, Ai and Aii). These sequences were indistinguishable from that obtained from thalamic stimulation, suggesting that spindle-related IPSPs were triggered by thalamic inputs. To further characterize the IPSP component, dual intracellular recordings were performed in which one cell was recorded using a KCl-filled pipette. Cells recorded with chloride pipettes fired bursts of four to seven action potentials at 100 Hz with spike inactivation, in phase with spindle waves (Fig. 18Aiii). These experiments revealed
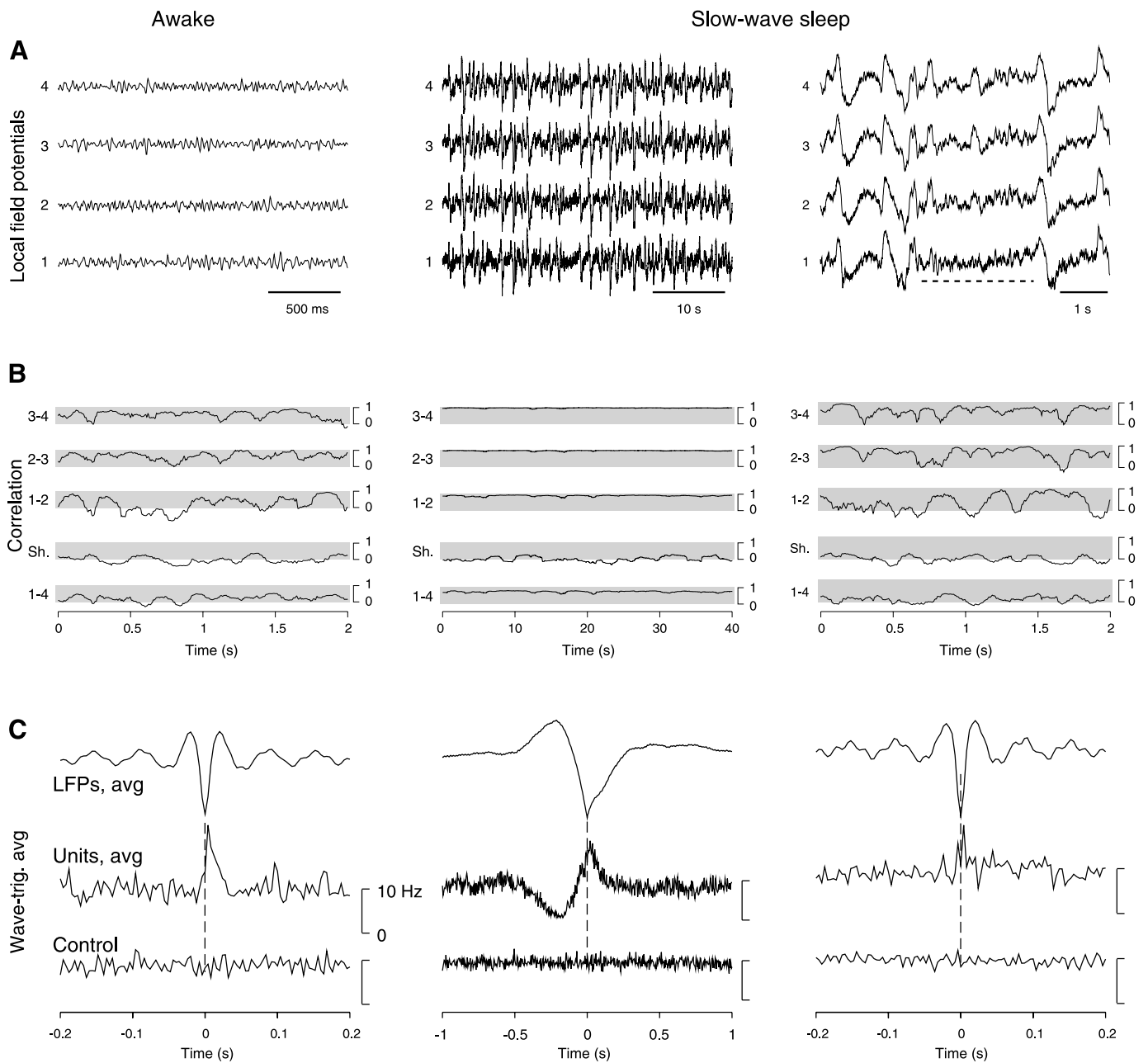
FIG. 17. Spatial and temporal coherence of wake and sleep oscillations. *A*: bipolar local field potential (LFP) recordings at 4 equidistant sites (1 mm interelectrode distance) in suprasylvian cortex of cats during natural wake (*left*) and slow-wave sleep states (*middle*; note different time scale). Awake periods consisted in low-amplitude fast (20–60 Hz) activity while slow-wave sleep was dominated by waves of slower frequency (0.5–4 Hz) and larger amplitude. *Right panel* shows a period of slow-wave sleep with higher magnification, in which a brief episode of fast oscillations was apparent (dotted line). *B*: correlations between different sites, calculated in moving time windows. Correlations were fluctuating between high and low values between neighboring sites during fast oscillations (*left*), but rarely attained high values for distant sites (1–4; "Sh." indicates the control correlation obtained between electrode 1 and the same signal taken 20 s later). In contrast, correlations always stayed high during slow-wave sleep (*middle*). Episodes of fast oscillations during slow-wave sleep (*right*) revealed similar correlation patterns as during the wake state. *C*: wave-triggered averages between extracellularly recorded units and LFP activity. During the wake state, the negativity of fast oscillations was correlated with an increase of firing (*left*; "control" indicates randomly shuffled spikes). The negativity of slow-wave complexes was correlated with an increased firing preceded by a silence in the units (*middle*; note different time scale). During the brief episodes of fast oscillations of slow-wave sleep (*right*), the correspondence between units and LFP was similar as in wakefulness. [Modified from Destexhe et al. (101).]
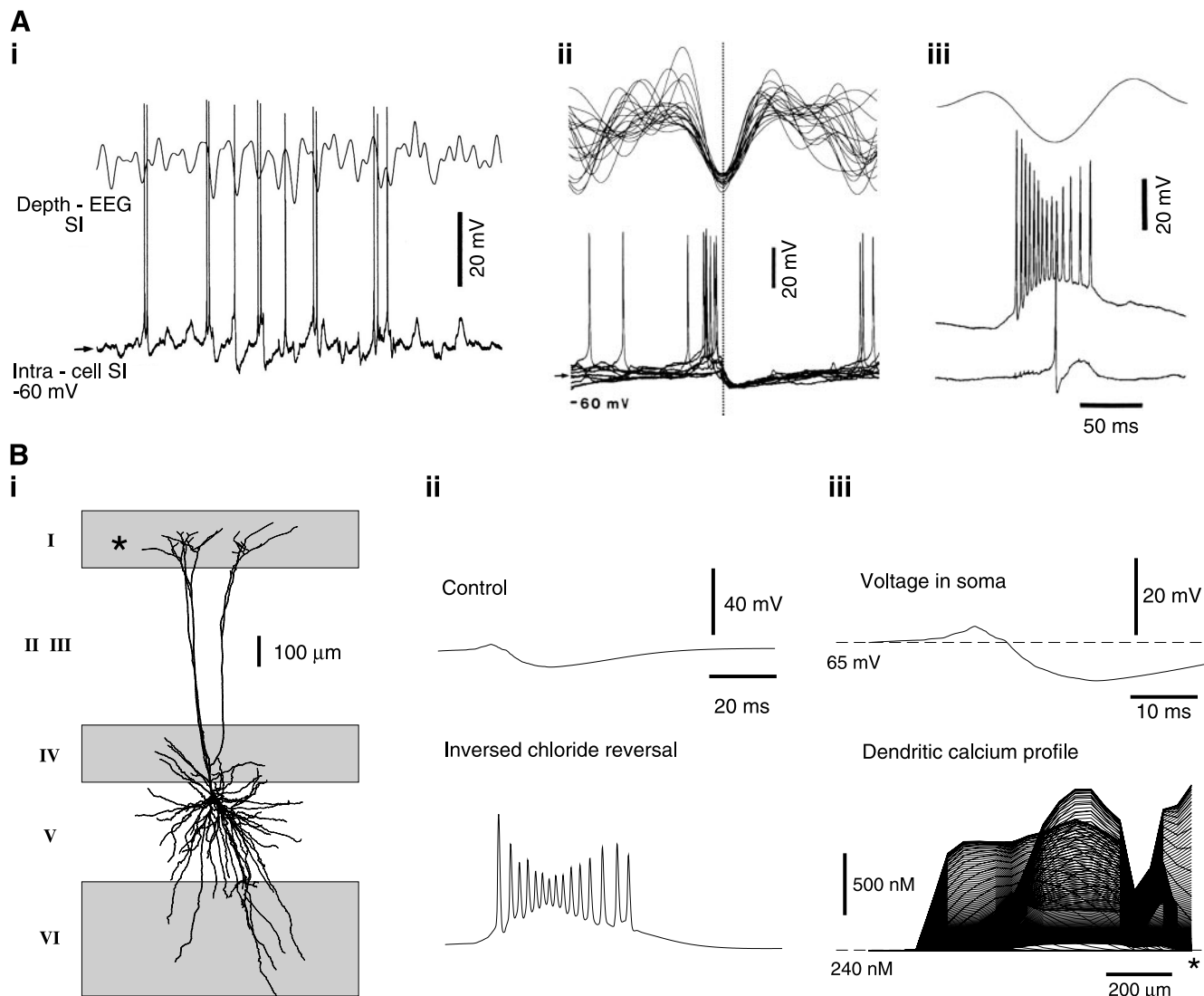
FIG. 18. Evidence that spindle oscillations evoke calcium entry in pyramidal neurons. *A*: in vivo intracellular recordings in suprasylvian cortical neurons during spindle oscillations under barbiturate anesthesia. *i*: Simultaneous recording of intracellular and extracellular activity. *ii*: Each cycle of the spindle oscillation corresponds to EPSP/IPSP sequences in the recorded pyramidal neuron. *iii*: Dual intracellular recording in which one of the neurons (*middle trace*) was recorded with chloride-filled pipettes. In this case, the EPSP/IPSP sequence transformed into a powerful burst of action potentials. *B*: computational models of thalamic inputs in pyramidal neurons. *i*: Morphology used in the simulations. A layer V pyramidal neuron recorded intracellularly in *A* was filled and its morphology was integrated into simulations. Simulations of thalamic inputs in layers I, IV, and VI (gray areas) were directly compared with the experimental recordings of thalamic inputs in that cell. *ii*: Simulated EPSP/IPSP sequences and bursts after inversion of the chloride reversal potential. The model could match experiments only if both excitatory and inhibitory conductances were strong. *iii*: Calcium transients in the dendrites of the model following thalamic inputs. The membrane potential at the soma (*top trace*) consisted in an EPSP/IPSP sequence. However, representing the profile of calcium concentration (*bottom trace*) along a path from soma (*left*) to distal apical dendrite (*) shows large calcium transients in response to strong dendritic depolarization. [Modified from Contreras et al. (63).]

that a strong feedforward inhibition is recruited in the cortex when the thalamus fires bursts in synchrony (63).

Computational models were used to estimate the exact amount and distribution of synaptic conductances and concluded that during synchronized thalamic input, there is a mixture of strong excitatory and inhibitory conductances (63). This conclusion was reached based on three-dimensional reconstructions and simulations of

some of the neurons recorded experimentally (Fig. 18*Bi*), and constraining the model directly using the recordings obtained in those neurons. Simulating the control and IPSP-reversed responses (Fig. 18*Bii*) could only be obtained if there was an asymmetry of conductance distribution in the cell: the proximal region had to be dominated by GABAergic conductances, while the dendrites had to be dominated by strong glutamatergic conduc-

tances. This distribution is in agreement with morphological data indicating that excitation and inhibition are not evenly distributed in pyramidal neurons; the dendrites are dominated by excitatory synapses while the soma essentially receives inhibitory synapses (77). This imbalance necessarily implies that during strong afferent activity, the dendrites must experience strong depolarization, in parallel with a strong inhibition around the soma. This conclusion is in agreement with direct measurements of conductances during visual inputs in cortical neurons that also revealed large GABAergic conductances (35).

Taken together, morphological data, in vivo intracellular recordings, and computational models suggest that during spindling there is a strong increase of both excitatory and inhibitory conductances in pyramidal neurons. This conductance increase induces a massive depolarization in the dendrites, combined with a strong proximal inhibition preventing the cell from firing excessively. Models (63) further indicate that this type of conductance distribution is ideal to evoke a massive calcium entry in dendrites through voltage-dependent Ca^{2+} channels, and at the same time keep the neuron at low levels of firing (Fig. 18*Biii*). This is consistent with in vitro studies showing that dendritic depolarization is accompanied by Ca^{2+} entry (370).

4. Cellular mechanisms for memory reprocessing during slow-wave sleep

Various calcium-dependent mechanisms are involved in synaptic plasticity (reviewed in Ref. 127). Thus calcium entry during sleep may serve to activate cortical plasticity mechanisms (reviewed in Ref. 106b). In particular, calmodulin kinase II (CaMKII), an enzyme that is abundant at synapses and is implicated in synaptic plasticity of excitatory synapses in the cortex and elsewhere (287, 365), is not only sensitive to Ca^{2+} but also to the frequency of Ca^{2+} spikes (78). It is possible that sleep spindles provide a signal to optimally activate CaMKII in the dendrites of cortical pyramidal neurons.

Another possible consequence of massive Ca^{2+} entry in pyramidal neurons is calcium-dependent gene expression, which is also frequency sensitive (141, 195) in the delta range of frequencies (1–4 Hz). Calcium that enters dendrites during spindles may accumulate in the endoplasmic reticulum, which forms a continuous compartment within the neuron, and is also continuous with the nucleus. Calcium-stimulated calcium release from the endoplasmic reticulum during delta waves may then deliver the calcium signal to the nucleus (26).

A third possibility is that the repeated Ca^{2+} entry activates a molecular "gate," opening the door to gene expression (106b). This possibility is based on the observation that repeated high-frequency stimuli, but not isolated stimuli, activate protein kinase A (PKA), an enzyme

implicated in long-lasting synaptic changes and long-term memory (1). The proposed mechanism is that PKA acts like a gate by inhibiting phosphoprotein phosphatases, which themselves exert a tonic inhibition over biochemical cascades leading to gene expression (1, 29, 30) (for a model of these biochemical cascades, see Ref. 27). The evidence for this hypothetical mechanism is based on observations that activation of PKA alone does not induce synaptic changes, but blocking PKA suppresses long-term synaptic changes in the hippocampus (122). All the necessary enzymes for this mechanism are located at or near the active zone of the synapse (51, 108, 180, 233).

A cellular mechanism for memory reprocessing was proposed (106b), based on complementary roles in network reorganization for two types of sleep oscillation, spindles, and slow waves. At sleep onset, the thalamus enters a burst mode and generates synchronized spindle oscillations. During these oscillations, the high-frequency bursts of thalamic relay cells occur synchronously in the thalamus and therefore provide unusually strong excitatory/inhibitory inputs in cortical pyramidal neurons. The repetition of these inputs at ~10 Hz is particularly efficient to trigger periodic calcium entry in cortical dendrites and activate intracellular mechanisms, such as CaMKII or molecular gates. This process could serve to open the door between synaptic activation and gene expression or mobilize particular molecular machinery needed for synaptic plasticity so that pyramidal neurons are ready to produce permanent changes in response to subsequent synaptic events that need to be consolidated.

As sleep deepens, slow waves such as delta oscillations progressively dominate the EEG. A slow-wave complex is a remarkably synchronized network event, in which a concerted period of silence is seen across the network, followed by a rebound firing in most of the cells. Some synapses could be "tagged" by short-term potentiation during the brief episodes of fast oscillations. During the subsequent slow-wave(s), these tagged synapses would then be selected by the synchronized pattern of firing, through a calcium-mediated signal evoked in pyramidal cells. This calcium signal could be routed to the nucleus (assuming the gate has been opened by spindles) or to local protein synthesis in dendrites, leading to long-term modifications or even morphological changes. A brief episode of fast oscillations that follows next would then potentiate or tag another subset of synapses; these tagged synapses would be selected by the next slow waves for permanent changes, and the cycle repeats itself several hundred times during the slow-wave sleep episode.

This "recall-store" hypothesis (106b) thus proposes that slow-wave sleep iterates a process of memory reprocessing; the brief periods of fast oscillations represent a recall of information acquired previously during wakefulness, which are subsequently stored by highly synchro-

nized events that appear as slow waves in the EEG. Slow-wave sleep would thus begin by spindle oscillations that open molecular gates to plasticity, then proceed by iteratively "recalling" and "storing" information primed in neural assemblies. Although speculative, this scenario is consistent with what is currently known about the biophysical mechanisms of sleep oscillations (see details in Ref. 106b). It is also consistent with the growing evidence that sleep serves to consolidate memories, as well as with models that require a "sleep" phase for the long-term learning of generative representations (155). The key prediction is that slow-wave sleep is a specific state in which information is consolidated by activating Ca^{2+}-mediated intracellular cascades in pyramidal neurons.

V. SUMMARY AND CONCLUSIONS

We present here a synopsis of the main concepts in this review, the questions that are still open, the predictions that would allow them to be tested, and prospects for future studies.

A. A Framework for Thalamic and Thalamocortical Oscillations

Models provide a unifying framework to account for apparently inconsistent experimental observations. Different experiments point to different ways to generate spindle oscillations in the thalamus,. The original TC-interneuron model proposed by Andersen and Eccles (9) identified two basic mechanisms for generating thalamic oscillations: inhibition and the rebound burst. These two mechanisms were essentially correct, except that they proposed that the interneurons provided the inhibition, but TC cells and interneurons are not reciprocally interconnected. Later, a TC-RE variant of this model, based on the same mechanisms, was proposed by Scheibel and Scheibel (269–271), in which the inhibitory neurons in the RE nucleus provided the reciprocal loop with TC cells. The TC-RE loop also generates spindles in thalamic (170, 351, 346) and thalamocortical (322) slices. An alternative mechanism was suggested in an in vivo study (308), which reported that the isolated RE nucleus can generate oscillations without the need for interactions with TC cells. This RE pacemaker hypothesis has not yet been confirmed by in vitro experiments, but given the difficulty of preserving the connectivity of the RE in a slice preparation, this hypothesis is still a viable one (297).

Computational models proposed different scenarios to account for these experiments. The RE pacemaker hypothesis found support from computational models which showed that the known intrinsic properties and synaptic connectivity between RE cells can plausibly generate synchronized oscillations. Interconnected RE cells

with slow ($GABA_B$) synapses can generate slow synchronized oscillations at a frequency of ~3 Hz (135, 354, 355). Alternatively, RE cells with extended connectivity through fast ($GABA_A$) synapses can generate synchronized oscillations around 10 Hz (23, 90, 97, 98). Models also reported that RE oscillations can show waxing-and-waning patterns, similar to experiments, which are generated by traveling waves of activity within the RE nucleus (23, 97).

The TC-RE hypothesis also found support from modeling studies, based on the intrinsic properties of TC and RE cells, and the excitatory (AMPA) and inhibitory ($GABA_A$ and $GABA_B$) connectivity between the two types of cells (96, 105, 136, 353). The subharmonic bursting of TC cells during spindles was due to interactions between IPSPs and the I_T and I_h currents (352, 353), as found earlier in cortical models (185). The typical waxing-and-waning patterns of spindle waves were due to Ca^{2+}-mediated upregulation of I_h (96, 105). The TC-RE pacemaker could also be reconstructed by hybrid recording methods in which real cells are connected to model cells (193).

Different models support both RE pacemaker and TC-RE hypotheses, but an explanation was still needed for why the RE nucleus does not oscillate in vitro. One modeling study proposed that this apparent contradiction can be relaxed based on the action of neuromodulators (98). This model reproduced the quiescent state of the RE nucleus in the absence of neuromodulators, similar to in vitro recordings, as well as ~10 Hz waxing-and-waning oscillations in the presence of weak neuromodulatory drive, which may represent a situation closer to in vivo recordings. When both TC-RE and RE pacemakers were assembled in the same model, the results were consistent with the initiation and propagation of spindle waves observed in thalamic slices (96).

At the level of the thalamocortical system, experiments demonstrated the large-scale coherence of spindle waves in vivo (60, 61), but the same oscillations typically show traveling wave patterns in thalamic slices (182). Models showed that these two states can be obtained in the same circuits (100). The model suggests that these differences are primarily due to the presence of thalamocortical loops, which act through the RE nucleus (thalamo-cortico-reticular loops) and which provide a more global synchronization compared with what can be achieved by intrathalamic loops alone (Fig. 12). Thalamocortical loops are highly efficient at synchronizing large areas because the diverging cascade of axonal projection systems reaches a wide area of the cortex on a single cycle (cortex-to-RE, RE-to-TC, TC-to-cortex). In addition, spindles may be initiated at roughly the same time at different sites because of similar refractory periods in TC cells; as a consequence, oscillations may spread over large regions of the cortical mantle within a few cycles. Thalamic slices deprived of this powerful synchronizing

mechanism display systematic traveling wave propagation through the topographic structure of intrathalamic connections (Fig. 12*A*).

This strong impact of corticothalamic inputs on thalamic circuits also accounted for pathological phenomena such as absence seizures. The recruitment of the thalamus through the RE nucleus results in a dominant inhibition, which normally activates only GABA$_A$ receptors because the discharge of RE cells is controlled by intra-RE inhibitory interactions. However, if the cortex generates too strong descending feedback, the RE cells are forced into large burst discharges and activate GABA$_B$-mediated inhibition, in addition to GABA$_A$ responses, in TC cells. Consequently, this slower inhibition imposes a slower oscillation frequency, and the thalamus will therefore tend to oscillate at 3 Hz with a strong corticothalamic feedback. These predictions of the model (86) were corroborated in thalamic slices (18, 31). Thalamocortical loops combined with a hyperexcitable cortex can generate hypersynchronous 3-Hz oscillations, which generate spike and waves in the simulated field potentials (86). This model accounts for a large body of experimental data on absence seizures (see sect. IV*B*).

Consistent with intracellular recordings, models predict that the thalamus has a strong impact on the cortex during spindles, perhaps leading to massive calcium entry in these cells and activating calcium-dependent plasticity mechanisms. This leads to the hypothesis that slow-wave sleep processing occurs in two stages (106b): *1*) spindle oscillations would activate molecular gates, enabling further plasticity to be initiated in the activated neurons; and *2*) the iteration between short "wakelike" episodes and highly synchronized slow waves would perform "recall-store" operations, in which information acquired previously is consolidated through permanent synaptic changes.

B. Successful, Unsuccessful, and Untested Predictions

Formulating predictions is probably one of the most important contributions that models can make. They can directly test the relevance of the model, lead to new directions for further experimentation, and perhaps collectively provide new insights. We enumerate below key predictions that were formulated by the models reviewed above; some of these predictions have been already tested experimentally.

1. Successful predictions

1) One of the main predictions of the modeling studies was that the waxing and waning of TC cell oscillations is due to Ca^{2+}-mediated upregulation of I_h (85, 95, 96). This mechanism was inspired from heart cells (144) and was later demonstrated experimentally in thalamic neu-

rons (19, 212). However, the direct binding of Ca^{2+} postulated initially (85, 95) was shown to be incorrect (44). Ca^{2+} seems to act through an intermediate messenger, cAMP (213), as also predicted by a more elaborate version of the model (96). The model predicted that the upregulation of I_h occurs through Ca^{2+} (or cAMP) binding to the open state of the channel, which was also found to be the best possible explanation to the data (213). Recent data, however, indicate that cyclic nucleotide-gated channels are regulated by cAMP through the release of an inhibitory mechanism internal to the protein complex (347). It is possible that similar mechanisms also apply to I_h, which is a possible direction for future investigation.

2) A second successful prediction was that the "waning" of spindle waves is due to upregulation of I_h (95). In particular, the unbinding of calcium (or calcium-bound messenger) from I_h channels during the silent period results in a slow recovery of these channels, which induces a progressive hyperpolarization of the membrane in TC cells.[6] This progressive hyperpolarization and the critical role of I_h in spindle termination were both demonstrated in ferret thalamic slices (19).

3) The model predicted that natural sleep and barbiturate anesthesia should correspond to different levels of resting membrane potential in cortical pyramidal cells (102). The model predicts that intracellular recordings performed in neocortical pyramidal cells during natural sleep should have a relatively depolarized resting level, close to -60 mV, compared with the hyperpolarized resting level of -70 to -80 mV typical of barbiturate anesthesia. Recent results show that neocortical neurons in naturally sleeping animals are maintained at approximately -65 mV, except during slow (0.5–4 Hz) wave complexes, when they hyperpolarize (314).

4) A fourth successful prediction of the model was that the characteristic nonlinearity of GABA$_B$ responses is a consequence of mechanisms intrinsic to single terminals containing these receptors (106a). Single-synapse GABA$_B$ responses should not be activated by isolated presynaptic spikes, but by high-frequency bursts of a large number of presynaptic spikes. This property was essential to explain the hypersynchronous 3-Hz oscillations in thalamic slices (96, 136) and is a central component in the mechanism proposed for absence seizures (86). Dual intracellular recordings of single-axon GABA$_B$ responses demonstrated this property in both thalamic (183) and neocortical slices (327). Interestingly, the number of presynaptic spikes needed to start activating GABA$_B$ IPSPs was lower in neocortex (>3 spikes) compared with thalamus (>10 spikes), presumably because the probability

---

[6] This may also be described as an afterdepolarization (ADP) following the spindle wave, which is actually the terminology used in the in vitro experiments (19).

of release is low in thalamic inhibitory synapses. The biophysical mechanism postulated by the model was that four G proteins must bind to activate the K^+ channels associated with $GABA_B$ receptors (106a), consistent with the tetrameric structure and activation properties of K^+ channels (150). The predicted multiplicity of G protein binding sites could be tested experimentally by application of activated G proteins on membrane patches (see Ref. 339), or by voltage-clamp experiments. Application of G proteins on membrane patches was performed for muscarinic K^+ channels, and a nonlinear response was observed with a Hill coefficient >3 (169); thus, at least in this system, several G protein bindings are needed to activate the K^+ channels. Other kinetic studies have also suggested that G proteins act on ion channels at multiple binding sites (see Ref. 366 for the muscarinic current and Refs. 32, 132 for Ca^{2+} currents in sympathetic neurons).

5) The models predicted that strong corticothalamic feedback should force physiologically intact thalamic circuits to oscillate at ~3 Hz (86). In particular, this mechanism explicitly predicted that stimulation of corticothalamic fibers in vitro should force the intact slice to oscillate in a slower, more synchronized mode. This prediction was successfully tested in slices (18, 31). Moderate stimulation of corticothalamic fibers did not affect the spontaneous rhythms besides entrainment, but strong stimuli transformed spindle waves into hypersynchronous rhythms at ~3 Hz (Fig. 16).

6) It was found recently that the antiepileptic drug vigabatrin strongly affects spike-and-wave discharges in rats (36). This drug increases GABA concentrations by inhibiting GABA transaminase, one of the major enzymes implicated in GABA degradation. In particular, this study (36) demonstrated that vigabatrin decreases the frequency of spike-and-wave discharges (from 7.5 to 5.6 Hz), as well as prolongs the duration of seizures (from 1.04 to 1.52 s). This effect occurs presumably through boosting of both $GABA_A$ and $GABA_B$ responses and is in agreement with predictions of the model (see Fig. 3 in Ref. 87).

2. Unsuccessful or unclear predictions

1) Several modeling studies have predicted that networks of RE cells reciprocally connected through fast inhibitory synapses should oscillate at ~10 Hz (23, 90, 97). RE cells are indeed sensitive to $GABA_A$ agonists (17, 164, 227, 291), and intracellularly recorded RE neurons display fast GABAergic IPSPs (21, 97, 265, 266, 280, 336, 372). There is evidence that some RE cells are connected through dendro-dendritic synapses (83, 252, 368), and axon collaterals also interconnect RE cells (174, 252, 368). These data support an oscillatory mechanism implicating mutual $GABA_A$ interactions in the RE nucleus. However, several lines of evidence suggest more complex mechanisms. First, there are circumstances when GABAergic

interactions in the RE nucleus may act as "desynchronizers" (166) and protect against epileptic discharges (266). Models suggest that this protective role depends on the membrane potential (106a); intra-RE connections may serve as a synchronizer at depolarized levels, but protect against synchronization at more hyperpolarized levels (see Fig. 2 in Ref. 96 for a simulation of this effect in thalamic networks). Second, there is still a controversy about the type and proportion of $GABA_A$ synapses in the RE nucleus that mediate synaptic interactions between these cells. A recent study reported few dendro-dendritic synapses or axon collaterals, but found gap junctions between RE neurons in mice (189), which might also support oscillations between RE cells. Third, whether $GABA_A$-mediated interactions between RE cells are sufficiently powerful to entrain synchronized oscillations is still unclear. A dynamic-clamp study showed that $GABA_A$-mediated rebound bursts occur with a significant delay, questioning the relevance of inhibitory rebound mechanisms to RE oscillations at a frequency above 3 Hz (338). However, other studies have shown that $GABA_A$ IPSPs in RE cells, although of small apparent amplitude at the soma, can have powerful effects such as completely shunting the burst discharges of these cells (265). It has been proposed that the dendritic localization of the I_T in RE cells may explain these observations (106c); dendritic I_T gives RE cells a high sensitivity to IPSPs, and rebound bursts could be initiated in dendrites with small apparent GABAergic conductances measured at the soma. In this case, RE oscillations could arise from T-type and $GABA_A$ currents interacting locally in dendrites with little or no involvement of the soma. These possibilities constitute interesting directions to explore with future models.

2) The oscillatory mechanism proposed for RE oscillations based on depolarizing $GABA_A$ interactions (23) has not yet been confirmed. First, the evidence for depolarizing $GABA_A$ interactions comes from only a single study (337). Hyperpolarizing fast IPSPs were observed in intracellularly recorded RE cells in vivo (see Fig. 3 in Ref. 97), as well as in a number of in vitro studies of RE cells (21, 97, 265, 266, 280, 336, 372). It is possible that species differences may explain these conflicting observations. Second, this model predicted that slow oscillations (~2.5 Hz) should occur when RE neurons have hyperpolarized resting levels (around −80 mV). However, such oscillations have never been observed in slices where the resting levels of RE cells are typically around −80 mV. This prediction awaits experimental confirmation.

3) Models predict a significant contribution of $GABA_B$-mediated K^+ currents to the wave component of spike-and-wave field potentials during seizures (86). Experiments (299, 313) have shown that the wave is not $GABA_A$ mediated and is significantly affected by cesium, a K^+ channel blocker. The authors suggested that the wave is a mixture of Ca^{2+}-dependent K^+ currents and disfacili-

tation (299). However, these experiments show that the wave is mediated in large part by K^+ currents, consistent with the mixture of voltage-dependent and $GABA_B$-mediated K^+ currents predicted by the model. Further experiments should be performed in the presence of more specific antagonists (TEA, apamin, $GABA_B$ antagonists) to evaluate the respective contribution of different K^+ currents to the wave.

4) Models have predicted that the fast (5–10 Hz) type of spike-and-wave oscillation, as observed experimentally in rats, is based on a thalamocortical loop mechanism involving rebound bursts in TC cells (87). During spike-and-wave seizures in GAERS rats, TC cells display moderate firing and rarely display full-blown bursts (251). However, the bursts displayed by the model were weak and often consisted of single spikes (87). Such "weak" rebound bursts may therefore be difficult to identify, which may explain this experimental observation. Other experiments in rats reported burst firing of TC cells during seizures (224, 273, 293) and that seizures seem to start in a focus located in somatosensory cortex (231), suggesting that not all of the thalamus participates in seizures and that full-blown bursts are seen only in some nuclei. Other experiments showed that mice lacking the genes for the T-channel subunits specific to TC cells do not display seizures (181), which clearly demonstrates that thalamic I_T are involved in this type of seizure activity.

3. Yet untested predictions

Several of the predictions made by the models have not yet been tested experimentally (or are too difficult to be tested with current techniques).

1) The discrepancy between in vivo and in vitro experiments on RE oscillations could be reconciled by models postulating that RE oscillations critically depend on the resting membrane potential and should be sensitive to neuromodulators (98). In particular, application of neuromodulators such as NE or 5-HT, at low concentration, should depolarize RE cells and restore the ability of the RE nucleus to oscillate in vitro. Alternatively, the infusion of noradrenergic and serotonergic antagonists in vivo should alter the oscillatory capabilities of the isolated RE nucleus.

2) A second central prediction of the models is that the inhibitory-dominant nature of the cortical feedback on TC cells is critical in explaining large-scale synchrony (100).[7] This mechanism predicts that diminishing the efficiency of IPSPs evoked by RE cells onto TC cells should not only change the genesis of the oscillations, but should also impair the large-scale synchrony of spindle or spike-

and-wave oscillations. On the other hand, antagonizing excitatory synapses on TC cells should not alter the large-scale synchrony of these oscillations. This mechanism could be tested by locally applying synaptic antagonists in thalamocortical slices.

3) The models predict that horizontal propagation in neocortical slices should be highly sensitive to the excitability of pyramidal neurons and that such horizontal discharges tighten the synchrony of oscillations (102). Local stimulation of the white matter in neocortical slices produces limited horizontal propagation (5, 53, 64), but the application of $GABA_A$ antagonists generates epileptic discharges that propagate horizontally (5, 53, 64). The model predicts that, in addition to $GABA_A$ antagonists, propagation should also be facilitated by neuromodulators such as ACh. Discharges evoked in the "modulated" slice should easily propagate at a speed of ~100–200 mm/s, depending on the level of excitability (see details in Ref. 102) and therefore should depend on the concentration of neuromodulator. This value is consistent with current estimates of propagation velocity (42, 140). Such rapidly propagating cortical discharges should also be detectable by high-resolution optical recording methods in awake or naturally sleeping animals.

4) A fourth prediction of the model is that evoked propagation of spindle waves should not occur during natural sleep (102). Low-intensity electrical stimulation of the cortex can induce propagating oscillatory waves during barbiturate anesthesia, and these propagating oscillations persist after cortical cuts (61), suggesting that horizontal intracortical connections were not responsible. However, intracortical connections should have an important role in supporting the simultaneous bursting of natural sleep spindles. This directly implies that it should not be possible to evoke propagating oscillations by cortical stimulation during natural sleep. A corollary to this prediction is that cortical cuts should significantly affect the spatiotemporal patterns and synchrony of natural sleep spindle oscillations. This is supported by the observation of diminished interhemispheric synchrony of spindles following callosal transection (41).

5) The model predicts mechanisms for spike-and-wave oscillations, at either 3 or 5–10 Hz, and which in both cases involve inhibitory-rebound sequences in TC cells (86, 87). This predicts that blocking the I_T in TC cells should suppress seizures.[8] This is consistent with a presumed effect of the antiabsence drug ethosuximide on reducing the effectiveness of the I_T in thalamic neurons (67) (for a model, see Ref. 214). This is also consistent with recent genetic studies showing that mice lacking the gene for the T-channel subunits present in TC cells (while

---

[7] Inhibitory dominance was not by itself a prediction, given the large body of experimental evidence showing that cortical stimulation primarily evoke IPSPs in TC cells (4, 45, 66, 82, 196, 263, 315, 330, 359).

[8] This is converse to the claims that the low-threshold spike in TC cells is not involved in generating seizures in GAERS rats (251).

not affecting RE cells) display a specific resistance to the generation of spike-and-wave seizures (181).

6) The genesis of spike-and-wave discharges in the model depends on an abnormally strong corticothalamic feedback. This therefore predicts that during seizures, there should be an increased output of cortical layer 6 neurons projecting to the thalamus. This increased output could result from either an increase in the discharge of individual neurons or an increase in the synchrony of the population of neurons in layer 6 that project to the thalamus. This prediction could be tested in vivo or with appropriate stimulation protocols in cortical or thalamocortical slices.

7) In the model for the fast (5–10 Hz) type of spike-and-wave oscillation in rodents, the frequency is higher than in cats because of a different balance between $GABA_A$ and $GABA_B$ conductances in TC cells (87). The mechanism is the same as that for the slow ($\sim$3 Hz) spike and wave, except that the $GABA_B$ component here is sustained and not phasic as for the 3-Hz spike and wave. Therefore, the same feedback paradigm as outlined in section IV*B5* applied to rat thalamic slices should lead to highly synchronized 5- to 10-Hz oscillations that are different from spindles.

8) Inhibition between the RE and TC cells in the thalamus is critical in generating spike-and-wave oscillations. The model predicts that fast (5–10 Hz) and slow ($\sim$3 Hz) spike-and-wave oscillations should be transformable into each other by manipulating GABAergic conductances in TC cells (87): *1*) enhancing $GABA_B$ conductances in TC cells should slow down the frequency of spike and wave to $\sim$3 Hz, *2*) blocking $GABA_B$ receptors in TC cells should reduce or suppress seizures, and *3*) suppressing thalamic $GABA_A$ conductances should either completely suppress seizures or slow down the faster spike-and-wave discharges (see details in Ref. 87).

9) The model predicts that corticothalamic synapses should be efficient targets for antiabsence drugs (86). This prediction is a direct consequence of the thalamocortical loop mechanism proposed for generating seizure. There is currently no selective antagonist for this synapse, but it should be possible to target these synapses with modern genetic techniques.

10) The model predicts that the upregulation of I_h by Ca^{2+} is responsible for the transient nature of absence seizures. Seizures terminate by the same mechanism as for spindle waves, by a progressive upregulation of I_h. This predicts that thalamic infusion of pharmacological agents that block I_h should lead to long-lasting seizures, or alternatively, agents that potentiate I_h (for example, neuromodulators) should shorten the duration of absence seizures or even suppress them. This is consistent with the decreased probability of seizures in awake and attentive states compared with slow-wave sleep (179).

11) Models predict that attention can be imple-

mented through the complex interactions between dendritic calcium currents and the activity of corticothalamic synapses (88). High levels of background activity (of cortical origin) can prevent burst generation in TC and RE cells through local dendritic interactions between glutamatergic and calcium conductances in dendrites (88, 99, 106c). This mechanism is fast, in contrast to other mechanisms implicating metabotropic receptors (see Ref. 222). This mechanism directly predicts that high levels of cortical activity should switch the thalamus from burst mode to tonic mode, therefore implementing a fast switch to a more responsive state. This prediction could be tested in slices by sustained random stimulation of corticothalamic fibers, paired with stimulation of afferent activity.[9] The control of the responsiveness of thalamic neurons by cortical activity is a highly important problem that can be investigated by combining experiments and models.

12) Finally, the model predicts that synchronized thalamic inputs should be associated with a strong increase of both excitatory and inhibitory conductances in pyramidal neurons (63). This conductance increase should induce a massive calcium entry localized in the dendrites. This prediction should be testable using two-photon imaging studies of pyramidal neurons (320). The model predicts a strong calcium signal in the dendrites, but not in the soma, following strong afferent inputs, such as during thalamic stimulation, spindle oscillations, or slow-wave complexes.

C. Concluding Remarks

Two of the intuitions of Bremer (38–40) still form the basis of our present understanding of the mechanisms of brain rhythmicity. First, his proposition that oscillations depend on the "excitability cycle" of cortical neurons, or on neuronal autorhythmicity, constitute the first explicit recognition for the importance of intrinsic neuronal properties (39). Studies in invertebrates, in vitro physiology of central neurons, and molecular genetic approaches, have contributed to our detailed understanding of these intrinsic properties based on ion channel conductances. Second, Bremer proposed that the EEG results from the synchronized oscillatory activity of large assemblies of oscillating cortical neurons, rather than arising from circulating action potentials. This concept of synchrony is now well established, and the mechanisms leading to the synchrony of large assemblies of neurons are still being investigated.

Recent studies have revealed the intricate complexity of ion channel types and subunits, their uneven distribution in soma and dendrites, their expression at various

---

[9] This is possible in slices from the visual thalamus, in which the corticothalamic and retinal fibers are both accessible (18, 334).

developmental stages, the mapping of the different receptor types in various classes of synapses, as well as the characterization of their dynamics in fine detail. Progress in pharmacology and molecular genetics has provided tools to focus on a given type or subtype of ion channel and establish its function. One of the conceptual advances made in our understanding of the genesis of thalamic oscillations is that oscillations can result from the synaptic interaction between different neuronal types, none of which alone constitutes an oscillator (see sects. III*B* and III*C*).

In another conceptual advance, the commonly held "thalamocentric" view is being replaced by one in which feedback projections from cortex to thalamus are crucial. Corticothalamic feedback is needed to account for the initiation, spread, and termination of oscillations (see sect. IV*A*), as well as pathological states. This new view agrees with morphological observations that the majority of thalamic synapses originate from cortical axons (115, 116, 197, 198). Thus the thalamocortical system is a loop in which the "feed-forward" part is the classic pathway relaying sensory information to cortex and the "feedback" part is the control of the cortex over thalamic operations, which may be excitatory or inhibitory depending on cortical activity, and possibly implement attentional mechanisms (88). Sensory information in this view serves to modulate this intrinsic activity (203).

New methods are needed to investigate this intricate web of molecular properties and relate it to the macroscopic behavior of neuronal populations. By integrating both electrophysiological and molecular data, computational models can be an efficient way to improve our interpretation of experimental data and try to assemble them into a coherent framework, as we have done here. This approach has made it possible to integrate knowledge of thalamic and thalamocortical oscillations from the molecular level to large-scale networks (106b). Not only the models reproduced experiments, but they have also generated a multitude of predictions that motivated new experiments and a new generation of models. This experimental-modeling loop has been realized in studies in which computational models and real neurons interact in functional circuits (193, 194, 259). Theory and experiment have led to important advances in physics, and the same approach could also be effective in biology.

Finally, accurate models can be used in exploring possible functions for these oscillations. We reviewed here a possible role for slow-wave sleep oscillations in synaptic plasticity. The fact that we are now able to propose plausible mechanisms that are compatible with the available experimental data is itself an important milestone. The proposed hypotheses are probably incomplete or even incorrect, but we anticipate they will trigger imaginative experiments and better models, which together could ultimately lead us to uncover the true nature of the sleeping brain.

Address for reprint requests and other correspondence: A. Destexhe, Unité de Neurosciences Intégratives et Computationnelles, CNRS, UPR-2191, Avenue de la Terrasse, Bat. 33, 91198 Gif-sur-Yvette, France (E-mail: Destexhe@iaf.cnrs-gif.fr).

REFERENCES

1. **Abel T, Nguyen PV, Barad M, Deuel TAS, Kandel ER, and Bourtchouladze R.** Genetic demonstration of a role for PKA in the late phase of LTP and in hippocampus-based long-term memory. *Cell* 88: 615–626, 1997.
2. **Adams DJ, Smith SJ, and Thompson SH.** Ionic currents in molluscan soma. *Annu Rev Neurosci* 3: 141–167, 1980.
3. **Adrian ED.** Afferent discharges to the cerebral cortex from peripheral sense organs. *J Physiol* 100: 159–191, 1941.
4. **Ahlsen G, Grant K, and Lindström S.** Monosynaptic excitation of principal cells in the lateral geniculate nucleus by corticofugal fibers. *Brain Res* 234: 454–458, 1982.
5. **Albowitz B and Kuhnt U.** Spread of epileptiform potentials in the neocortical slice: recordings with voltage-sensitive dyes. *Brain Res* 631: 329–333, 1993.
6. **Alonso A and Llinas RR.** Subthreshold Na^+-dependent theta-like rhythmicity in stellate cells of entorhinal cortex layer II. *Nature* 342: 175–177, 1989.
7. **Alvarez P, Zola-Morgan S, and Squire LR.** Damage limited to the hippocampal region produces long-lasting memory impairment in monkeys. *J Neurosci* 15: 3796–3807, 1995.
8. **Andersen P and Andersson SA.** *Physiological Basis of the Alpha Rhythm.* New York: Appelton Century Crofts, 1968.
9. **Andersen P and Eccles JC.** Inhibitory phasing of neuronal discharge. *Nature* 196: 645–647, 1962.
10. **Andersen P and Rutjord T.** Simulation of a neuronal network operating rhythmically through recurrent inhibition. *Nature* 204: 289–190, 1964.
11. **Andersen P, Andersson SA, and Lømo T.** Nature of thalamocortical relations during spontaneous barbiturate spindle activity. *J Physiol* 192: 283–307, 1967.
12. **Antal K, Emri Z, Toth TI, and Crunelli V.** Model of a thalamocortical neurone with dendritic voltage-gated ion channels. *Neuroreport* 8: 1063–1066, 1997.
13. **Antoniadis G and Kostopoulos G.** Simulation study for the transition from spindles to spike and wave epileptogenesis. *Med Biol Engineer Comput* 33: 241–246, 1995.
14. **Avanzini G, de Curtis M, Panzica F, and Spreafico R.** Intrinsic properties of nucleus reticularis thalami neurones of the rat studied in vitro. *J Physiol* 416: 111–122, 1989.
15. **Avoli M and Gloor P.** The effect of transient functional depression of the thalamus on spindles and bilateral synchronous epileptic discharges of feline generalized penicillin epilepsy. *Epilepsia* 22: 443–452, 1981.
16. **Avoli M, Gloor P, Kostopoulos G, and Gotman J.** An analysis of penicillin-induced generalized spike and wave discharges using simultaneous recordings of cortical and thalamic single neurons. *J Neurophysiol* 50: 819–837, 1983.
17. **Bal T and McCormick DA.** Mechanisms of oscillatory activity in guinea-pig nucleus reticularis thalami in vitro: a mammalian pacemaker. *J Physiol* 468: 669–691, 1993.
18. **Bal T, Debay D, and Destexhe A.** Cortical feedback controls the frequency and synchrony of oscillations in the visual thalamus. *J Neurosci* 20: 7478–7488, 2000.

19. **Bal T and McCormick DA.** What stops synchronized thalamocortical oscillations? *Neuron* 17: 297–308, 1996.

20. **Bal T, von Krosigk M, and McCormick DA.** Synaptic and membrane mechanisms underlying synchronized oscillations in the ferret LGN in vitro. *J Physiol* 483: 641–663, 1995.

21. **Bal T, von Krosigk M, and McCormick DA.** Role of the ferret perigeniculate nucleus in the generation of synchronized oscillations in vitro. *J Physiol* 483: 665–685, 1995.

22. **Ball GJ, Gloor P, and Schaul N.** The cortical electromicrophysiology of pathological delta waves in the electroencephalogram of cats. *Electroencephalogr Clin Neurophysiol* 43: 346–361, 1977.

23. **Bazhenov M, Timofeev I, Steriade M, and Sejnowski TJ.** Self-sustained rhythmic activity in the thalamic reticular nucleus mediated by depolarizing GABA$_A$ receptor potentials. *Nature Neurosci* 2: 168–174, 1999.

24. **Bazhenov M, Timofeev I, Steriade M, and Sejnowski TJ.** Spiking-bursting activity in the thalamic reticular nucleus initiates sequences of spindle oscillations in thalamic networks. *J Neurophysiol* 84: 1076–1087, 2000.

25. **Berger H.** über den zeitlichen verlauf der negativen schwankung des nervenstroms. *Arch Ges Physiol* 1: 173, 1929.

26. **Berridge MJ.** Neuronal calcium signaling. *Neuron* 21: 13–26, 1998.

27. **Bhalla US and Iyengar R.** Emergent properties of networks of biological signaling pathways. *Science* 283: 381–387, 1999.

28. **Bishop GH.** The interpretation of cortical potentials. *Cold Spring Harbor Symp Quant Biol* 4: 305–319, 1936.

29. **Blitzer RD, Connor JH, Brown GP, Wong T, Shenolikar S, Iyengar R, and Landau EM.** Gating of CaMKII by cAMP-regulated protein phosphatase activity during LTP. *Science* 280: 1940–1942, 1998.

30. **Blitzer RD, Wong T, Nouranifar R, Iyengar R, and Landau EM.** Postsynaptic cAMP pathway gates early LTP in hippocampal CA1 region. *Neuron* 15: 1403–1414, 1995.

31. **Blumenfeld H and McCormick DA.** Corticothalamic inputs control the pattern of activity generated in thalamocortical networks. *J Neurosci* 20: 5153–5162, 2000.

32. **Boland LM and Bean BP.** Modulation of N-type calcium channels in bullfrog sympathetic neurons by luteinizing hormone-releasing hormone: kinetics and voltage dependence. *J Neurosci* 13: 516–533, 1993.

33. **Bonnet V and Bremer F.** Étude des potentiels électriques de la moelle épinière faisant suite chez la grenouille spinale à une ou deux vollées d'influx centripètes. *C R Soc Biol Paris* 127: 806–812, 1938.

34. **Bontempi B, Laurent-Demir C, Destrade C, and Jaffard R.** Time-dependent reorganization of brain circuitry underlying long-term memory storage. *Nature* 400: 671–675, 1999.

35. **Borg-Graham LJ, Monier C, and Frégnac Y.** Visual input evokes transient and strong shunting inhibition in visual cortical neurons. *Nature* 393: 369–373, 1998.

36. **Bouwman BM, van den Broek PL, van Luijtelaar G, and van Rijn CM.** The effects of vigabatrin on type II spike wave discharges in rats. *Neurosci Lett* 338: 177–180, 2003.

37. **Bremer F.** Effets de la déafférentation complète d'une région de l'écorce cérébrale sur son activité électrique. *C R Soc Biol Paris* 127: 355–359, 1938.

38. **Bremer F.** L'activité électrique de l'écorce cérébrale. *Actual Sci Industriel* 658: 3–46, 1938.

39. **Bremer F.** Considérations sur l'origine et la nature des "ondes" cérébrales. *Electroencephalogr Clin Neurophysiol* 1: 177–193, 1949.

40. **Bremer F.** Cerebral and cerebellar potentials. *Physiol Rev* 38: 357–388, 1958.

41. **Bremer F, Brihaye J, and André-Balisaux G.** Physiologie et pathologie du corps calleux. *Schweiz Arch Neurol Psychiat* 78: 31–87, 1956.

42. **Bringuier V, Chavane F, Glaeser L, and Frégnac Y.** Horizontal propagation of visual activity in the synaptic integration field of area 17 neurons. *Science* 283: 695–699, 1999.

43. **Brock LG, Coombs JS, and Eccles JC.** The recording of potential from monotneurones with an intracellular electrode. *J Physiol* 117: 431–460, 1952.

44. **Budde T, Biella G, Munsch T, and Pape HC.** Lack of regulation by intracellular Ca^{2+} of the hyperpolarization-activated cation current in rat thalamic neurones. *J Physiol* 503: 79–85, 1997.

45. **Burke W and Sefton AJ.** Inhibitory mechanisms in lateral geniculate nucleus of rat. *J Physiol* 187: 231–246, 1966.

46. **Buzsáki G.** Two-stage model of memory trace formation: a role for "noisy" brain states. *Neuroscience* 31: 551–570, 1989.

47. **Buzsáki G.** The hippocampo-neocortical dialogue. *Cerebral Cortex* 6: 81–92, 1996.

48. **Buzsáki G, Bickford RG, Ponomareff G, Thal LJ, Mandel R, and Gage FH.** Nucleus basalis and thalamic control of neocortical activity in the freely moving rat. *J Neurosci* 8: 4007–4026, 1988.

49. **Carbone E and Lux HD.** A low voltage-activated, fully inactivating Ca channel in vertebrate sensory neurones. *Nature* 310: 501–502, 1984.

50. **Carbone E and Lux HD.** A low voltage-activated calcium conductance in embryonic chick sensory neurons. *Biophys J* 46: 413–418, 1984.

51. **Carr DW, Stofko-Hahn RE, Fraser ID, Cone RD, and Scott JD.** Localization of the cAMP-dependent protein kinase to the postsynaptic densities by A-kinase anchoring proteins. Characterization of AKAP 79. *J Biol Chem* 267: 16816–16823, 1992.

52. **Castro-Alamancos MA.** Neocortical synchronized oscillations induced by thalamic disinhibition in vivo. *J Neurosci Online* 19: RC27, 1999.

53. **Chagnac-Amitai Y and Connors BW.** Horizontal spread of synchronized activity in neocortex and its control by GABA-mediated inhibition. *J Neurophysiol* 61: 747–758, 1989.

54. **Chrobak JJ and Buzsáki G.** Selective activation of deep layer (V-VI) retrohippocampal cortical neurons during hippocampal sharp waves in the behaving rat. *J Neurosci* 14: 6160–6170, 1994.

55. **Connor JA and Stevens CF.** Inward and delayed outward membrane currents in isolated neural somata under voltage clamp. *J Physiol* 213: 1–19, 1971.

56. **Connor JA and Stevens CF.** Voltage clamp studies of a transient outward membrane current in gastropod neural somata. *J Physiol* 213: 21–30, 1971.

57. **Connor JA and Stevens CF.** Prediction of repetitive firing behaviour from voltage clamp data on an isolated neurone soma. *J Physiol* 213: 31–53, 1971.

58. **Contreras D.** *Oscillatory Properties of Cortical and Thalamic Neurons and the Generation of Synchronized Rhythmicity in the Corticothalamic Network* (PhD thesis). Québec, Canada: Laval Univ., 1996.

59. **Contreras D, Curro Dossi R, and Steriade M.** Electrophysiological properties of cat reticular thalamic neurones in vivo. *J Physiol* 470: 273–294, 1993.

60. **Contreras D, Destexhe A, Sejnowski TJ, and Steriade M.** Control of spatiotemporal coherence of a thalamic oscillation by corticothalamic feedback. *Science* 274: 771–774, 1996.

61. **Contreras D, Destexhe A, Sejnowski TJ, and Steriade M.** Spatiotemporal patterns of spindle oscillations in cortex and thalamus. *J Neurosci* 17: 1179–1196, 1997.

62. **Contreras D, Destexhe A, and Steriade M.** Spindle oscillations during cortical spreading depression in naturally sleeping cats. *Neuroscience* 77: 933–936, 1997.

63. **Contreras D, Destexhe A, and Steriade M.** Intracellular and computational characterization of the intracortical inhibitory control of synchronized thalamic inputs in vivo. *J Neurophysiol* 78: 335–350, 1997.

64. **Contreras D and Llinás RR.** Voltage-sensitive dye imaging of neocortical spatiotemporal dynamics to afferent activation frequency. *J Neurosci* 21: 9403–9413, 2001.

65. **Contreras D and Steriade M.** Cellular basis of EEG slow rhythms: a study of dynamic corticothalamic relationships. *J Neurosci* 15: 604–622, 1995.

66. **Contreras D and Steriade M.** Spindle oscillation in cats: the role of corticothalamic feedback in a thalamically-generated rhythm. *J Physiol* 490: 159–179, 1996.

67. **Coulter DA, Huguenard JR, and Prince DA.** Calcium currents in rat thalamocortical relay neurones: kinetic properties of the transient, low-threshold current. *J Physiol* 414: 587–604, 1989.

68. **Creutzfeldt O, Watanabe S, and Lux HD.** Relation between EEG phenomena and potentials of single cortical cells. I. Evoked re-

sponses after thalamic and epicortical stimulation. *EEG Clin Neurophysiol* 20: 1–18, 1966.

69. **Creutzfeldt O, Watanabe S, and Lux HD.** Relation between EEG phenomena and potentials of single cortical cells. II. Spontaneous and convulsoid activity. *EEG Clin Neurophysiol* 20: 19–37, 1966.

70. **Cruikshank SJ and Weinberger NM.** Receptive-field plasticity in the adult auditory cortex induced by Hebbian covariance. *J Neurosci* 16: 861–875, 1996.

71. **Crunelli V, Lightowler S, and Pollard CE.** A T-type Ca^{2+} current underlies low-threshold Ca^{2+} potentials in cells of the cat and rat lateral geniculate nucleus. *J Physiol* 413: 543–561, 1989.

72. **Crunelli V, Soltesz I, Toth TI, Turner J, and Leresche N.** Intrinsic low-frequency oscillations of thalamocortical cells and their modulation by synaptic potentials. In: *Thalamic Networks for Relay and Modulation,* edited by Miniciacchi A, Molinari M, Macchi G, and Jones EG. New York: Pergamon, 1993, p. 375–384.

73. **Curro Dossi R, Nunez A, and Steriade M.** Electrophysiology of a slow (0.5–4 Hz) intrinsic oscillation of cat thalamocortical neurones in vivo *J Physiol* 447: 215–234, 1992.

74. **Danober L, Deransart C, Depaulis A, Vergnes M, and Marescaux C.** Pathophysiological mechanisms of genetic absence epilepsy in the rat. *Prog Neurobiol* 55: 27–57, 1988.

75. **Davies CH, Davies SN, and Collingridge GL.** Paired-pulse depression of monosynaptic GABA-mediated inhibitory postsynaptic responses in rat hippocampus. *J Physiol* 424: 513–531, 1990.

76. **Debarbieux F, Brunton J, and Charpak S.** Effect of bicuculline on thalamic activity: a direct blockade of IAHP in reticularis neurons. *J Neurophysiol* 79: 2911–2918, 1998.

77. **DeFelipe J and Fariñas I.** The pyramidal neuron of the cerebral cortex: morphological and chemical characteristics of the synaptic inputs. *Prog Neurobiol* 39: 563–607, 1992.

78. **De Koninck P and Schulman H.** Sensitivity of CaM kinase II to the frequency of Ca^{2+} oscillations. *Science* 279: 227–230, 1998.

79. **De la Pena E and Geijo-Barrientos E.** Laminar organization, morphology and physiological properties of pyramidal neurons that have the low-threshold calcium current in the guinea-pig frontal cortex. *J Neurosci* 16: 5301–5311, 1996.

80. **Dement W.** The effect of dream deprivation. *Science* 131: 1705–1707, 1960.

81. **Derbyshire AJ, Rempel B, Forbes A, and Lambert EF.** The effects of anesthetics on action potentials in the cerebral cortex of the cat. *Am J Physiol* 116: 577–596, 1936.

82. **Deschênes M and Hu B.** Electrophysiology and pharmacology of the corticothalamic input to lateral thalamic nuclei: an intracellular study in the cat. *Eur J Neurosci* 2: 140–152, 1990.

83. **Deschênes M, Madariaga-Domich A, and Steriade M.** Dendrodendritic synapses in the cat reticularis thalami nucleus: a structural basis for thalamic spindle synchronization. *Brain Res* 334: 165–168, 1985.

84. **Deschênes M, Paradis M, Roy JP, and Steriade M.** Electrophysiology of neurons of lateral thalamic nuclei in cat: resting properties and burst discharges. *J Neurophysiol* 55: 1196–1219, 1984.

85. **Destexhe A.** *Nonlinear Dynamics of the Rhythmical Activity of the Brain* (PhD thesis). Brussels, Belgium: Université Libre de Bruxelles, 1992.

86. **Destexhe A.** Spike-and-wave oscillations based on the properties of GABA_A receptors. *J Neurosci* 18: 9099–9111, 1998.

87. **Destexhe A.** Can GABA_A conductances explain the fast oscillation frequency of absence seizures in rodents? *Eur J Neurosci* 11: 2175–2181, 1998.

88. **Destexhe A.** Modeling corticothalamic feedback and the gating of the thalamus by the cerebral cortex. *J Physiol (Paris)* 94: 391–410, 2000.

89. **Destexhe A and Babloyantz A.** Pacemaker-induced coherence in cortical networks. *Neural Computat* 3: 145–154, 1991.

90. **Destexhe A and Babloyantz A.** Cortical coherent activity induced by thalamic oscillations. In: *Neural Network Dynamics,* edited by Taylor JG, Caianello ER, Cotterill RMJ, and Clark JW. Berlin: Springer-Verlag, 1992, p. 234–249.

91. **Destexhe A and Babloyantz A.** A model of the inward current I_h and its possible role in thalamocortical oscillations. *Neuroreport* 4: 223–226, 1993.

95. **Destexhe A, Babloyantz A, and Sejnowski TJ.** Ionic mecha-

nisms for intrinsic slow oscillations in thalamic relay neurons. *Biophys J* 65: 1538–1552, 1993.

96. **Destexhe A, Bal T, McCormick DA, and Sejnowski TJ.** Ionic mechanisms underlying synchronized oscillations and propagating waves in a model of ferret thalamic slices. *J Neurophysiol* 76: 2049–2070, 1996.

97. **Destexhe A, Contreras D, Sejnowski TJ, and Steriade M.** A model of spindle rhythmicity in the isolated thalamic reticular nucleus. *J Neurophysiol* 72: 803–818, 1994.

98. **Destexhe A, Contreras D, Sejnowski TJ, and Steriade M.** Modeling the control of reticular thalamic oscillations by neuromodulators. *Neuroreport* 5: 2217–2220, 1994.

99. **Destexhe A, Contreras D, Steriade M, Sejnowski TJ, and Huguenard JR.** In vivo, in vitro and computational analysis of dendritic calcium currents in thalamic reticular neurons. *J Neurosci* 16: 169–185, 1996.

100. **Destexhe A, Contreras D, and Steriade M.** Mechanisms underlying the synchronizing action of corticothalamic feedback through inhibition of thalamic relay cells. *J Neurophysiol* 79: 999–1016, 1998.

101. **Destexhe A, Contreras D, and Steriade M.** Spatiotemporal analysis of local field potentials and unit discharges in cat cerebral cortex during natural wake and sleep states. *J Neurosci* 19: 4595–4608, 1999.

102. **Destexhe A, Contreras D, and Steriade M.** Cortically-induced coherence of a thalamic-generated oscillation. *Neuroscience* 92: 427–443, 1999.

103. **Destexhe A, Contreras D, and Steriade M.** LTS cells in cerebral cortex and their role in generating spike-and-wave oscillations. *Neurocomputing* 38: 555–563, 2001.

104. **Destexhe A, Mainen Z, and Sejnowski TJ.** Kinetic models of synaptic transmission. In: *Methods in Neuronal Modeling,* edited by Koch C and Segev I. Cambridge, MA: MIT, 1998, p. 1–26.

105. **Destexhe A, McCormick DA, and Sejnowski TJ.** A model for 8–10 Hz spindling in interconnected thalamic relay and reticularis neurons. *Biophys J* 65: 2474–2478, 1993.

106. **Destexhe A, Neubig M, Ulrich D, and Huguenard JR.** Dendritic low-threshold calcium currents in thalamic relay cells. *J Neurosci* 18: 3574–3588, 1998.

106a.**Destexhe A and Sejnowski TJ.** G-protein activation kinetics and spill-over of GABA may account for differences between inhibitory responses in the hippocampus and thalamus. *Proc Natl Acad Sci USA* 92: 9515–9519, 1995.

106b.**Destexhe A and Sejnowski TJ.** *Thalamocortical Assemblies.* Oxford, UK: Oxford Univ. Press, 2001.

106c.**Destexhe A and Sejnowski TJ.** The initiation of bursts in thalamic neurons and the cortical control of thalamic sensitivity. *Phil Trans R Soc Lond B Biol Sci* 357: 1649–1657, 2002.

107. **Domich L, Oakson G, and Steriade M.** Thalamic burst patterns in the naturally sleeping cat: a comparison between cortically projecting and reticularis neurones. *J Physiol* 379: 429–449, 1986.

108. **Dosemeci A and Reese TS.** Inhibition of endogenous phosphatase in a postsynaptic density fraction allows extensive phosphorylation of the major postsynaptic density protein. *J Neurochem* 61: 550–555, 1993.

109. **Dutar P and Nicoll RA.** A physiological role for GABA_A receptors in the central nervous system. *Nature* 332: 156–158, 1988.

110. **Eccles JC.** Interpretation of action potentials evoked in the cerebral cortex. *J Neurophysiol* 3: 449–464, 1951.

111. **Eckhorn R, Bauer R, Jordan W, Brosch M, Kruse W, Munk M, and Reitboek HJ.** Coherent oscillations: a mechanism of feature linking in the visual cortex? Multiple electrode and correlation analyses in the cat. *Biol Cybernetics* 60: 121–130, 1988.

112. **Edeline JM, Manunta Y, and Hennevin E.** Auditory thalamus neurons during sleep: changes in frequency selectivity, threshold, and receptive field size. *J Neurophysiol* 84: 934–952, 2000.

113. **Emri Z, Antal K, Toth TI, Cope DW, and Crunelli V.** Backpropagation of the delta oscillation and the retinal excitatory postsynaptic potential in a multi-compartment model of thalamocortical neurons. *Neuroscience* 98: 111–127, 2000.

114. **Erickson KR, Ronnekleiv OK, and Kelly MJ.** Electrophysiology of guinea-pig supraoptic neurones: role of a hyperpolarization-

activated cation current in phasic firing. *J Physiol* 460: 407–425, 1993.

115. **Erisir A, VanHorn SC, Bickford ME, and Sherman SM.** Immunocytochemistry and distribution of parabrachial terminals in the lateral geniculate nucleus of the cat: a comparison with corticogeniculate terminals. *J Comp Neurol* 377: 535–549, 1997.

116. **Erisir A, VanHorn SC, and Sherman SM.** Relative numbers of cortical and brainstem inputs to the lateral geniculate nucleus. *Proc Natl Acad Sci USA* 94: 1517–1520, 1997.

117. **Evarts EV.** Temporal patterns of discharge of pyramidal tract neurons during sleep and waking in the monkey. *J Neurophysiol* 27: 152–171, 1964.

118. **Fishbein W and Gutwein BM.** Paradoxical sleep and memory storage processes. *Behav Biol* 19: 425–464, 1977.

119. **FitzGibbon T, Tevah LV, and Jervie-Sefton A.** Connections between the reticular nucleus of the thalamus and pulvinar-lateralis posterior complex: a WGA-HRP study. *J Comp Neurol* 363: 489–504, 1995.

120. **Fowler MJ, Sullivan MJ, and Ekstrand BR.** Sleep and memory. *Science* 179: 302–304, 1973.

121. **Frank MG, Issa NP, and Stryker MP.** Sleep enhances plasticity in the developing visual cortex. *Neuron* 30: 275–287, 2001.

122. **Frey U, Huang YY, and Kandel ER.** Effects of cAMP simulate a late phase of LTP in hippocampal CA1 neurons. *Science* 260: 1661–1664, 1993.

123. **Frost JD, Kellaway PR, and Gol A.** Single-unit discharges in isolated cerebral cortex. *Exp Neurol* 14: 305–316, 1966.

124. **Gais S, Plihal W, Wagner U, and Born J.** Early sleep triggers memory for early visual discrimination skills. *Nat Neurosci* 3: 1335–1339, 2000.

125. **Galligan JJ, Tatsumi H, Shen KZ, Surprenant A, and North RA.** Cation current activated by hyperpolarization (I_h) in guinea pig enteric neurons. *Am J Physiol Gastrointest Liver Physiol* 259: G966–G972, 1990.

126. **Getting PA.** Emerging principles governing the operation of neuronal networks. *Annu Rev Neurosci* 12: 185–204, 1989.

127. **Ghosh A and Greenberg ME.** Calcium signaling in neurons: molecular mechanisms and cellular consequences. *Science* 268: 239–247, 1995.

128. **Gibbs JW, Berkow-Schroeder G, and Coulter DA.** GABA$_A$ receptor function in developing rat thalamic reticular neurons: whole cell recordings of GABA-mediated currents and modulation by clonazepam. *J Neurophysiol* 76: 2568–2579, 1996.

129. **Gloor P and Fariello RG.** Generalized epilepsy: some of its cellular mechanisms differ from those of focal epilepsy. *Trends Neurosci* 11: 63–68, 1988.

130. **Gloor P, Quesney LF, and Zumstein H.** Pathophysiology of generalized penicillin epilepsy in the cat: the role of cortical and subcortical structures. II. Topical application of penicillin to the cerebral cortex and subcortical structures. *EEG Clin Neurophysiol* 43: 79–94, 1977.

131. **Gluck MA and Myers CE.** *Gateway to Memory: An Introduction to Neural Network Modeling of the Hippocampus and Learning.* Cambridge, MA: MIT, 2000.

132. **Golard A and Siegelbaum SA.** Kinetic basis for the voltage-dependent inhibition of N-type calcium current by somatostatin and norepinephrine in chick sympathetic neurons. *J Neurosci* 13: 3884–3894, 1993.

133. **Golomb D and Rinzel J.** Dynamics of globally coupled inhibitory neurons with heterogeneity. *Phys Rev E* 48: 4810–4814, 1993.

134. **Golomb D and Rinzel J.** Clustering in globally coupled inhibitory neurons. *Physica* 72: 259–282, 1994.

135. **Golomb D, Wang XJ, and Rinzel J.** Synchronization properties of spindle oscillations in a thalamic reticular nucleus model. *J Neurophysiol* 72: 1109–1126, 1994.

136. **Golomb D, Wang XJ, and Rinzel J.** Propagation of spindle waves in a thalamic slice model. *J Neurophysiol* 75: 750–769, 1996.

137. **Golshani P, Liu XB, and Jones EG.** Differences in quantal amplitude reflect GluR4-subunit number at corticothalamic synapses on two populations of thalamic neurons. *Proc Natl Acad Sci USA* 98: 4172–4177, 2001.

138. **Gonzalo-Ruiz A and Lieberman AR.** Topographic organization of projections from the thalamic reticular nucleus to the anterior thalamic nuclei in the rat. *Brain Res Bull* 37: 17–35, 1995.

139. **Gray CM and Singer W.** Stimulus-specific neuronal oscillations in orientation columns of cat visual cortex. *Proc Natl Acad Sci USA* 86: 1698–1702, 1989.

140. **Grinvald A, Lieke EE, Frostig RD, and Hildesheim R.** Cortical point-spread function and long-range lateral interactions revealed by real-time optical imaging of macaque monkey primary visual cortex. *J Neurosci* 14: 2545–2568, 1994.

141. **Gu X and Spitzer NC.** Distinct aspects of neuronal differentiation encoded by frequency of spontaneous Ca^{2+} transients. *Nature* 375: 784–787, 1995.

142. **Guido W, Lu SM, and Sherman SM.** Relative contributions of burst and tonic responses to the receptive field properties of lateral geniculate neurons in the cat. *J Neurophysiol* 68: 2199–2211, 1992.

143. **Guido W and Weyand T.** Burst responses in thalamic relay cells of the awake behaving cat. *J Neurophysiol* 74: 1782–1786, 1995.

144. **Hagiwara N and Irisawa H.** Modulation by intracellular Ca^{2+} of the hyperpolarization-activated inward current in rabbit single sino-atrial node cells. *J Physiol* 409: 121–141, 1989.

145. **Hamos JE, Van Horn SC, Raczkowski D, and Sherman SM.** Synaptic circuits involving an individual retinogeniculate axon in the cat. *J Comp Neurol* 259: 165–192, 1987.

146. **Harris-Warrick RM and Marder E.** Modulation of neural networks for behavior. *Annu Rev Neurosci* 14: 39–57, 1991.

147. **Herculano-Houzel S, Munk MH, Neuenschwander S, and Singer W.** Precisely synchronized oscillatory firing patterns require electroencephalographic activation. *J Neurosci* 19: 3992–4010, 1999.

148. **Hernandez-Cruz A and Pape HC.** Identification of two calcium currents in acutely dissociated neurons from the rat lateral geniculate nucleus. *J Neurophysiol* 61: 1270–1283, 1989.

149. **Hersch SM and White EL.** Thalamocortical synapses on corticothalamic projections neurons in mouse SmI cortex: electron microscopic demonstration of a monosynaptic feedback loop. *Neurosci Lett* 24: 207–210, 1981.

150. **Hille B.** *Ion Channels of Excitable Membranes* (3rd ed.). Sunderland, MA: Sinauer, 2001.

151. **Hindmarsh JL and Rose RM.** A model for rebound bursting in mammalian neurons. *Philos Trans R Soc Lond B Biol Sci* 346: 129–150, 1994.

152. **Hindmarsh JL and Rose RM.** A model of intrinsic and driven spindling in thalamocortical neurons. *Philos Trans R Soc Lond B Biol Sci* 346: 165–183, 1994.

153. **Hines ML.** NEURON: a program for simulation of nerve equations. In: *Neural Systems: Analysis and Modeling*, edited by Eeckman F. Norwell, MA: Kluwer Academic, p. 127–136.

154. **Hines ML and Carnevale NT.** The NEURON simulation environment. *Neural Computat* 9: 1179–1209, 1997.

155. **Hinton GE, Dayan P, Frey BJ, and Neal RM.** The "wake-sleep" algorithm for unsupervised neural networks. *Science* 268: 1158–1161, 1995.

156. **Hobson JA.** *The Dreaming Brain.* New York: Basic, 1988.

157. **Hodgkin AL and Huxley AF.** A quantitative description of membrane current and its application to conduction and excitation in nerve. *J Physiol* 117: 500–544, 1952.

158. **Horne JA and McGrath MJ.** The consolidation hypothesis for REM sleep function: stress and other confounding factors—a review. *Biol Psychol* 18: 165–184, 1984.

159. **Hosford DA, Clark S, Cao Z, Wilson WA Jr, Lin FH, Morrisett RA, and Huin A.** The role of GABA$_B$ receptor activation in absence seizures of lethargic (*lh/lh*) mice. *Science* 257: 398–401, 1992.

160. **Hosford DA, Wang Y, and Cao Z.** Differential effects mediated by GABA$_A$ receptors in thalamic nuclei of *lh/lh* model of absence seizures. *Epilepsy Res* 27: 55–65, 1997.

161. **Hughes SW, Cope DW, and Crunelli V.** Dynamic clamp study of I_h modulation of burst firing and delta oscillations in thalamocortical neurons in vitro. *Neuroscience* 87: 541–550, 1998.

162. **Huguenard JR and McCormick DA.** Simulation of the currents involved in rhythmic oscillations in thalamic relay neurons. *J Neurophysiol* 68: 1373–1383, 1992.

163. **Huguenard JR and Prince DA.** A novel T-type current underlies

prolonged calcium-dependent burst firing in GABAergic neurons of rat thalamic reticular nucleus. *J Neurosci* 12: 3804–3817, 1992.

164. **Huguenard JR and Prince DA.** Clonazepam suppresses GABA$_A$-mediated inhibition in thalamic relay neurons through effects in nucleus reticularis. *J Neurophysiol* 71: 2576–2581, 1994.

165. **Huguenard JR and Prince DA.** Intrathalamic rhythmicity studied in vitro: nominal T-current modulation causes robust anti-oscillatory effects. *J Neurosci* 14: 5485–5502, 1994.

166. **Huntsman MM, Porcello DM, Homanics GE, DeLorey TM, and Huguenard JR.** Reciprocal inhibitory connections and network synchrony in the mammalian thalamus. *Science* 283: 541–543, 1999.

167. **Imbert M and Buisseret P.** Receptive field characteristics and plastic properties of visual cortical cells in kittens reared with or without visual experience. *Exp Brain Res* 22: 25–36, 1975.

168. **Inoue M, Duysens J, Vossen JMH, and Coenen AML.** Thalamic multiple-unit activity underlying spike-wave discharges in anesthetized rats. *Brain Res* 612: 35–40, 1993.

169. **Ito H, Tung RT, Sugimoto T, Kobayashi I, Takahashi K, Katada T, Ui M, and Kurachi Y.** On the mechanism of G-protein beta gamma subunit activation of the muscarinic K^+ channel in guinea pig atrial cell membrane. Comparison with the ATP-sensitive K^+ channel. *J Gen Physiol* 99: 961–983, 1992.

170. **Jacobsen RB, Ulrich D, and Huguenard JR.** GABA(B) and NMDA receptors contribute to spindle-like oscillations in rat thalamus in vitro. *J Neurophysiol* 86: 1365–1375, 2001.

171. **Jahnsen H and Llinás RR.** Electrophysiological properties of guinea-pig thalamic neurons: an in vitro study. *J Physiol* 349: 205–226, 1984.

172. **Jahnsen H and Llinás RR.** Ionic basis for the electroresponsiveness and oscillatory properties of guinea-pig thalamic neurons in vitro. *J Physiol* 349: 227–247, 1984.

173. **Jasper H and Kershman J.** Electroencephalographic classification of the epilepsies. *Arch Neurol Physchiat* 45: 903–943, 1941.

174. **Jones EG.** *The Thalamus.* New York: Plenum, 1985.

175. **Kamondi A and Reiner PB.** Hyperpolarization-activated inward current in histaminergic tuberomammillary neurons of the rat hypothalamus. *J Neurophysiol* 66: 1902–1911, 1991.

176. **Kandel ER.** *Cellular Basis of Behavior.* San Francisco, CA: Freeman, 1976.

177. **Kao CQ and Coulter DA.** Physiology and pharmacology of corticothalamic stimulation-evoked responses in rat somatosensory thalamic neurons in vitro. *J Neurophysiol* 77: 2661–2676, 1997.

178. **Kapur N and Brooks DJ.** Temporally-specific retrograde amnesia in two cases of discrete bilateral hippocampal pathology. *Hippocampus* 9: 247–254, 1999.

179. **Kellaway P.** Sleep and epilepsy. *Epilepsia* 26 *Suppl*: S15–S30, 1985.

180. **Kennedy MB, Bennett MK, and Erondu NE.** Biochemical and immunochemical evidence that the "major postsynaptic density protein" is a subunit of a calmodulin-dependent protein kinase. *Proc Natl Acad Sci USA* 80: 7357–7361, 1983.

181. **Kim D, Song U, Keum S, Lee T, Jeong MJ, Kim SS, McEnery MW, and Shin HS.** Lack of the burst firing of thalamocortical relay neurons and resistance to absence seizures in mice lacking the α_{1G} T-type Ca^{2+} channels. *Neuron* 31: 35–45, 2001.

182. **Kim U, Bal T, and McCormick DA.** Spindle waves are propagating synchronized oscillations in the ferret LGNd in vitro. *J Neurophysiol* 74: 1301–1323, 1995.

183. **Kim U, Sanchez-Vives MV, and McCormick DA.** Functional dynamics of GABAergic inhibition in the thalamus. *Science* 278: 130–134, 1997.

184. **Klee MR, Offenloch K, and Tigges J.** Cross-correlation analysis of electroencephalographic potentials and slow membrane transients. *Science* 147: 519–521, 1965.

185. **Kopell N and LeMasson G.** Rhythmogenesis, amplitude modulation, and multiplexing in a cortical architecture. *Proc Natl Acad Sci USA* 91: 10586–10590, 1994.

186. **Kostopoulos G, Gloor P, Pellegrini A, and Siatitsas I.** A study of the transition from spindles to spike and wave discharge in feline generalized penicillin epilepsy: EEG features. *Exp Neurol* 73: 43–54, 1981.

187. **Kostopoulos G, Gloor P, Pellegrini A, and Gotman J.** A study of the transition from spindles to spike and wave discharge in feline generalized penicillin epilepsy: microphysiological features. *Exp Neurol* 73: 55–77, 1981.

188. **Lagerlund TD and Sharbrough FW.** Computer simulation of neuronal circuit models of rhythmic behavior in the electroencephalogram. *Comput Biol Med* 18: 267–304, 1988.

189. **Landisman CE, Long MA, Beierlein M, Deans MR, Paul DL, and Connors BW.** Electrical synapses in the thalamic reticular nucleus. *J Neurosci* 22: 1002–1009, 2002.

190. **Leresche N, Jassik-Gerschenfeld D, Haby M, Soltesz I, and Crunelli V.** Pacemaker-like and other types of spontaneous membrane potential oscillations in thalamocortical cells. *Neurosci Lett* 113: 72–77, 1990.

191. **Leresche N, Lightowler S, Soltesz I, Jassik-Gerschenfeld D, and Crunelli V.** Low-frequency oscillatory activities intrinsic to rat and cat thalamocortical cells. *J Physiol* 441: 155–174, 1991.

192. **Lee JH, Daud A, Cribbs LL, Lacerda AE, Pereverzev A, Klöckner U, Schneider T, and Perez-Reyes E.** Cloning and expression of a novel member of the low voltage-activated T-type calcium channel family. *J Neurosci* 19: 1912–1921, 1999.

193. **LeMasson G, Renaud-LeMasson S, Debay D, and Bal T.** Feedback inhibition controls spike transfer in hybrid thalamic circuits. *Nature* 417: 854–858, 2002.

194. **LeMasson G, Renaud-LeMasson S, Sharp A, Abbott LF, and Marder E.** Real time interaction between a model neuron and the crustacean somatogastric nervous system. *Soc Neurosci Abstr* 18: 1055, 1992.

195. **Li W, Llopis J, Whitney M, Zlokarnik G, and Tsien RY.** Cell-permanent caged InsP$_3$ ester shows that Ca^{2+} spike frequency can optimize gene expression. *Nature* 392: 936–941, 1998.

196. **Lindström S.** Synaptic organization of inhibitory pathways to principal cells in the lateral geniculate nucleus of the cat. *Brain Res* 234: 447–453, 1982.

197. **Liu XB, Honda CN, and Jones EG.** Distribution of four types of synapse on physiologically identified relay neurons in the ventral posterior thalamic nucleus of the cat. *J Comp Neurol* 352: 69–91, 1995.

198. **Liu XB and Jones EG.** Predominance of corticothalamic synaptic inputs to thalamic reticular nucleus neurons in the rat. *J Comp Neurol* 414: 67–79, 1999.

199. **Liu Z, Vergnes M, Depaulis A, and Marescaux C.** Evidence for a critical role of GABAergic transmission within the thalamus in the genesis and control of absence seizures in the rat. *Brain Res* 545: 1–7, 1991.

200. **Liu Z, Vergnes M, Depaulis A, and Marescaux C.** Involvement of intrathalamic GABA$_B$ neurotransmission in the control of absence seizures in the rat. *Neuroscience* 48: 87–93, 1992.

201. **Livingstone MS and Hubel DH.** Effects of sleep and arousal on the processing of visual information in the cat. *Nature* 291: 554–561, 1981.

202. **Llinás RR.** The intrinsic electrophysiological properties of mammalian neurons: a new insight into CNS function. *Science* 242: 1654–1664, 1988.

203. **Llinás RR and Paré D.** Of dreaming and wakefulness. *Neuroscience* 44: 521–535, 1991.

204. **Llinás RR and Sugimori M.** Electrophysiological properties of in vitro Purkinje cell somata in mammalian cerebellar slices. *J Physiol* 305: 171–195, 1980.

205. **Llinás RR and Sugimori M.** Electrophysiological properties of in vitro Purkinje cell dendrites in mammalian cerebellar slices. *J Physiol* 305: 197–213, 1980.

206. **Llinás R and Yarom Y.** Electrophysiology of mammalian inferior olivary neurones in vitro. Different types of voltage-dependent ionic conductances. *J Physiol* 315: 549–567, 1981.

207. **Llinás R and Yarom Y.** Properties and distribution of ionic conductances generating electroresponsiveness of mammalian inferior olivary neurones in vitro. *J Physiol* 315: 569–584, 1981.

208. **Llinás RR and Geijo-Barrientos E.** In vitro studies of mammalian thalamic and reticularis thalami neurons. In: *Cellular Thalamic Mechanisms*, edited by Bentivoglio M and Spreafico R. Amsterdam: Elsevier, 1988, p. 23–33.

209. **Llinás RR and Jahnsen H.** Electrophysiology of thalamic neurones in vitro. *Nature* 297: 406–408, 1982.

210. **Lopes da Silva FH, Hoeks A, Smits H, and Zetterberg LH.**

Model of brain rhythmic activity, the alpha rhythm of the thalamus. *Kybernetik* 15: 27–37, 1974.

211. **Lüthi A, Bal T, and McCormick DA.** Periodicity of thalamic spindle waves is abolished by ZD7288, a blocker of I_h. *J Neurophysiol* 79: 3284–3289, 1998.

212. **Lüthi A and McCormick DA.** Periodicity of thalamic synchronized oscillations: the role of Ca^{2+}-mediated upregulation of I_h. *Neuron* 20: 553–563, 1998.

213. **Lüthi A and McCormick DA.** Modulation of a pacemaker current through Ca^{2+}-induced stimulation of cAMP production. *Nature Neurosci* 2: 634–641, 1999.

214. **Lytton W and Sejnowski TJ.** Computer model of ethosuximide's effect on a thalamic cell. *Ann Neurol* 32: 131–139, 1992.

215. **Lytton WW.** Computer model of clonazepam's effect in thalamic slice. *Neuroreport* 8: 3339–3343, 1997.

216. **Lytton WW, Contreras D, Destexhe A, and Steriade M.** Dynamic interactions determine partial thalamic quiescence in a computer network model of spike-and-wave seizures. *J Neurophysiol* 77: 1679–1696, 1997.

217. **Lytton WW, Destexhe A, and Sejnowski TJ.** Control of slow oscillations in the thalamocortical neuron: a computer model. *Neuroscience* 70: 673–684, 1996.

218. **Magee JC and Carruth M.** Dendritic voltage-gated ion channels regulate the action potential firing mode of hippocampal CA1 pyramidal neurons. *J Neurophysiol* 82: 1895–1901, 1999.

219. **Marcus EM and Watson CW.** Bilateral synchronous spike wave electrographic patterns in the cat: interaction of bilateral cortical foci in the intact, the bilateral cortical-callosal and adiencephalic preparations. *Arch Neurol* 14: 601–610, 1966.

220. **Marr D.** Simple memory: a theory for the archicortex. *Philos Trans R Soc Lond B Biol Sci* 262: 23–81, 1971.

221. **McClelland JL, McNaughton BL, and O'Reilly RC.** Why there are complementary learning systems in the hippocampus and neocortex: insights from the successes and failures of connectionist models of learning and memory. *Psychol Rev* 102: 419–457, 1995.

222. **McCormick DA.** Neurotransmitter actions in the thalamus and cerebral cortex and their role in neuromodulation of thalamocortical activity. *Prog Neurobiol* 39: 337–388, 1992.

223. **McCormick DA and Feeser HR.** Functional implications of burst firing and single spike activity in lateral geniculate relay neurons. *Neuroscience* 39: 103–113, 1990.

224. **McCormick DA and Hashemiyoon R.** Thalamocortical neurons actively participate in the generation of spike-and-wave seizures in rodents. *Soc Neurosci Abstr* 24: 129, 1998.

225. **McCormick DA and Huguenard JR.** A model of the electrophysiological properties of thalamocortical relay neurons. *J Neurophysiol* 68: 1384–1400, 1992.

226. **McCormick DA and Pape HC.** Properties of a hyperpolarization-activated cation current and its role in rhythmic oscillations in thalamic relay neurones. *J Physiol* 431: 291–318, 1990.

227. **McCormick DA and Prince DA.** Mechanisms of action of acetylcholine in the guinea-pig cerebral cortex in vitro. *J Physiol* 375: 169–194, 1986.

228. **McCormick DA and Wang Z.** Serotonin and noradrenaline excite GABAergic neurones of the guinea-pig and cat nucleus reticularis thalami. *J Physiol* 442: 235–255, 1991.

229. **McLachlan RS, Avoli M, and Gloor P.** Transition from spindles to generalized spike and wave discharges in the cat: simultaneous single-cell recordings in the cortex and thalamus. *Exp Neurol* 85: 413–425, 1984.

230. **McMullen TA and Ly N.** Model of oscillatory activity in thalamic neurons: role of voltage and calcium-dependent ionic conductances. *Biol Cybernetics* 58: 243–259, 1988.

231. **Meeren HK, Pijn JP, Van Luijtelaar EL, Coenen AM, and Lopes da Silva FH.** Cortical focus drives widespread corticothalamic networks during spontaneous absence seizures in rats. *J Neurosci* 22: 1480–1495, 2002.

232. **Minderhoud JM.** An anatomical study of the efferent connections of the thalamic reticular nucleus. *Exp Brain Res* 112: 435–446, 1971.

233. **Mons N, Harry A, Dubourg P, Premont RT, Iyengar R, and Cooper DM.** Immunohistochemical localization of adenylyl cy-

clase in rat brain indicates a highly selective concentration at synapses. *Proc Natl Acad Sci USA* 92: 8473–8477, 1995.

234. **Morison RS and Bassett DL.** Electrical activity of the thalamus and basal ganglia in decorticate cats. *J Neurophysiol* 8: 309–314, 1945.

235. **Moruzzi G.** The functional significance of sleep with particular regard to the brain mechanisms underlying consciousness. In: *Brain and Conscious Experience*, edited by Eccles JC. Berlin: Springer, 1966, p. 345–379.

236. **Muhlethaler M and Serafin M.** Thalamic spindles in an isolated and perfused preparation in vitro. *Brain Res* 524: 17–21, 1990.

237. **Mulle C, Madariaga A, and Deschênes M.** Morphology and electrophysiological properties of reticularis thalami neurons in cat: in vivo study of a thalamic pacemaker. *J Neurosci* 6: 2134–2145, 1986.

238. **Munsch T, Budde T, and Pape HC.** Voltage-activated intracellular calcium transients in thalamic relay cells and interneurons. *Neuroreport* 11: 2411–2418, 1997.

239. **Nadasdy Z, Hirase H, Czurko A, Csicsvari J, and Buzsaki G.** Replay and time compression of recurring spike sequences in the hippocampus. *J Neurosci* 19: 9497–9507, 1999.

240. **Niedermeyer E.** Primary (idiopathic) generalized epilepsy and underlying mechanisms. *Clin Electroencephalogr* 27: 1–21, 1996.

241. **Niedermeyer E and Lopes da Silva F (Editors).** *Electroencephalography* (4th ed.). Baltimore, MD: Williams & Wilkins, 1998.

242. **Nowycky MC, Fox AP, and Tsien RW.** Three types of neuronal calcium channel with different calcium agonist sensitivity. *Nature* 316: 440–443, 1985.

243. **Nunez PL.** *Electric Fields of the Brain. The Neurophysics of EEG.* Oxford, UK: Oxford Univ. Press, 1981.

244. **Pape HC.** Queer current and pacemaker: the hyperpolarization-activated cation current in neurons. *Annu Rev Physiol* 58: 299–327, 1996.

245. **Partridge LD and Swandulla D.** Calcium-activated non-specific cation channels. *Trends Neurosci* 11: 69–72, 1988.

246. **Paulsen O and Heggelund P.** The quantal size at retinogeniculate synapses determined from spontaneous and evoked EPSCs in guinea-pig thalamic slices. *J Physiol* 480: 505–511, 1994.

247. **Paulsen O and Heggelund P.** Quantal properties of spontaneous EPSCs in neurones of the guinea-pig dorsal lateral geniculate nucleus. *J Physiol* 496: 759–772, 1996.

248. **Pellegrini A, Musgrave J, and Gloor P.** Role of afferent input of subcortical origin in the genesis of bilaterally synchronous epileptic discharges of feline generalized epilepsy. *Exp Neurol* 64: 155–173, 1979.

249. **Perkel DH and Mulloney B.** Motor pattern production in reciprocally inhibitory neurons exhibiting postinhibitory rebound. *Science* 185: 181–183, 1974.

250. **Peters A and Jones EG (Editors).** *Cerebral Cortex: Cellular Components of the Cerebral Cortex.* New York: Plenum, 1984, vol. 1.

251. **Pinault D, Leresche N, Charpier S, Deniau JM, Marescaux C, Vergnes M, and Crunelli V.** Intracellular recordings in thalamic neurones during spontaneous spike and wave discharges in rats with absence epilepsy. *J Physiol* 509: 449–456, 1998.

252. **Pinault D, Smith Y, and Deschênes M.** Dendrodendritic and axosomatic synapses in the thalamic reticular nucleus of the adult rat. *J Neurosci* 17: 3215–3233, 1997.

253. **Pollard CE and Crunelli V.** Intrinsic membrane currents in projection cells of the cat and rat lateral geniculate nucleus. *Neurosci Lett* 32: S39, 1988.

254. **Pollen DA.** Intracellular studies of cortical neurons during thalamic induced wave and spike. *Electroencephalogr Clin Neurophysiol* 17: 398–404, 1964.

255. **Prevett MC, Duncan JS, Jones T, Fish DR, and Brooks DJ.** Demonstration of thalamic activation during typical absence seizures during $H_2^{15}O$ and PET. *Neurology* 45: 1396–1402, 1995.

256. **Prince DA and Farrell D.** "Centrencephalic" spike-wave discharges following parenteral penicillin injection in the cat. *Neurology* 19: 309–310, 1969.

257. **Puigcerver A, Van Luijtenaar EJLM, Drinkenburg WHIM, and Coenen ALM.** Effects of the $GABA_A$ antagonist CGP-35348 on

sleep-wake states, behaviour and spike-wave discharges in old rats. *Brain Res Bull* 40: 157–162, 1996.

258. **Ralston B and Ajmone-Marsan C.** Thalamic control of certain normal and abnormal cortical rhythms. *EEG Clin Neurophysiol* 8: 559–582, 1956.

259. **Renaud-Le Masson S, Le Masson G, Marder E, and Abbott LF.** Hybrid circuits of interacting computer model and biological neurons. In: *Advanced in Neural Information Processing Systems*, edited by Hanson SJ, Cowan JD, and Giles GL. San Mateo, CA: Morgan Kaufmann, 1993, vol. 5, p. 813–819.

260. **Renshaw B, Forbes A, and Morison BR.** Activity of isocortex and hippocampus: electrical studies with microelectrodes. *J Neurophysiol* 3: 74–105, 1940.

261. **Robinson HP and Kawai N.** Injection of digitally synthesized synaptic conductance transients to measure the integrative properties of neurons. *J Neurosci Methods* 49: 157–165, 1993.

262. **Rose RM and Hindmarsh JL.** The assembly of ionic currents in a thalamic neuron. I. The three-dimensional model. *Proc R Soc Lond B Biol Sci* 237: 267–288, 1989.

263. **Roy JP, Clercq M, Steriade M, and Deschênes M.** Electrophysiology of neurons in lateral thalamic nuclei in cat: mechanisms of long-lasting hyperpolarizations. *J Neurophysiol* 51: 1220–1235, 1984.

264. **Sakmann B and Neher E (Editors).** *Single-Channel Recording* (2nd ed.). New York: Plenum, 1995.

265. **Sanchez-Vives MV, Bal T, and McCormick DA.** Inhibitory interactions between perigeniculate GABAergic neurons. *J Neurosci* 17: 8894–8908, 1997.

266. **Sanchez-Vives MV and McCormick DA.** Functional properties of perigeniculate inhibition of dorsal lateral geniculate nucleus thalamocortical neurons in vitro. *J Neurosci* 17: 8880–8893, 1997.

267. **Sanchez-Vives MV and McCormick DA.** Cellular and network mechanisms of rhythmic recurrent activity in neocortex. *Nature Neurosci* 3: 1027–1034, 2000.

268. **Sanderson KJ.** The projection of the visual field to the lateral geniculate and medial interlaminar nuclei in the cat. *J Comp Neurol* 143: 101–108, 1971.

269. **Scheibel ME and Scheibel AB.** The organization of the nucleus reticularis thalami: a Golgi study. *Brain Res* 1: 43–62, 1966.

270. **Scheibel ME and Scheibel AB.** Patterns of organization in specific and nonspecific thalamic fields. In: *The Thalamus*, edited by Purpura DP and Yahr M. New York: Columbia Univ. Press, 1966, p. 13–46.

271. **Scheibel ME and Scheibel AB.** Structural organization of nonspecific thalamic nuclei and their projection toward cortex. *Brain Res* 6: 60–94, 1967.

272. **Schlag J and Waszak M.** Electrophysiological properties of units of the thalamic reticular complex. *Exp Neurol* 32: 79–97, 1971.

273. **Seidenbecher T, Staak R, and Pape HC.** Relations between cortical and thalamic cellular activities during absence seizures in rats. *Eur J Neurosci* 10: 1103–1112, 1998.

274. **Selverston AI (Editor).** *Model Neural Networks and Behavior.* New York: Plenum, 1985.

275. **Sharp AA, Abbott LF, and Marder E.** Artificial electrical synapses in oscillatory networks. *J Neurophysiol* 67: 1691–1694, 1992.

276. **Sharp AA, O'Neil MB, Abbott LF, and Marder E.** The dynamic clamp: artificial conductances in biological neurons. *Trends Neurosci* 16: 389–394, 1993.

277. **Sharp AA, O'Neil MB, Abbott LF, and Marder E.** Dynamic clamp: computer-generated conductances in real neurons. *J Neurophysiol* 69: 992–995, 1993.

278. **Sherman SM.** A wake-up call from the thalamus. *Nat Neurosci* 4: 344–346, 2001.

279. **Sherman SM and Guillery RW.** *Exploring the Thalamus.* New York: Academic, 2001.

280. **Shu Y and McCormick DA.** Inhibitory interactions between ferret thalamic reticular neurons. *J Neurophysiol* 87: 2571–2576, 2002.

281. **Siapas AG and Wilson MA.** Coordinated interactions between hippocampal ripples and cortical spindles during slow-wave sleep. *Neuron* 21: 1123–1128, 1998.

282. **Siegel JM.** The REM sleep-memory consolidation hypothesis. *Science* 294: 1058–1063, 2001.

283. **Slaght SJ, Leresche N, Deniau JM, Crunelli V, and Charpier S.** Activity of thalamic reticular neurons during spontaneous genetically determined spike and wave discharges. *J Neurosci* 22: 2323–2334, 2002.

284. **Smith GD, Cox CL, Sherman M, and Rinzel J.** Fourier analysis of sinusoidally driven thalamocortical relay neurons and a minimal integrate-and-fire-or-burst model. *J Neurophysiol* 83: 588–610, 2000.

285. **Smith KA and Fisher RS.** The selective GABA$_B$ antagonist CGP-35348 blocks spike-wave bursts in the cholesterol synthesis rat absence epilepsy model. *Brain Res* 729: 147–150, 1996.

286. **Snead OC.** Evidence for GABA$_B$-mediated mechanisms in experimental generalized absence seizures. *Eur J Pharmacol* 213: 343–349, 1992.

287. **Soderling TR.** Calcium/calmodulin-dependent protein kinase II: role in learning and memory. *Mol Cell Biochem* 127/128: 93–101, 1993.

288. **Sohal VS and Huguenard JR.** Long-range connections synchronize rather than spread intrathalamic oscillations: computational modeling and in vitro electrophysiology. *J Neurophysiol* 80: 1736–1751, 1998.

289. **Soltesz I and Crunelli V.** GABA$_A$ and pre- and post-synaptic GABA$_B$ receptor-mediated responses in the lateral geniculate nucleus. *Prog Brain Res* 90: 151–169, 1992.

290. **Soltesz I, Lightowler S, Leresche N, Jassik-Gerschenfeld D, Pollard CE, and Crunelli V.** Two inward currents and the transformation of low frequency oscillations of rat and cat thalamocortical cells. *J Physiol* 441: 175–197, 1991.

291. **Spreafico R, de Curtis M, Frassoni C, and Avanzini G.** Electrophysiological characteristics of morphologically identified reticular thalamic neurons from rat slices. *Neuroscience* 27: 629–638, 1988.

292. **Squire LR and Zola-Morgan S.** The medial temporal lobe memory system. *Science* 253: 1380–1386, 1991.

293. **Staak R and Pape HC.** Contribution of GABA(A) and GABA(B) receptors to thalamic neuronal activity during spontaneous absence seizures in rats. *J Neurosci* 21: 1378–1384, 2001.

294. **Steriade M.** Interneuronal epileptic discharges related to spike-and-wave cortical seizures in behaving monkeys. *Electroencephalogr Clin Neurophysiol* 37: 247–263, 1974.

295. **Steriade M.** Cortical long-axoned cells and putative interneurons during the sleep-waking cycle. *Behav Brain Sci* 3: 465–514, 1978.

296. **Steriade M.** To burst, or rather, not to burst. *Nat Neurosci* 4: 671, 2001.

297. **Steriade M.** *The Intact and Sliced Brain.* Cambridge, MA: MIT, 2001.

298. **Steriade M and Amzica F.** Intracortical and corticothalamic coherency of fast spontaneous oscillations. *Proc Natl Acad Sci USA* 93: 2533–2538, 1996.

299. **Steriade M and Amzica F.** Intracellular study of excitability in the seizure-prone neocortex in vivo. *J Neurophysiol* 82: 3108–3122, 1999.

300. **Steriade M, Amzica F, and Contreras D.** Synchronization of fast (30–40 Hz) spontaneous cortical rhythms during brain arousal. *J Neurosci* 16: 392–417, 1996.

301. **Steriade M and Contreras D.** Relations between cortical and thalamic cellular events during transition from sleep patterns to paroxysmal activity. *J Neurosci* 15: 623–642, 1995.

302. **Steriade M and Contreras D.** Spike-wave complexes and fast components of cortically generated seizures. I. Role of neocortex and thalamus. *J Neurophysiol* 80: 1439–1455, 1998.

303. **Steriade M, Contreras D, Curró Dossi R, and Nunez A.** The slow (<1 Hz) oscillation in reticular thalamus and thalamocortical neurons. Scenario of sleep rhythms generation in interacting thalamic and neocortical networks. *J Neurosci* 13: 3284–3299, 1993.

304. **Steriade M, Curro Dossi R, and Contreras D.** Electrophysiological properties of intralaminar thalamocortical cells discharging rhythmic (~40 Hz) spike-bursts at ~1000 Hz during waking and rapid eye movement sleep. *Neuroscience* 56: 1–9, 1993.

305. **Steriade M and Deschênes M.** The thalamus as a neuronal oscillator. *Brain Res Rev* 8: 1–63, 1984.

306. **Steriade M, Deschênes M, Domich L, and Mulle C.** Abolition of spindle oscillations in thalamic neurons disconnected from nucleus reticularis thalami. *J Neurophysiol* 54: 1473–1497, 1985.

307. **Steriade M, Domich L, and Oakson G.** Reticularis thalami neurons revisited: activity changes during shifts in states of vigilance. *J Neurosci* 6: 68–81, 1986.

308. **Steriade M, Domich L, Oakson G, and Deschênes M.** The deafferented reticular thalamic nucleus generates spindle rhythmicity. *J Neurophysiol* 57: 260–273, 1987.

309. **Steriade M, Jones EG, and Llinás RR.** *Thalamic Oscillations and Signalling.* New York: Wiley, 1990.

310. **Steriade M and Llinás RR.** The functional states of the thalamus and the associated neuronal interplay. *Physiol Rev* 68: 649–742, 1988.

311. **Steriade M and McCarley RW.** *Brainstem Control of Wakefulness and Sleep.* New York: Plenum, 1990.

312. **Steriade M, McCormick DA, and Sejnowski TJ.** Thalamocortical oscillations in the sleeping and aroused brain. *Science* 262: 679–685, 1993.

313. **Steriade M, Timofeev I, and Grenier F.** Inhibitory components of cortical spike-wave seizures in vivo. *Soc Neurosci Abstr* 24: 2143, 1998.

314. **Steriade M, Timofeev I, and Grenier F.** Natural waking and sleep states: a view from inside neocortical neurons. *J Neurophysiol* 85: 1969–1985, 2001.

315. **Steriade M, Wyzinski P, and Apostol V.** Corticofugal projections governing rhythmic thalamic activity. In: *Corticothalamic Projections and Sensorimotor Activities*, edited by Frigyesi TL, Rinvik E, and Yahr MD. New York: Raven, 1972, p. 221–272.

316. **Stickgold R, Hobson JA, Fosse R, and Fosse M.** Sleep, learning, and dreams: off-line memory reprocessing. *Science* 294: 1052–1057, 2001.

317. **Stickgold R, Whidbee D, Schirmer B, Patel V, and Hobson JA.** Visual discrimination task improvement: a multi-step process occurring during sleep. *J Cogn Neurosci* 12: 246–254, 2000.

318. **Sutherland GR and McNaughton B.** Memory trace reactivation in hippocampal and neocortical neuronal ensembles. *Curr Opin Neurobiol* 10: 180–186, 2000.

319. **Suzuki S and Rogawski MA.** T-type calcium channels mediate the transition between tonic and phasic firing in thalamic neurons. *Proc Natl Acad Sci USA* 86: 7228–7232, 1989.

320. **Svoboda K, Denk W, Kleinfeld D, and Tank DW.** In vivo dendritic calcium dynamics in neocortical pyramidal neurons. *Nature* 385: 161–165, 1997.

321. **Talley EM, Cribbs LL, Lee JH, Daud A, Perez-Reyes E, and Bayliss DA.** Differential distribution of three members of a gene family encoding low-voltage activated (T-type) calcium channels. *J Neurosci* 19: 1895–1911, 1999.

322. **Tancredi V, Biagini G, D'Antuono M, Louvel J, Pumain R, and Avoli M.** Spindle-like thalamocortical synchronization in a rat brain slice preparation. *J Neurophysiol* 84: 1093–1097, 2000.

323. **Terman D, Bose A, and Koppell N.** Functional reorganization in thalamocortical networks: transition between spindling and delta sleep rhythms. *Proc Natl Acad Sci USA* 93: 15417–15422, 1996.

324. **Thomas E and Grisar T.** Increased synchrony with increase of a low-threshold calcium conductance in a model thalamic network: a phase-shift mechanism. *Neural Comput* 12: 1553–1571, 2000.

325. **Thomas E and Lytton WW.** Computer model of antiepileptic effects mediated by alterations in GABA(A)-mediated inhibition. *Neuroreport* 9: 691–696, 1998.

326. **Thomas E and Wyatt RE.** A computational model of spindle oscillations. *Math Comput Simul* 40: 35–69, 1995.

327. **Thomson AM and Destexhe A.** Dual intracellular recordings and computational models of slow IPSPs in rat neocortical and hippocampal slices. *Neuroscience* 92: 1193–1215, 1999.

328. **Thomson AM and West DC.** Local-circuit excitatory and inhibitory connections in slices of the rat thalamus (Abstract). *J Physiol* 438: 113P, 1991.

329. **Timofeev I, Bazhenov M, Sejnowski TJ, and Steriade M.** Cortical hyperpolarization-activated depolarizing current takes part in the generation of focal paroxysmal activities. *Proc Natl Acad Sci USA* 99: 9533–9537, 2002.

330. **Timofeev I, Contreras D, and Steriade M.** Synaptic responsiveness of cortical and thalamic neurones during various phases of slow sleep oscillation in cat. *J Physiol* 494: 265–278, 1996.

331. **Timofeev I, Grenier F, Bazhenov M, Sejnowski TJ, and Steriade M.** Origin of slow cortical oscillations in deafferented cortical slabs. *Cereb Cortex* 10: 1185–1199, 2000.

332. **Toth T and Crunelli V.** Computer simulations of the pacemaker oscillations of thalamocortical cells. *Neuroreport* 3: 65–68, 1992.

333. **Tsakiridou E, Bertollini L, de Curtis M, Avanzini G, and Pape HC.** Selective increase in T-type calcium conductance of reticular thalamic neurons in a rat model of absence epilepsy. *J Neurosci* 15: 3110–3117, 1995.

334. **Turner JP and Salt TE.** Characterization of sensory and corticothalamic excitatory inputs to rat thalamocortical neurones in vitro. *J Physiol* 510: 829–843, 1998.

335. **Uchimura N, Cherubini E, and North RA.** Cation current activated by hyperpolarization in a subset of rat nucleus accumbens neurons. *J Neurophysiol* 64: 1847–1850, 1990.

336. **Ulrich D and Huguenard JR.** GABA$_B$ receptor-mediated responses in GABAergic projection neurones of rat nucleus reticularis thalami in vitro. *J Physiol* 493: 845–854, 1996.

337. **Ulrich D and Huguenard JR.** Nucleus-specific chloride homeostasis in the thalamus. *J Neurosci* 17: 2348–2354, 1997.

338. **Ulrich D and Huguenard JR.** GABA$_A$-receptor-mediated rebound burst firing and burst shunting in thalamus. *J Neurophysiol* 78: 1748–1751, 1997.

339. **VanDongen AMJ, Codina J, Olate J, Mattera R, Joho R, Birnbaumer L, and Brown AM.** Newly identified brain potassium channels gated by the guanine nucleotide binding protein G$_o$. *Science* 242: 1433–1437, 1988.

340. **Van Ginneken ACG and Giles W.** Voltage-clamp measurements of the hyperpolarization-activated inward current I_f in single cells from rabbit sino-atrial node. *J Physiol* 434: 57–83, 1991.

341. **Vergnes M and Marescaux C.** Cortical and thalamic lesions in rats with genetic absence epilepsy. *J Neural Transm* 35 *Suppl*: 71–83, 1992.

342. **Vergnes M, Marescaux C, Micheletti G, Depaulis A, Rumbach L, and Warter JM.** Enhancement of spike and wave discharges by GABA mimetic drugs in rats with spontaneous petit-mal-like epilepsy. *Neurosci Lett* 44: 91–94, 1984.

343. **Vertes RP and Eastman KE.** The case against memory consolidation in REM sleep. *Behav Brain Sci* 23: 867–876, 2000.

344. **Verzeano M.** Pacemakers, synchronization, and epilepsy. In: *Synchronization of EEG Activity in Epilepsies*, edited by Petsche H and Brazier MAB. Berlin: Springer, 1972, p. 154–158.

345. **Verzeano M and Negishi K.** Neuronal activity in cortical and thalamic networks. A study with multiple microelectrodes. *J Gen Physiol* 43: 177–195, 1960.

346. **Von Krosigk M, Bal T, and McCormick DA.** Cellular mechanisms of a synchronized oscillation in the thalamus. *Science* 261: 361–364, 1993.

347. **Waigner BJ, Degennaro M, Santoro B, Seigelbaum SA, and Tibbs GR.** Molecular mechanism of cAMP modulation of HCN pacemaker channels. *Nature* 411: 805–810, 2001.

348. **Wallenstein GV.** A model of the electrophysiological properties of nucleus reticularis thalami neurons. *Biophys J* 66: 978–988, 1994.

349. **Wallenstein GV.** The role of thalamic $I_{GABA(B)}$ in generating spike-wave discharges during petit mal seizures. *Neuroreport* 5: 1409–1412, 1994.

350. **Wallenstein GV.** Adenosinic modulation of 7–14 Hz spindle rhythms in interconnected thalamic relay and nucleus reticularis neurons. *Neuroscience* 73: 93–98, 1996.

351. **Warren RA, Agmon A, and Jones EG.** Oscillatory synaptic interactions between ventroposterior and reticular neurons in mouse thalamus in vitro. *J Neurophysiol* 72: 1993–2003, 1994.

352. **Wang XJ.** Multiple dynamical modes of thalamic relay neurons: rhythmic bursting and intermittent phase-locking. *Neuroscience* 59: 21–31, 1994.

353. **Wang XJ, Golomb D, and Rinzel J.** Emergent spindle oscillations and intermittent burst firing in a thalamic model: specific neuronal mechanisms. *Proc Natl Acad Sci USA* 92: 5577–5581, 1995.

354. **Wang XJ and Rinzel J.** Alternating and synchronous rhythms in reciprocally inhibitory model neurons. *Neural Computat* 4: 84–97, 1992.

355. **Wang XJ and Rinzel J.** Spindle rhythmicity in the reticularis thalami nucleus: synchronization among inhibitory neurons. *Neuroscience* 53: 899–904, 1993.

356. **Wang XJ, Rinzel J, and Rogawski MA.** A model of the T-type calcium current and the low-threshold spike in thalamic neurons. *J Neurophysiol* 66: 839–850, 1991.

357. **Weyand TG, Boudreaux M, and Guido W.** Burst and tonic response modes in thalamic neurons during sleep and wakefulness. *J Neurophysiol* 85: 1107–1118, 2001.

358. **White EL and Hersch SM.** A quantitative study of thalamocortical and other synapses involving the apical dendrites of corticothalamic cells in mouse SmI cortex. *J Neurocytol* 11: 137–157, 1982.

359. **Widen K and Ajmone Marsan C.** Effects of corticopetal and corticofugal impulses upon single elements of the dorsolateral geniculate nucleus. *Exp Neurol* 2: 468–502, 1960.

360. **Williams D.** A study of thalamic and cortical rhythms in Petit Mal. *Brain* 76: 50–69, 1953.

361. **Williams SR and Stuart GJ.** Action potential backpropagation and somato-dendritic distributions of ion channels in thalamocortical neurons. *J Neurosci* 20: 1307–1317, 2000.

362. **Wilson MA and McNaughton BL.** Reactivation of hippocampal ensemble memories during sleep. *Science* 265: 676–679, 1994.

363. **Worgotter F, Suder K, Zhao Y, Kerscher N, Eysel UT, and Funke K.** State-dependent receptive-field restructuring in the visual cortex. *Nature* 396: 165–168, 1998.

364. **Wright JJ, Robinson PA, Rennie CJ, Gordon E, Bourke PD, Chapman CL, Hawthorn N, Lees GJ, and Alexander D.** Toward an integrated continuum model of cerebral dynamics: the cerebral rhythms, synchronous oscillation and cortical stability. *Biosystems* 63: 71–88, 2001.

365. **Wu GY and Cline HT.** Stabilization of dendritic arbor structure in vivo by CaMKII. *Science* 279: 222–226, 1998.

366. **Yamada M, Jahangir A, Hosoya Y, Inanobe A, Katada T, and Kurachi Y.** GK* and brain G beta gamma activate muscarinic K^+ channel through the same mechanism. *J Biol Chem* 268: 24551–24554, 1993.

367. **Yarom Y.** Rhythmogenesis in a hybrid system-interconnecting an olivary neuron to an analog network of coupled oscillators. *Neuroscience* 44: 263–275, 1991.

368. **Yen CT, Conley M, Hendry SH, and Jones EG.** The morphology of physiologically identified GABAergic neurons in the somatic sensory part of the thalamic reticular nucleus in the cat. *J Neurosci* 5: 2254–2268, 1985.

369. **Yingling CD and Skinner JE.** Gating of thalamic input to the cerebral cortex by nucleus reticularis thalami. *Prog Clin Neurophysiol* 1: 70–96, 1977.

370. **Yuste R and Tank DW.** Dendritic integration in mammalian neurons, a century after Cajal. *Neuron* 16: 701–716, 1996.

371. **Zhan XJ, Cox CL, and Sherman SM.** Dendritic depolarization efficiently attenuates low-threshold calcium spikes in thalamic relay cells. *J Neurosci* 15: 3909–3914, 2000.

372. **Zhang SJ, Huguenard JR, and Prince DA.** $GABA_A$ receptor-mediated Cl^- currents in rat thalamic reticular and relay neurons. *J Neurophysiol* 78: 2280–2286, 1997.

373. **Zhou Q, Godwin DW, O'Malley DM, and Adams PR.** Visualisation of calcium influx through channels that shape the burst and tonic firing modes of thalamic relay cells. *J Neurophysiol* 77: 2816–2825, 1997.

374. **Zola-Morgan SM and Squire LR.** The primate hippocampal formation: evidence for a time-limited role in memory storage. *Science* 250: 288–290, 1990.